# *IN VITRO* CULTURE CONDITIONS AND MECHANICAL STIMULATION ON INORGANIC POLYPHOSPHATE PRODUCTION IN CHONDROCYTES

**Wendy Wu**

Thesis submitted to the University of Ottawa
in partial Fulfillment of the requirements for the degree of
Master of Applied Science in Biomedical Engineering

Department of Chemical and Biological Engineering
Faculty of Engineering
University of Ottawa

## ABSTRACT

Osteoarthritis (OA) is degenerative joint disease that is characterized by the progressive loss and destruction of articular cartilage, the connective tissue that provides a smooth and lubricated surface for articulation and the transmission of mechanical forces. OA affects almost 5 million Canadians and can cause individuals to experience pain, joint stiffness, and a decreased range of motion, all of which have a significant impact on their quality of life. There is currently no cure to stop the progression of OA; hence, current treatments are solely focused on symptom management, while the disease progresses.

The lack of effective treatments is largely attributed to our limited knowledge of cartilage biology and of the mechanisms involved in the pathogenesis of the disease. Inorganic polyphosphate (polyP) is a linear polymer of orthophosphates that are linked together by high energy phosphoanhydride bonds. Previous studies have shown that the exogenous administration of polyP to cultures of chondrocytes stimulates matrix accumulation, while intra-articular injection in an OA animal model protected the cartilage from degenerative changes. Polyphosphate has also been observed in native articular cartilage. Therefore, polyP demonstrates the potential to be integrated into therapeutics to address the degenerative nature of OA. Despite this potential as a chondroprotective agent, polyP remains understudied in cartilage. In this work, we investigated the impact of culture conditions, exogenous polyP administration, and static compression on the levels of polyP and other key metabolites in cartilage tissue.

Our work demonstrated that the polyP found in cultures of chondrocytes can be synthesized by the cells, as opposed to accumulated from media supplements. Cultures grown in the combination of DMEM 4.5 g/L glucose and fetal bovine serum (FBS) yielded the greatest accumulation of polyP in the tissue constructs. PolyP levels were influenced by media

composition, as greater levels of polyP per cell were quantified in DMEM compared to Ham's F12. Glucose, lactate, and polyP content were monitored over a 72-hour period between media changes, with a downward trend observed in the glucose content and an upward trend in lactate and polyP accumulation. Exogenous polyP administration elicited minimal differences in glucose consumption and lactate build-up. Static compression of tissue constructs resulted in an increase in cell proliferation and depletion of collagen and proteoglycans, the two major components of the extracellular matrix. The metabolic response to static loading appeared to be minimal due to the stable levels of glucose, lactate and polyP quantified, suggesting the chondrocytes may reach a state of equilibrium similar to the controls within the compression session. Results from this thesis provide insight into the factors that influence polyP metabolism, furthering our understanding of this biomolecule's role in cartilage tissue. Further work needs to be done to identify the key factors involved in modulating polyP levels, the effect of exogenous polyP administration on metabolic pathways, and short-term effects of static compression on metabolism.

## RÉSUMÉ

L’arthrose est une maladie dégénérative des articulations caractérisée par la perte et la destruction progressives du cartilage articulaire, le tissu conjonctif qui fournit une surface lisse et lubrifiée pour l’articulation et qui participe à la transmission des forces mécaniques. L’arthrose touche près de 5 millions de Canadiens et peut provoquer des douleurs, une raideur articulaire et une diminution de l’amplitude des mouvements, qui ont tous un impact significatif sur la qualité de vie. Il n’existe actuellement aucun traitement thérapeutique pour arrêter la progression de l’arthrose. Par conséquent, les traitements actuels se concentrent uniquement sur la gestion des symptômes sans pouvoir arrêter la progression de la maladie. Le manque de traitements efficaces est en grande partie attribué à notre connaissance limitée de la biologie du cartilage et des mécanismes impliqués dans la pathogenèse de l’arthrose. Le polyphosphate inorganique (polyP) est un polymère linéaire d’orthophosphates liés entre eux par des liaisons phosphoanhydrides à haute énergie. Des études antérieures ont montré que l’administration exogène de polyP à des cultures de chondrocytes stimule l’accumulation de matrice extracellulaire, tandis que l’injection intra-articulaire de la molécule dans un modèle animal d’arthrose protège le cartilage des changements dégénératifs. Le polyphosphate a également été observé dans le cartilage articulaire naturel. Par conséquent, le polyP démontre le potentiel d'être intégré dans les thérapies pour traiter la nature dégénérative de l'arthrose. Malgré ce potentiel en tant qu'agent chondroprotecteur, le polyP reste sous-étudié dans le cartilage. Dans cette thèse, nous avons étudié l'impact des conditions de culture des chondrocytes, de l'administration de polyP exogène et de la compression statique sur les niveaux de polyP et d'autres métabolites dans le tissu cartilagineux. Nos travaux ont démontré que le polyP trouvé dans les cultures de chondrocytes peut être synthétisé par les cellules, par opposition à une accumulation à partir de suppléments

des milieux de culture. Les cultures cultivées dans la combinaison de DMEM comprenant 4,5 g/L de glucose et de sérum bovin fœtal (FBS) ont donné la plus grande accumulation de polyP dans les constructions tissulaires. Les niveaux de polyP étaient principalement influencés par la densité cellulaire dans les cultures. De plus, des niveaux plus élevés de polyP par cellule ont été observés lors de cultures dans le DMEM par rapport au F12, suggérant un effet de l'environnement sur l'accumulation de polyP. Les teneurs en glucose, en lactate et en polyP ont été mesurés sur une période de 72 heures, avec une tendance à la baisse observée dans la teneur en glucose et une tendance à la hausse dans l'accumulation de lactate et de polyP. L'administration de polyP exogène a provoqué des différences minimes dans la consommation de glucose et l'accumulation de lactate. La compression statique des structures tissulaires a entraîné une augmentation de la prolifération cellulaire et une diminution du collagène et des protéoglycanes, les deux principaux composants de la matrice extracellulaire. La réponse métabolique à la charge statique semble être minimale en raison des niveaux stables de glucose, de lactate et de polyP quantifiés, suggérant que les chondrocytes peuvent atteindre un état d'équilibre similaire aux conditions contrôles au cours de la séance de compression. Les résultats de cette thèse donnent un aperçu des facteurs qui influencent le métabolisme des polyP, approfondissant ainsi notre compréhension du rôle de cette biomolécule dans le tissu cartilagineux. Des travaux supplémentaires doivent être effectués pour identifier les facteurs clés impliqués dans la modulation des niveaux de polyP, l'effet de l'administration de polyP exogène sur les voies métaboliques et les effets à court terme de la compression statique sur le métabolisme.

## ACKNOWLEDGEMENTS

To start, I would like to thank my supervisor, Dr. Jean-Philippe St-Pierre for his support and guidance throughout the duration of my Master's and this project. I have learned so much from this experience and I am so grateful for the opportunity to explore the field of research and academia which has helped me to develop skills for my future endeavours.

I would like to thank my colleagues from the St-Pierre lab past and present (Jordan Nhan, Abrie Girgis, Noor Ghadie, Luisa Metzler, Michael Mulholland, Rayehe Ghofrani, Olivia Stenier) for their help in supporting my research and all the fun memories we created outside of the lab. I would also like to extend my gratitude to my students Justin Wong and Athena Prattas who have helped me immensely to complete this project. I wish to thank Dr. Xuodong Cao, Dr. Elena Baranova and their students for sharing their laboratory space and equipment with us. I am especially grateful to my friends and family for their continuous love and support for the past two years. Thank you Sarah and Heather for being my two closest friends in the Biomedical Engineering program and being there through all the ups and downs our Master's had to offer. Lastly, I'd like to thank my best friend Sabrina Rasna for being my rock and biggest cheerleader, despite the 400 km distance between us your unwavering support is the reason I'm here today and I am forever grateful.

## TABLE OF CONTENTS

## LIST OF FIGURES

## LIST OF ABBREVIATIONS

| | |
|---|---|
| AC | Articular cartilage |
| ACI | Autologous chondrocyte implantation |
| ADAMTS | A disintegrin and metalloproteinase with thrombospondin motifs |
| ADP | Adenosine diphosphate |
| AGE | Advanced glycation end-product |
| ALP | Alkaline phosphatase |
| ANOVA | Analysis of variance |
| ATP | Adenosine triphosphate |
| BMP | Bone morphogenetic protein |
| BSA | Bovine serum albumin |
| DAPI | 4’,6-diamidino-2-phenylindole |
| DMEM | Dulbecco’s modified Eagle medium |
| DMMB | Dimethylmethylene blue |
| DMOAD | Disease modifying OA drugs |
| DNA | Deoxyribose nucleic acid |
| ECM | Extracellular matrix |
| EDTA | Ethylenediaminetetraacetic acid |
| ERK | Extracellular signal-regulated kinase |
| ETC | Electron transport chain |
| $FADH_2$ | Flavin adenine dinucleotide |
| FBS | Fetal bovine serum |

| | |
|---|---|
| GAG | Glycosaminoglycan |
| diH2O | Deionized water |
| HA | Hyaluronic acid |
| HCl | Hydrochloric acid |
| HK | Hexokinase |
| IDH | Isocitrate dehydrogenase |
| IL | Interleukin |
| iPSC | Induced pluripotent stem cells |
| ITS | Insulin-transferrin-selenium |
| LDH | Lactate dehydrogenase |
| MMP | Matrix metalloproteinase |
| mPTP | Mitochondrial permeability transition pore |
| MAPK | Mitogen-activated protein kinase |
| MSC | Mesenchymal stem cells |
| MTT | 3-(4,5-dimethylthiazol-2-yl)-2,5-diphenyl tetrazolium bromide |
| NAD | Nicotinamide adenine dinucleotide |
| NADH | Nicotinamide adenine dinucleotide hydride |
| NMR | Nuclear magnetic resonance |
| NSAID | Nonsteroidal anti-inflammatory drugs |
| OA | Osteoarthritis |
| OXPHOS | Oxidative phosphorylation |
| PAGE | Polyacrylamide gel electrophoresis |

| | |
|---|---|
| PBS | Phosphate buffered saline |
| PCM | Pericellular matrix |
| PFK | Phosphofructokinase |
| PG | Proteoglycan |
| Pi | Inorganic phosphate |
| PK | Pyruvate kinase |
| P NMR | Phosphorous nuclear magnetic resonance |
| PPK | Polyphosphate kinases |
| PPN | Endopolyphosphatases |
| PPX | Exopolyphosphatases |
| RNA | Ribonucleic acid |
| SD | Standard deviation |
| $SO_4$ | Sulfate |
| TCA | Tricarboxylic acid |
| TGF | Transforming growth factor |
| TNF | Tumor necrosis factor |
| UTP | Uridine triphosphate |
| UV | Ultraviolet |
| VTC | Vacuolar transporter chaperone |

# INTRODUCTION

## 1.1 Purpose and Research Objectives

Arthritis is a group of degenerative joint diseases and is Canada's most prevalent chronic health condition [1]. Osteoarthritis (OA) is the most common type of arthritis, affecting more than 4 million Canadians [2]. It is characterized by the progressive loss and destruction of articular cartilage [3], the connective tissue that provides a smooth and lubricated surface for articulation and that helps distribute and transmit mechanical forces to the underlying bone [4]. Individuals suffering from OA experience pain, joint stiffness, and a decreased range of motion, all of which have a significant impact on their quality of life and, in many cases, their capacity to lead fulfilling professional lives. There is currently no cure to stop the course of OA; hence, current pharmacological treatments solely address the management of symptoms as the disease progresses. Localized cartilage defects can be surgically repaired with cell- and biomaterial-based techniques, although doing so only offers limited and temporary relief in many patients. In the end, joint replacement with permanent prosthetic materials is required [5]. The lack of effective treatments is largely attributed to our limited knowledge of cartilage biology and of the mechanisms involved in the pathogenesis of the disease.

Inorganic polyphosphate (polyP) is a linear polymer of orthophosphate groups that are linked by phosphoanhydride bonds. It is ubiquitous in nature as it has been found in organisms from all branches of the "tree of life" [6]. Although polyP has been extensively studied in lower-level organisms, their functions in mammalian tissues have only recently started to be uncovered. Interestingly, previous work by my supervisor found that the exogenous administration of polyP to cultures of chondrocytes, the resident cell of cartilage tissue, stimulates cartilage matrix accumulation, while intra-articular injection in a guinea pig model of OA protects the cartilage

from some degenerative changes [7, 8]. These results suggest that polyP may promote tissue synthesis and the structural maintenance of the cartilage extracellular matrix (ECM). While research efforts have been made to better understand and characterize this understudied biopolymer, in cartilage, many open questions must be answered to exploit its potential as an untapped therapeutic target to stimulate tissue repair.

In the work presented in this thesis, we are interested in monitoring the endogenous polyP levels in *in-vitro*-formed cartilage constructs to gain insights into its metabolism and how different culture conditions and mechanical cues influence chondrocyte's ability to produce the biomolecule. More specifically, this thesis will discuss work pertaining to three main objectives:

1. Determination of independent polyP production from chondrocytes by quantifying the polyP levels of tissue constructs grown in culture with and without polyP present.
2. Evaluation of metabolic activity in chondrocytes over time in culture to evaluate the relationship between polyP and other key biomolecules.
3. Determination of how mechanical stresses known to lead to tissue degradation, impacts the metabolic activity and biochemical composition cartilage tissue.

## 1.2 Organization of Thesis

There are seven chapters in this thesis. A review of the current literature on polyP metabolism and characterization will be provided in Chapter 2. An overview of the pertinent techniques used in this project is detailed in Chapter 3. Chapter 4 outlines the statistical analyses conducted. The study's results and discussions are presented together in Chapters 5 and 6. Lastly, chapter 7 concludes this thesis by providing a brief overview of the main takeaways of this study and the possible future directions for the project's advancement.

# LITERATURE REVIEW

## 2.1 Articular Cartilage

### *2.1.1 Functions of Articular Cartilage*

Articular cartilage (AC) is a specialized connective tissue that overlies the bone surface in diarthrodial joints, such as the knees, shoulders, and hips. The articular cartilage is subject to a dynamic biomechanical environment by undergoing various compressive, sheer, friction, and tension forces [9] and withstanding high cyclic loads through ECM structure and osmotic pressure changes between the tissue and synovial fluid [4,10]. The main functions of the AC are to provide a smooth and lubricated surface for articulation, minimize friction from diarthrosis, and distribute loads to the underlying bone.

### *2.1.2 Composition of Articular Cartilage*

AC is made up of a dense extracellular matrix (ECM) composed primarily of water, collagen, proteoglycans, and non-collagenous proteins. Water makes up 65-80% [11] of the weight in AC, while collagen, proteoglycans and non-collagenous proteins make up 60%, 25-35%, and 15-25% in dry weight, respectively [12]. Among these components, chondrocytes are the sole cell type in AC [13] and occupy 1-5% of the volume depending on location in the joint, joint type and age. Chondrocytes are responsible for maintaining the integrity and function of the cartilage tissue through the synthesis of matrix components and enzymes for matrix degradation to facilitate dynamic ECM remodeling [4, 11, 12]. The composition and organization of the ECM is crucial for providing the cartilage tissue with ability to carry out its diverse functions.

#### 2.1.2.1 Proteoglycans

Proteoglycans (PGs) are comprised of a protein core and one or more glycosaminoglycan (GAG) chains. These glycosaminoglycan chains form long unbranched polysaccharide chains

with repeating disaccharide units containing amino sugars [12]. The most common GAGs found in cartilage include chondroitin sulfate, keratan sulfate, dermatan sulfate, and hyaluronic acid [12]. Notably, the fixed negative charge imparted by the sulfate and carboxylate groups within these disaccharide units can attract positively charged ions inside the matrix, enhancing the osmolarity of the AC and attracting water [12]. The resulting swelling contributes to providing compressive strength to the cartilage while regulating the fluid and electrolyte balance within the tissue, ensuring optimal function to support joint movement and resistance to mechanical stresses [12].

2.1.2.2 Collagens

Collagen is the most abundant component in the cartilage ECM, with types II, VI, IX, X, and XI found more prominently in articular cartilage [11]. Each collagen molecule is composed of three polypeptide chains that form a triple helix structure [14]. The polypeptide chains contain an amino acid sequence that has glycine for every third residue, resulting in a repeating sequence of X-Y-glycine, where X and Y can be any amino acid [14]. Proline and hydroxyproline are the most common amino acids for the X and Y position, respectively [14]. Type II collagen accounts for 90-95% [11] of the collagens in the ECM and is responsible for providing the cartilage tissue with tensile strength by forming cross-band fibrils that are organized in tight meshwork [11, 12]. The collagen network also provides a restraining force to counter the osmotic pressure attributed to the GAGs [15], hence, the ratio of collagen to GAG is crucial to the compressive strength of the cartilage tissue. Collagen type VI is located in the pericellular matrix [11, 16] and facilitate chondrocytes to attach to the matrix through the interaction of various integrin receptors and transmembrane proteoglycans [11, 17]. Type IX collagen is cross-linked to the surface of collagen fibrils that provide tensile strength and facilitate inter-fibrillar connections [11, 18].

Collagen X is found specifically in the deeper aspects of the tissue and has a role in cartilage mineralization and compartmentalizing matrix components [11, 19]. Type XI is found within or on the collagen fibrils and initiates fibril formation.

#### 2.1.2.3 Fluid Phase

The fluid phase is the aqueous component of cartilage and is mainly comprised of water and electrolytes. This phase also contains small proteins, metabolites, gases, and a high concentration of positively charged ions [12]. It acts as a medium for joint lubrication by creating a low-friction surface and a medium for nutrient delivery by enabling the diffusion and transport of nutrients to the chondrocytes. Additionally, the interaction between the water from fluid phase and the proteoglycans and collagens from the matrix influence the mechanical properties of the tissue.

### *2.1.3 Mechanical Properties of Cartilage Tissue*

Cartilage tissue encompasses several mechanisms attributable to its mechanical properties. A key characteristic is the viscoelastic behaviour of cartilage in response to applied loads. Two mechanisms are responsible for the viscoelasticity of AC – flow dependent and flow independent responses [20]. The flow dependent mechanism responds to mechanical loads by undergoing fluid flow within the ECM and relies on the interstitial fluid and its associated frictional drag [4]. When a compressive load is applied, fluid from the matrix is displaced and causes an increase in interstitial fluid pressure. If there is deformation, the fluid can flow through the layers of cartilage, across the articular surface, and subsequently out of the ECM [20, 21]. When the load is removed, the tissue is rehydrated by the Donnan effect where negatively charged proteoglycan attract cations from the interstitial fluid leading to higher osmolarity within the cartilage [11]. The flow independent response is caused by the intrinsic behaviour of the collagen and

proteoglycans in the matrix. When the cartilage undergoes compressive forces, the negatively charged aggregated proteoglycans are in closer contact to each other and create a repulsive force that causes them spread out within the collagen framework [21]. The combined effect of these repulsive forces attribute to the compressive stiffness of the cartilage tissue. Swelling of the aggregated proteoglycans against the collagen framework play an important role in the mechanical response of cartilage.

### *2.1.4 Organization of ECM*

#### 2.1.4.1 Zonal Organization

AC can be divided into four zones – the superficial, middle, and deep zones, as well as the zone of calcified cartilage (Figure 1). Every zone possesses different biomechanical properties due to variations in water, collagen, and proteoglycan concentrations and organization. Each zone also differs biochemically due to variations in chondrocyte phenotype and metabolism.

The superficial zone is the outermost most layer of tissue in the articular cartilage that is adjacent to the synovial fluid in the joint cavity. It is the thinnest layer and make up 10-20% of the total AC thickness [20]. In this zone, the chondrocytes are flat in shape and the ECM comprises a high amount of collagen and low levels of proteoglycans. This zone has the highest water content due to its close contact with the synovial fluid and increased tissue permeability when deformed, leading to greater fluid exchange with its surroundings [20]. Collagen fibrils in the superficial zone are tightly packed and oriented parallel to the articular surface [4, 20]. This collagen organization provides high tensile stiffness and strength compared to other zones to endure the sheer stresses and strains produced by the joints during articulation. Moreover, the tight packing of the collagen fibrils of this zone can act as a barrier for the AC that could limit the diffusion of molecules in and out of cartilage tissue [12].

The middle zone is the intermediate layer between the superficial and deep zones of the articular cartilage and makes up 40-60% of total cartilage volume [20]. Chondrocytes in this zone are low in density and spherical in shape. The collagen fibers in the middle zone are larger diameter and arranged obliquely to the surface [4]. Proteoglycan concentration is elevated in this zone and contributes to providing swelling pressure to resist compressive forces caused by the joint.

The deep zone is directly beneath the middle zone and accounts for 30% of the AC volume [20]. Chondrocytes density and water concentration are the lowest in this area, while proteoglycan concentrations are at its highest compared to the other zones. This region contains the thickest collagen fibers oriented perpendicularly to the articular surface. Chondrocytes in the deep zone are arranged in a columnar orientation, that is parallel to the collagen fibers and perpendicular to the joint line. Functionally, the deep zone provides the greatest resistance to compressive forces due to its high concentration of proteoglycans.

The zone of calcified cartilage (ZCC) is the mineralized layer situated in the deepest region in the articular cartilage and interfacing with subchondral bone. The anisotropic structure of the collagen fibers is responsible for anchoring the hyaline cartilage into the ZCC [22] and the interface between these zones is marked by a tidemark. Its undulating interface with subchondral bone is marked by the cement line and is responsible for diffusing loads and contributing to the joint's mechanical properties [23]. Chondrocytes in this region are scarce in density, display a hypertrophic phenotype, and can synthesize collagen type X to provide structural integrity and distribute mechanical forces along the bone.

2.1.4.2 Regional Organization

The ECM can also be organized into three different regions based on distance from the chondrocytes – pericellular, territorial, and inter-territorial matrix (Figure 1). The pericellular region is thinnest layer and is located adjacent to the cell membrane. This region is rich in proteoglycans and non-collagenous proteins and has been implicated in signal transduction under load bearing conditions in cartilage [4, 24]. Its role as a transducer of mechanical signals is supported by cell-matrix studies that demonstrate mechanical changes in the PCM impact ECM components and in turn influence the chondrocytes' mechanical and physiochemical environment [25]. The territorial region surrounds the pericellular layer and is composed of thin collagen fibrils oriented in a transverse pattern. This collagen organization has been proposed to protect chondrocytes from mechanical stresses [26]. The inter-territorial region is the largest of the three layers and contains the largest collagen fibrils which are oriented parallel, oblique, and perpendicular to the superficial, middle, and deep zones, respectively [4]. It contributes the most to the biomechanical properties of AC due to proteoglycan abundance and collagen organization.

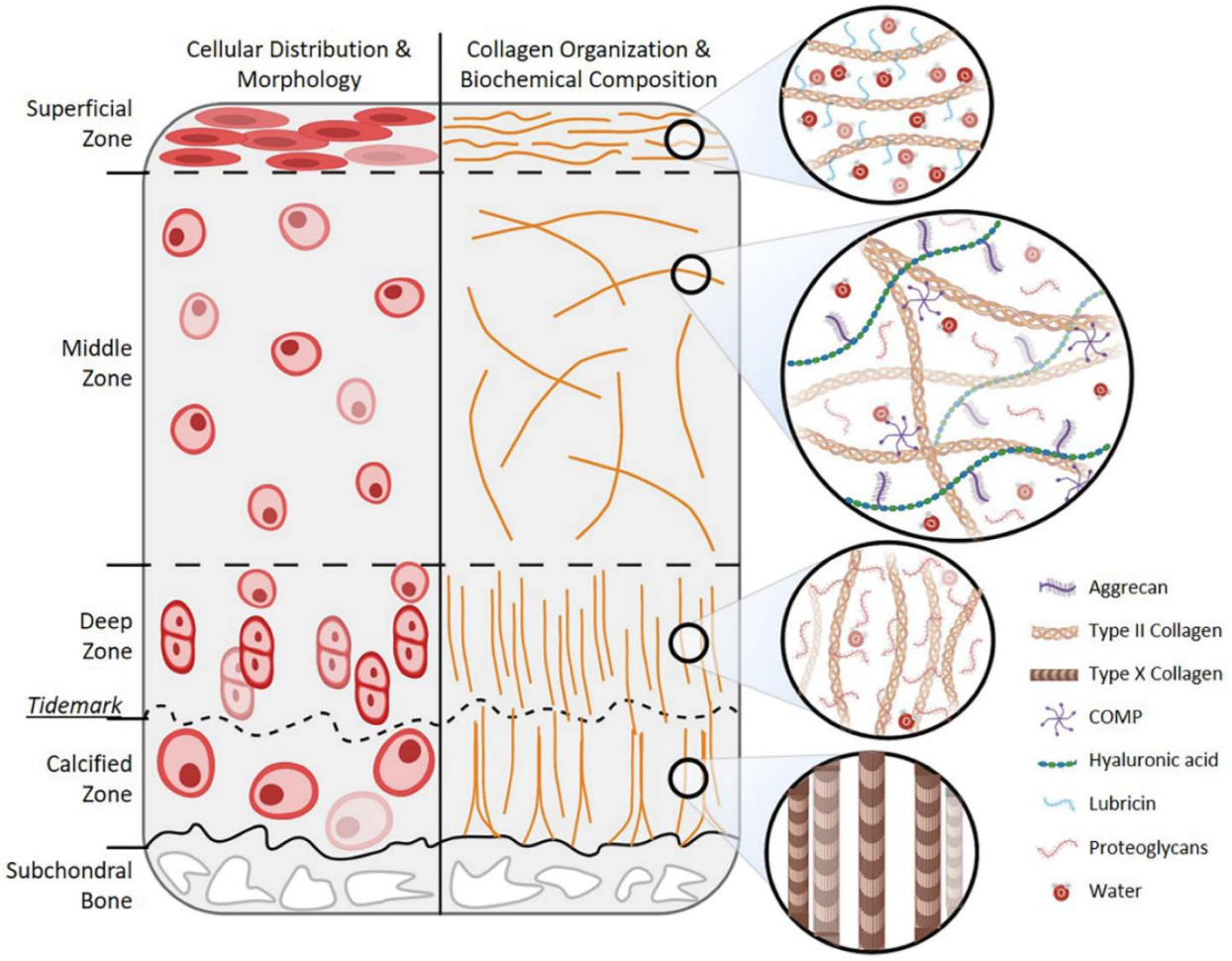


**Figure 1. Schematic representation of zonal and regional organization of articular cartilage.** Figure obtained from Trends in Articular Cartilage Tissue Engineering: 3D Mesenchymal Stem Cell Sheets as Candidates for Engineered Hyaline-Like Cartilage [27]. Used with permission under the Creative Commons Attribution license.

## 2.2 Osteoarthritis

Osteoarthritis (OA) is a debilitating joint disease that affects approximately 4 million Canadians. Although OA is commonly characterized by the progressive loss of AC, it also involves changes in the subchondral bone, synovium, and other tissues of the affected joint [28,

29, 30]. Individuals suffering from OA experience pain, joint stiffness, and decreased range of motion, all of which have a significant impact on their quality of life.

### 2.2.1 Etiology

OA is a multifactorial disease influenced by systemic and biomechanical factors that collectively contribute to the risk of OA onset. Systemic factors, such as age, sex, genetic predisposition, nutrition, and bone density increase the likelihood of joint susceptibility to injury [31]. Biomechanical factors influence load distribution along the joint and include factors such as joint injury, joint deformation, obesity, and muscle weakness [31].

On a molecular level in the cartilage tissue, chondrocytes are responsible for maintaining the matrix by expressing growth factors and cytokines that regulate the synthesis and break down of ECM components. A common event in the pathogenesis of OA is the disruption of cytokine levels, namely the overexpression of proinflammatory cytokines interleukin-1β (IL-1β), tumour necrosis factor α (TNF-α), and interleukin 6 (IL-6) [32]. These metabolic mediators activate signalling pathways to promote catabolic reactions, inhibit the synthesis of ECM components, and induce cell apoptosis [32]. As such, the expression of proinflammatory cytokines can modulate the activity of proteinases such as, matrix metalloproteinases (MMPs) and a disintegrin and metalloproteinase with thrombospondin motifs **(**ADAMTSs) which play a role in matrix degradation. The predominant MMPs in OA are MMP-1 and MMP-13, which are produced by the synovial cells and chondrocytes [33] respectively, and are responsible for degrading collagen type II [34]. Gelatinases MMP-2 and MMP-9 participate in the breakdown of various ECM components such as proteoglycans, fibronectin, and collagens [35]. Proteinases MMP-3, ADAMTS-4, and ADAMTS-5 function to break down proteoglycans, particularly aggrecan [34]. To compensate for these catabolic events, the chondrocytes increase their rate of proliferation

and synthesis of matrix components, however, despite these efforts, they fail to repair the cartilage tissue [36, 37]. The dysregulation of cartilage metabolism leads to the depletion of proteoglycan content and loss of integrity of the collagen network [38], which impedes on the compressive and tensile strength of the tissue.

Cartilage defects are injuries to the cartilage tissue that can be characterized based on their size and depth. Partial-thickness defects do not penetrate the full depth of the cartilage; however, they disrupt the smooth articular surface and impair its ability to facilitate low-friction joint movement [39]. These defects have poor healing capacity due in part to the entrapment of chondrocytes within their chondron and limiting their ability to migrate to the injury site, as well as to the avascular nature of the cartilage tissue, which restricts the access of progenitor cells to the defect site and the formation of fibrin clot that can serve as a scaffold to support repair mechanisms [40]. Over time, partial-thickness defects can expand and deepen progressively, and if left untreated, can lead to secondary OA. On the other hand, full-thickness defects penetrate the entire depth of the cartilage and reaches the subchondral bone. When these defects occur, blood from the marrow fills the space and forms a fibrin clot containing inflammatory cells. Subsequently, mesenchymal cells migrate to the injury site and differentiate into chondrocytes that produce fibrocartilaginous repair tissue with different properties to native hyaline cartilage. Despite these self-healing mechanisms, the resulting repair tissue is inferior to the hyaline cartilage and eventually undergoes degeneration [40, 41]. These degenerative changes in full-thickness defects can also manifest into OA over time and emphasize the importance of repairing these defects as a preventative measure.

### *2.2.2 Treatment Options*

There is currently no disease modifying OA drugs (DMOADs) to stop or reverse the course of the disease. The lack of effective treatments is largely attributed to our limited knowledge of the mechanisms involved in the pathogenesis of the disease. Hence, current pharmacological treatments solely address the management of symptoms, as the disease progresses. Localized cartilage defects can be surgically repaired with cell- and biomaterial-based techniques, although doing so only offers limited and temporary relief in many patients. In the end, joint replacement with permanent prosthetic materials is often prescribed [5].

#### 2.2.2.1 Conservative Therapy

Conservative therapies aim to provide non-invasive symptomatic relief of OA. They are the first-choice methods for managing the early stages of symptomatic OA and can be categorized into non-pharmacological and pharmacological strategies. Non-pharmacological methods include weight loss, exercise, and orthoses. Weight loss can reduce the compressive forces on the joints and subsequently improve pain and joint mobility [41], however, this treatment is not effective in addressing the inflammation state associated with obesity [42]. Exercise has a dynamic role in alleviating the pathological changes of OA by inhibiting the degradation of the ECM, apoptosis, inflammatory responses, and strengthening the joints to reduce loads on the cartilage [43, 44]. Orthoses such as lateral wedge insoles and braces provide joint support and stability to help improve pain and function [45]. Pharmacological interventions include opioids and nonsteroidal anti-inflammatory drugs (NSAIDs) which evoke an analgesic and anti-inflammatory response. Intra-articular injection is a targeted treatment that delivers therapeutic molecules directly into the joint space. The administration of corticosteroid injections reduces joint inflammation [46] and provides moderate pain relief [47] for at least one week [46]. Hyaluronic acid (HA)

injections aim to lubricate the joint and compensate for the depleted chondroprotective mechanisms of HA [48].

#### 2.2.2.2 Surgical Therapy

When conservative strategies are exhausted and fail to alleviate symptoms or disease progression, surgical interventions can be considered. These procedures aim to address the underlying structural issues within the joint that contribute to OA symptoms such as pain, stiffness, and limited joint mobility. Surgical strategies include cell-based interventions such as marrow stimulation, autologous chondrocyte implant (ACI), and tissue transplantation with osteochondral auto- and allo- grafts, as well as total joint replacement.

Marrow stimulation relies on the intrinsic cartilage repair system to heal lesions and defects. In this procedure, the lesion is debrided with arthroscopic curettes to remove any damaged cartilage on top or surrounding the defect and produce clear margins [49]. The underlying subchondral bone is then perforated to induce bleeding and the formation of a clot, into which mesenchymal stem cells (MSCs) can migrate. At the clot, MSCs can secrete bioactive molecules that have anti-inflammatory and immunomodulatory effects, to help reduce joint inflammation and slow the progression of OA [50]. It can also differentiate into chondrocytes for cartilage formation and stimulate tissue regeneration via MSC-derived paracrine signals [51]. The MSCs promote fibrocartilage formation within the defect space. Fibrocartilage is primarily composed of collagen type I as opposed to collagen type II, and due to this and other differences, fibrocartilage exhibits inferior biomechanical properties compared to native articular cartilage [52]. Although this procedure could lead to issues with biomechanical performance, it has shown to stimulate significant cartilage growth 9 months after surgery [53]. However, this treatment has

a limited lifespan with many patients beginning to experience treatment failures 5 years post-surgery [54].

ACI is a two-step cell-based technique for cartilage repair. The first step involves harvesting small samples of cartilage from a low or non-weight bearing area in the patient's knee [55]. The cartilage is then enzymatically digested and cultured *in*-vitro for 3-6 weeks to increase the number of chondrocytes [56]. The second step involves the implantation of the cultured chondrocytes into the cartilage lesion. To do so, the defect needs to undergo surgical debridement where careful care is taken to avoid penetration of the subchondral bone, releasing blood and bone marrow elements. A periosteal flap or collagen-membrane is secured on top of the lesion to create a pouch and the cultured chondrocytes are injected underneath. After the procedure, it can take months for the cartilage to mature which can be characterized into three distinct stages. Cellular proliferation is the first stage and involves the adherence of chondrocytes to the subchondral bone which can take up to 6 weeks [56]. The second stage of the maturation process is the transition phase where chondrocytes release ECM components and takes place 4-6 months after surgery [56]. The last stage is marked by the hardening of the cartilage tissue and begins 6 months post-operation and continues to mature for up to 3 years. Although ACI has been successful in alleviating patients from pain, it is not practiced in Canada due to its requirement of multiple surgeries, prolong return to activity, and risk of complications [57].

Osteochondral autografts are also used to treat small cartilage defects. In this procedure, healthy osteochondral tissue is harvested from a non-weight bearing area of the knee and transplanted into the cartilage defects. Autografts are advantageous as they avoid the potential risks of tissue rejection and infection [58]. However, several complications can arise, such as donor site morbidity and the graft not aligning with the joint topography [59]. Ultimately, this

technique cannot be used to treat large lesions due to the limited by the amount of cartilage available at the donor site. Osteochondral allografts can be used to treat larger lesions, but face issues with risk of infection, tissue rejection, limited availability, and high costs [60].

The prior techniques discussed focus on repairing cartilage lesions that could develop into secondary OA. Total joint replacement is an effective treatment option for severe cases of OA that helps patients improve their mobility and alleviate their pain. Prostheses are made from a combination of metals, ceramics, plastics, and biomaterials to replace the joint and restore articulating function [61]. After surgery, patients generally experience pain relief and an increase in mobility [62]. The long-term success of the joint replacement is dependent on the longevity and durability of the prostheses, with 90% of ceramic prostheses [63] and 95% of titanium prostheses [64] surviving 15 years post-operation. Implant failure can arise for a few reasons which include aseptic loosening, mechanical failure, and prosthetic joint inflections, all of which influence the need for revision surgery [65]. Total joint replacement is not an ideal therapeutic treatment for younger patients due to the invasive nature of the surgery and potential complications that arise with these implants such as aseptic loosening and joint infection [66, 67]. While it is a good alternative for end-stage disease, disease prevention and tissue regeneration strategies should be the main focus of research and development.

### 2.3 Cartilage Tissue Engineering

Cartilage tissue engineering techniques aim to regenerate damaged cartilage by utilizing cells, scaffolds, and bioactive molecules or a combination of multiple techniques. Cell-based techniques use a patient's own cells to facilitate the repair of cartilage defects. As discussed above, common cell-based interventions include marrow stimulation and ACI, however, emerging strategies are looking into utilizing stem cells as a source for repair.

Induced pluripotent stem cells (iPSCs) is a promising cell-based approach for treating OA. These cells are derived from the patient's somatic cells and reprogrammed into a pluripotent state, allowing them to differentiate into any cell type. For OA treatment, iPSCs are differentiated into chondrocytes and directly injected into the cartilage defect to facilitate repair. This approach is advantageous as it overcomes the hurdles of donor tissue availability, risk of immune rejection, and ethical concerns [68]. However, this technique is still in its early stages and poses various challenges that need to be addressed such as the ability to reliably differentiate iPSCs into chondrocytes and the risk for tumorigenicity [68].

Scaffold-based strategies are aimed to provide structural support for cell attachment, proliferation, and differentiation, and are often designed to mimic the ECM of the cartilage [69]. Scaffolds can be designed to incorporate bioactive molecules like growth factors such as transforming growth factor-beta (TGF-β) or bone morphogenetic protein-2 (BMP-2) to enhance tissue formation [70]. Although scaffolds provide immense promise for cartilage regeneration, there are existing challenges with biocompatibility, biodegradability, and suitable mechanical strength. Issues with biocompatibility could evoke unwanted inflammation and immune responses, while premature degradation could result in loss of mechanical support and poor load-bearing capacity, overall, compromising the long-term integrity of the scaffold [71].

### 2.4 Cartilage Bioenergetics

Given the avascular nature of AC, chondrocytes have restricted access to key metabolic substrates such as oxygen and glucose, which are obtained through diffusion from the synovial fluid. With the reduction of these substrates, chondrocytes mainly rely on anaerobic glycolysis to generate the energy necessary to maintain the structural integrity of cartilage tissue.

The low oxygen levels in the cartilage tissue, owing to the absence of vasculature, promotes the activity of anaerobic glycolysis for adenosine triphosphate (ATP) production as more than 75% of the total cellular ATP is derived from this pathway [72]. In this process, glucose is broken down into pyruvate through a series of enzymatic reactions, generating a net gain of two molecules of ATP per molecule of glucose. The end product of glycolysis, pyruvate, can either be transported into the mitochondria and converted to acetyl coenzyme A (acetyl CoA) by pyruvate dehydrogenase to enter the tricarboxylic acid (TCA) cycle, or alternatively, can be converted to lactate by lactate dehydrogenase (LDH) in order to exit the cell (Figure 2) [73].

Dysregulation of the three key glycolytic enzymes hexokinase (HK), phosphofructokinase (PFK), and pyruvate kinase (PK) have been reported in OA [72]. Hexokinase II is responsible for converting glucose to glucose-6-phosphate and is elevated in OA chondrocytes through the activation of transforming growth factor beta one (TGF-β1) [74]. PFK converts fructose 6-phosphate (F6P) and ATP into fructose 1,6-biphosphate (F1, 6BP) and adenosine diphosphate (ADP), respectively. Specifically, the expression of 6-phosphofructose-2-kinase/fructose-2,6-bisphos-phatase 3 (PFKFB3) was reported to be downregulated in human OA cartilage tissue [75]. PK catalyzes phosphoenolpyruvate to produce one molecule each of pyruvate and ATP. Pyruvate kinase M2 (PKM2) was upregulated in OA chondrocytes and facilitates LDH to transform pyruvate into lactate. This upregulation of PKM2 promotes an overexcitation of glycolysis, causing an accumulation of lactate [76] and creating an acidic environment that can inhibit chondrocytes to synthesize matrix components [77] and potentially encourage cartilage degradation in OA [76, 78]. Moreover, elevated lactate levels can induce inflammation by activating the nuclear factor kappa B (NF-κB) signalling pathway, which can lead to cell metabolism reprogramming and OA [79].

With the low levels of oxygen in the cartilage, up to 25% of total cellular ATP is produced through oxidative phosphorylation (OXPHOS) [72]. Acetyl CoA enters the TCA cycle to drive the synthesis of electron carriers NADH and $FADH_2$. Electrons derived from metabolic substrates are transferred by NADH and $FADH_2$ to the electron transport chain (ETC) to facilitate the production of ATP via OXPHOS. The energy from the electrons is used to pump protons across the mitochondrial membrane, generating a proton gradient that drives ATP synthase to produce ATP from ADP [73]. The complete oxidation of one glucose molecule through OXPHOS produces a total of 38 molecules of ATP [73].

Isocitrate dehydrogenase (IDH) is a TCA cycle enzyme responsible for oxidative decarboxylation of isocitrate to α-ketoglutarate. Interleukin-1-beta (IL-1β) induced chondrocytes displaying an osteoarthritic phenotype was reported to down regulate IDH1 and IDH2, in turn, decreasing the levels of α-ketoglutarate [80]. Supplementation of α-ketoglutarate on IL-1β induced chondrocytes alleviates OA associated metabolic dysregulation by promoting mitophagy and reducing oxidative stress, demonstrating its significance in easing OA pathogenesis [81].

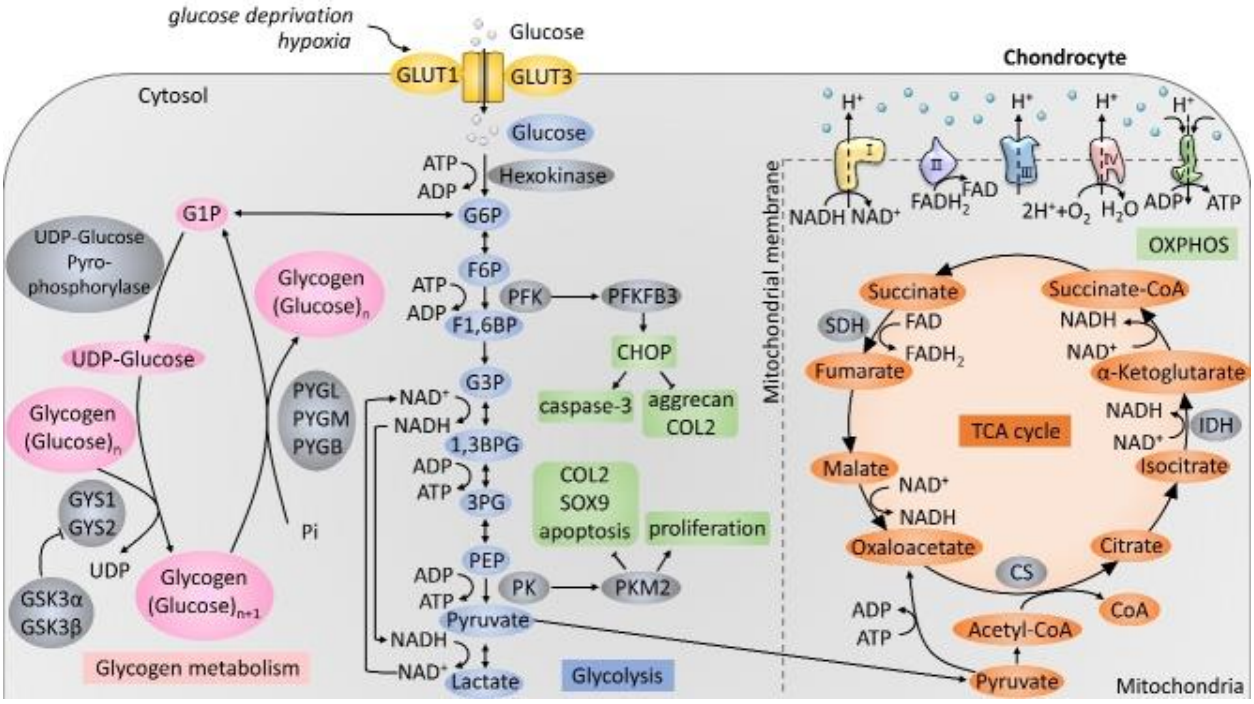


**Figure 2. Schematic representation of carbon metabolism pathways in chondrocytes.** Figure obtained from Wu et al. (2022) [72]. Used with permission under the Creative Commons Attribution license.

The choice between glycolysis and OXPHOS for ATP production is attributed to three factors: oxygen level, $NAD^+$/NADH availability, and mitochondrial function [72]. The glycolysis pathway does not require oxygen to catabolize glucose, while OXPHOS requires six molecules of oxygen to breakdown one molecule of glucose [72]. Cartilage is a relatively hypoxic tissue, as oxygen levels range from 6% on the surface to 1% in the deep zone [82], making anaerobic glycolysis the primary method for ATP synthesis. However, when chondrocytes are treated with IL-1β with sufficient oxygen, the rate of glycolysis was elevated suggesting other factors are involved in regulating glycolysis and OXPHOS balance [79]. The availability of $NAD^+$/NADH is another factor that affects this balance. In the presence of

oxygen, NADH, $H^+$, and oxygen can be used as substrates to enter OXPHOS to produce ATP [83].

However, in an oxygen deficient environment, cells cannot produce adequate energy through OXPHOS and shunts pyruvate away from the mitochondria and towards LDH [84] which catalyzes the conversion of pyruvate to lactate by utilizing the oxidation of NADH to $NAD^+$ and $H^+$. High levels of $NAD^+$ has a direct inhibitory effect on the conversion of pyruvate into lactate, while low levels of $NAD^+$ increase lactate production [85]. $NAD^+$ levels deplete with OA, pushing cells toward the glycolysis pathway and the conversion of pyruvate into lactate. Lastly, the mitochondrial function plays a significant role in regulating the glycolysis and OXPHOS pathways. Biomolecules such as glucose, amino acids, and fatty acids can be broken down in the TCA cycle and OXPHOS through acetyl-CoA, while amino acids can also be broken down into other substrates like oxaloacetate, fumarate, succinyl-CoA, and α-ketoglutarate [86, 87]. In OA, mitochondrial function in chondrocytes is impaired, causing an increase in cell death and depletion of collagen type II secretion [88, 89]. Mitochondrial dysfunction significantly impacts or completely shuts down the TCA cycle and OXPHOS (Figure 3), causing a metabolic reprogramming of the TCA cycle [72]. Moreover, this dysfunction reduces the membrane potential and the ability for pyruvate to cross the membrane [90], subsequently promoting the conversion to lactate through glycolysis in OA conditions.

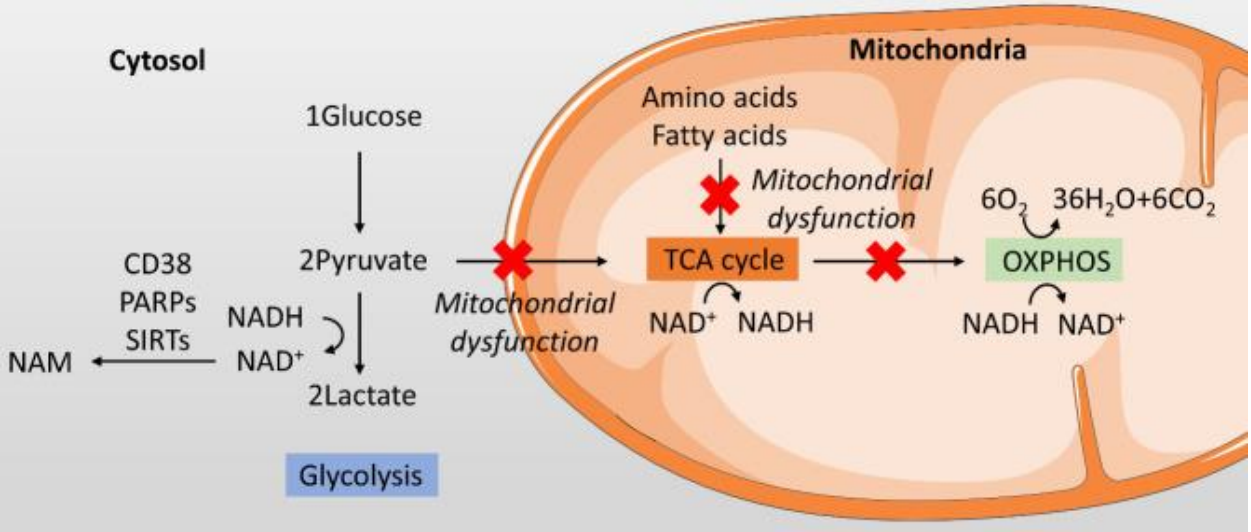


**Figure 3. Interaction between glycolysis and oxidative phosphorylation in chondrocytes.** Figure obtained from Wu et al. (2022) [72]. Used with permission under the Creative Commons Attribution license.

### 2.5 Inorganic Polyphosphate

PolyP is a linear polymer of orthophosphates linked together by high-energy phosphoanhydride bonds (Figure 4). The chain length can range from 2 to thousands phosphate residues [91]. Short-chains (60-100 phosphate residues) can be found in human platelets while long-chains occur in microbes and some mammalian cells [92]. PolyP is found in every branch in the tree of life spanning from prokaryotes to eukaryotes and is theorized to be conserved from prebiotic times [93]. PolyP has many diverse roles that are contingent upon the organism, cell type and cellular compartments the molecule is contained in, as well as the organism's need for it.

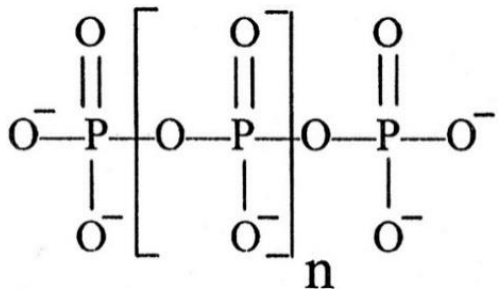

**Figure 4. Chemical structure of inorganic polyphosphate.**

2.5.1 Biological Roles of PolyP

The role of polyP is highly studied and well understood in microorganisms such as bacteria and yeast. One of its primary roles is to serve as an energy reserve during periods of stress. This is well observed in bacteria, which have shown to accumulate polyP during nutrient starvation [94, 95] by consuming ATP to create polyP granules that protect the bacteria from oxidative stress [94, 96, 97]. The yeast *C. humicola* demonstrates a similar behaviour with an increased accumulation of polyP when subjected to acidic growth conditions [98].

However, in mammalian cells, polyP is less well characterized. It has been found to act as a homeostatic regulator with its roles in mitochondrial ion transport and respiratory chain activity [99, 100]. PolyP interacts with the mitochondrial permeability transition pore (mPTP) by modifying the permeability of cations such as $Ca^{2+}$. In lower concentrations, polyP has been associated with increasing the uptake of mitochondrial $Ca^{2+}$ and decreasing the likelihood of the mPTP opening [101]. Elevated levels of polyP acts as a potent activator of $Ca^{2+}$-dependent mitochondrial permeability transition pore [101] and can potentially cause calcium dependent swelling and cell death triggered by excessive calcium influx [99, 102]. Moreover, polyP can chelate divalent cations like $Ca^{2+}$, thereby influencing its availability and transport within the mitochondria [101]. Additionally, polyP has been shown to have a direct role in influencing OXPHOS and in turn ATP production. In a study conducted by Domingues et al. [102] the

addition of polyP in mitochondria elevated the activity of complexes I-III and $F_1F_o$ ATP synthase, with longer polyP chains evoking a twice greater effect than shorter chains. By interacting with components of the respiratory chain, polyP affects the mitochondrial membrane potential, thereby influencing the efficiency of ATP production, and the mitochondrial $Ca^{2+}$-uptake capacity [101]. PolyP's involvement in these processes, helps to safeguard mitochondrial integrity, support energy metabolism, and protect cells from stress-induced damage. Although polyP has various implications in energy production, there is still limited knowledge on all its potential roles in energy metabolism in mammalian cells. Therefore, it is crucial to elucidate the metabolic relationship between polyP and other bioenergetic molecules such as glucose, lactate, and ATP.

PolyP's role in cartilage tissue is of significant interest to this project. St-Pierre et al. have previously shown the anabolic effect of polyP on in-vitro engineered and native AC grown ex-vivo. The exogenous administration of polyP to cultures of chondrocytes stimulated cartilage matrix accumulation through the elevation of sGAG and collagen levels [7]. Another study found that the intra-articular injection of polyP into the knee joint of an OA guinea pig model protected the cartilage from degenerative changes [8]. These results suggest that polyP may exert chondroprotective mechanisms such as tissue synthesis and structural maintenance of the ECM. While this biopolymer exhibits the potential as a therapeutic treatment for OA, the mechanisms to stimulate tissue repair is still unknown. For this project, we want to investigate the influence of mechanical stimulation known to elicit a catabolic response in cartilage and different culture conditions on endogenous polyP levels in cartilage.

### 2.5.2 Metabolism of PolyP

Understanding the metabolism of polyP is crucial due to its involvement in various cellular and physiological processes in prokaryotic and eukaryotic organisms. The synthesis of polyP is controlled by polyphosphate kinases (PPKs) and the vacuolar transporter chaperone complex, while its hydrolysis is mediated by exopolyphosphatases (PPXs), endopolyphosphatases (PPNs), and alkaline phosphatases (ALPs). The balance between the generation and degradation of polyP must be tightly regulated to ensure appropriate levels of phosphate for energy storage and stress response mechanisms [97, 103, 104].

The synthesis of polyP is primarily regulated by polyphosphate kinase 1 (PPK1). This enzyme is found in organisms such as bacteria, archaea, fungi, and yeast but has yet to be identified in mammalian cells [105]. PPK1 is bound to cell membranes and works to catalyze the transfer of the terminal phosphate from ATP to form ADP and a chain of polyP. ATP molecules can be used to elongate the polyP chain and once ATP levels are depleted, PPK1 releases the chain at a given length. This reversable reaction can generate polyP of various chains lengths and subsequently use these chains as a phosphate donor [106].

In eukaryotic cells, polyP synthesis is less well understood, however, the vacuolar transporter chaperone (VTC) complex in yeast has been identified to synthesize and accumulate polyP in the vacuoles. The VTC complex consists of five subunits: Vtc1, Vtc2, Vtc3, Vtc4, and Vtc5 [107]. The Vtc4 subunit facilitates the transfer of the terminal phosphate of ATP to produce polyP and ADP. Vtc4 is oriented towards the cytosol to allow it access to ATP to facilitate the elongation of polyP chains. Simultaneously, the transmembrane domains of Vtc4 creates an electropositive pathway for nascent polyP to ensure synthesis is coupled with translocation into the vacuolar lumen to prevent toxic polyP intermediates from accumulating in the cytosol [108, 109]. Once

synthesized, polyP is stored within the vacuole, it acts as a phosphate reservoir for various homeostatic functions such as osmoregulation and buffering against stress conditions. Vtc4 activity is regulated by the interaction between inositol-based signalling molecules and the SPX domain. Wild et al. [110] demonstrated that inositol pyrophosphate 5-PP-$InsP_5$ stimulates a 10 to 50-fold increase in polyP synthetase activity via SPX domain binding. Similarly, Liu et al. [109] found that PP-InsPs 5-$InsP_7$ and 1,5-$InsP_8$ positively regulates polyP synthesis when bound to the SPX domain. Although the SPX domain is highly conserved amongst eukaryotes, there is minimal research looking into its role in mammalian cells and polyP activity. This emphasizes the need to elucidate the mechanisms involved polyP synthesis and regulation in order to gain a deeper understanding of polyP's role in cellular functions and responses.

PolyP can be broken down by PPXs and PPNs to release Pi. PPX cleaves terminal phosphate residues from polyP chains releasing inorganic phosphate and shortening the chain length, while PPN cleaves internal phosphate bonds within the polyP chain [111]. PPXs are found in various organisms such as bacteria [112], archaea [113], and fungi [114] while PPNs are primarily found in eukaryotic cells and are of vacuolar origin [115]. The regulatory mechanisms of PPX and PPN are poorly understood, however, *in vitro* data suggests that PPN1 activity may be regulated by divalent cations such as $Mn^{2+}$, $Mg^{2+}$, $Co^{2+}$, or $Zn^{2+}$, while $Co^{2+}$ demonstrates the ability to enhance PPX activity [116, 117, 118]. Notably, PPX has a high affinity for long chains of polyP and a low affinity for chains shorter than 15 phosphate residues [119]. Lastly, ALP is a PPX that can catalyze the hydrolysis of phosphate esters found in polyP under alkaline conditions, releasing Pi. ALP is found in various tissues such as the bones where it has an active role in breaking down polyP during bone growth and repair [120]. It is also involved in mineral deposition by converting polyP to Pi, which replaces carbonate in amorphous calcium phosphate

where it eventually matures to hydroxyapatite [121, 122]. Mammalian ALP activity is regulated by phosphate supply and require two $Zn^{2+}$ and one $Mg^{2+}$ in the active site to facilitate enzymatic activity [123].

### 2.5.3 Characterization of PolyP

As mentioned above, polyP plays a vast range of roles in the biological functions of prokaryotic and eukaryotic organisms, requiring robust strategies to identify characteristics that are attributed to its biochemical and metabolic behaviour. However, assessing the characteristics of polyP in biological systems is challenging due to its heterogeneity in chain length which can impact the accuracy of detection methods and its highly anionic state which can lead to interactions with other cellular components, complicating purification and extraction techniques. Additionally, in mammalian organisms the levels of polyP are significantly lower than those found in bacteria and yeast [124], making it difficult to adapt quantification strategies for mammalian samples. PolyP can be analyzed and characterized based on six parameters which include the molecular structure, concentration, chain length, chain length distribution, cellular localization, and cation composition. In a review conducted by Christ et al. [125], they discuss the advantages and limitations of the various techniques to analyze the characteristics of polyP in biological samples. Below, we outline several methods currently available for characterizing polyP, which can be used to enhance our understanding of polyP's role in cartilage tissue.

#### 2.5.3.1 Methods of quantification of polyP concentration

To gain a thorough understanding of the metabolic nature of polyP, its concentration in an organism's cells, tissues, and fluids must be measured. There are several methods to measure polyP concentration which includes phosphorous nuclear magnetic resonance (P NMR) spectroscopy and enzymatic assays such as the polyphosphate kinase assay, the Christ et al.

assay [91] and Lee et al. assay [126]. P NMR is a non-destructive method that can quantitatively measure polyP concentration in samples as well as assess polyP structure, chain length, and chain length distribution. To measure polyP concentrations, the sample is dissolved in solvent and subsequently is placed in an NMR spectrometer and targets the phosophorus-31 nuclei to move these to an excited state. As the nuclei returns to their equilibrium state, they emit radiofrequency signals that are subsequently processed to generate an NMR spectrum of peaks corresponding to different phosphorus components in the sample. Within the spectrum, polyP chains can be detected at -7 ppm and -21.5 to -22.55 ppm, for molecules of 1-5 P-subunits [127, 128]. The concentration of polyP is determined by integrating the area under the resonance peaks and comparing the area to known standards. A downside of this technique is that it only detects phosphorus-containing molecules based on their bond class and cannot necessarily distinguish between polyP and other molecules containing phosphoanhydride bonds [129]. The polyphosphate kinase (PPK) assay is an enzymatic approach to quantify polyP that catalyzes the transfer of phosphate groups from polyP to ADP using PPK, generating ATP [130]. The ATP produced is quantified using a luciferase assay and provides the total concentration of polyP. This technique is highly sensitive and can detect polyP levels to the picomolar, however, it can only detect polyP with chain lengths of greater than 38 P-units. Another enzymatic technique to measure polyP concentration was created by Christ et al. [91] which uses *Saccharomyces cerevisiae* exopolyphosphatase 1 and inorganic pyrophosphatase 1 to hydrolyze polyP within samples into inorganic phosphate (Pi), which is subsequently quantified using a Pi colorimetric assay. This method not only measures total polyP concentration but also measures the average chain length by dividing the total concentration of polyP by the chain concentration. A challenge with this assay is its inability to detect and measure all forms of polyP due to exopolyphosphate

1 inability to break down cyclic polyP [91]. Lastly, a protocol developed by Lee et al. [126] leverages the use of silica spin columns to purify polyP in cartilage tissue. In this method, polyP is isolated by digesting the samples in proteinase K and loading them onto silica spin columns to adhere to the membrane. This is followed by multiple washing steps to remove contaminants. The bound polyP is then eluted and quantified fluorometrically using the fluorescence shift of 4′,6-diamidino-2-phenylindole (DAPI) when bound to polyP. A limitation of this technique is that it may not be suitable for measuring very short (less than 14 Pi residues) or very long polymers (greater than 130 Pi residues) [126].

2.5.3.2 Methods for the localization of polyP

Localizing polyP within cells and tissues can be accomplished through various microscopy and staining techniques. Light microscopy, often coupled with specific staining methods, provides a straightforward approach for visualizing polyP in biological samples. Specifically, polyP granules can be detected using stains containing methylene blue [131] by itself or in combination with a counter stain to improve the contrast between polyP granules and the cell [132, 133]. Fluorescence microscopy is another strategy that leverages fluorescent dyes like DAPI, JC-D7, and JC-D8 to localize polyP within organisms. Although traditionally used for DNA staining, DAPI concentrations between 3-50 µg/mL can be used to detect polyP [129, 134, 135]. DAPI staining is highly sensitive compared to the methylene blue-based stains [136], however, its specificity for polyP may be impacted by the presence of other polyanionic molecules. Fluorescent probes JC-D7 and JC-D8 created by Angelova et al. [137], offers improved polyP-binding specificity as it can bind to polyP without the interference of other biomolecules such as RNA. These dyes are suitable for live imaging due to their low toxicity compared to DAPI and exhibit high sensitivity for detecting polyP concentrations as low as 10

μM. Lastly, Raman spectroscopy offers a non-destructive and label-free method to detect polyP with high chemical specificity. The Raman spectrum of polyP has a strong peak between 1145–1177 $cm^{-1}$ which corresponds to $PO_2^-$ groups and a weaker peak between 682–700 $cm^{-1}$ corresponding to the P–O–P stretches of the phosphate ester linkages [138, 139, 140]. This strategy can be combined with confocal microscopy to localize polyP in relation to other biomolecules to gain insights on temporal and spatial dynamics [140, 141].

2.5.3.3 Methods for the evaluation of polyP chain length

Assessing the chain length of polyP can be accomplished through several techniques such as gel electrophoresis and end group titration. Polyacrylamide gel electrophoresis (PAGE) can be used to evaluate the average polyP chain length and chain length distribution of samples [125]. In this technique, polyP samples are loaded onto a polyacrylamide gel and subjected to an electric current to migrate the chains through the gel. The gel is then stained with a dye that specifically binds to polyP such as toluidine blue O or DAPI, neither of which can detect short polyP chains, subsequently skewing the average chain length and distribution to be larger. PolyP chain lengths can be estimated using polyP standards with known lengths or DNA ladders [142]. Another method to evaluate polyP chain length is end group titration, which estimates the average chain length by measuring the concentration of the end groups and dividing the value by the total concentration of phosphate in the sample. To accomplish this, polyP is hydrolyzed to release the terminal phosphates which are subsequently titrated to determine the concentration of the end groups. The total phosphate concentration is determined through a colorimetric assay. Although end group titration is one of the most used strategies for determining average polyP chain length, it requires the samples to be high in purity for accurate quantification.

# MATERIALS AND METHODOLOGY

## 3.1 Primary Bovine Chondrocyte Extraction

Full thickness cartilage tissue was excised sterilely from the metacarpal-phalangeal joints of cattle obtained from a local abattoir (Tom Henderson Meats & Abattoir) within 24 hours of death. The tissue was cultured in Dulbecco's modified Eagle medium (DMEM; 4.5 g/L glucose) supplemented with 1% antibiotic-antimycotic and kept in a cell incubator for three days at 37℃ at 5% $CO_2$. Cartilage tissue was then enzymatically digested by incubation with 0.2% (w/v) pronase protease (EMD Millipore) for 2 hours, followed by washing of the tissue three times with fresh DMEM and incubation with 0.1% (w/v) collagenase type I (Sigma-Aldrich) in 4.5g/L glucose DMEM for 48 hours to release chondrocytes. After digestion, the cell suspension was filtered through a 100 μm diameter cell strainer to remove undigested tissue. The cell suspension was then centrifuged to obtain a cell pellet and the supernatant containing collagenase was removed and the chondrocytes were resuspended in fresh DMEM. This washing step was repeated two more times, cells were counted and resuspended at a concentration of $2 \times 10^6$ cells per mL in Ham's F12 supplemented with 5% fetal bovine serum (FBS) and 100 units/mL penicillin, 100 units/mL streptomycin, and 250 ng/mL amphotericin B (1% antibiotic-antimycotic; Gibco).

## 3.2 3D Cartilage Tissue Constructs Culture

Millicell Cell Culture Inserts (EMD Millipore; hydrophilic PTFE membrane, diameter = 12 mm, pore size = 0.4 μm) were coated with 50 μg collagen type II from chicken sternal cartilage (Sigma-Aldrich) dissolved in 0.1 N acetic acid. The inserts were dried sterilely for 24 hours and subsequently underwent 15 minutes of UV radiation. Chondrocytes were seeded at a density of $1 \times 10^6$ cells per insert and cultured in Ham's F12 supplemented with 5% FBS and 1% antibiotic-

antimycotic. On day 5 after seeding, the culture media conditions were changed based on the experiment. To determine the impact of media and media supplements on endogenous polyP production, 4 media conditions were assessed: (i) DMEM with pyruvate and L-glutamine supplemented with 10% FBS, (ii) Ham's F12 with L-glutamine supplemented with 10% FBS, (iii) DMEM with pyruvate and L-glutamine supplemented with 1% insulin-transferrin-selenium (ITS), and (iv) Ham's F12 with L-glutamine supplemented with 1% ITS. Subsequent experiments were cultured in DMEM with pyruvate and L-glutamine supplemented with 10% heat-inactivated FBS. All culture media conditions were also supplemented with 1% antibiotic-antimycotic, and 100 μg/mL ascorbic acid. Medium was changed every 2-3 days throughout the culture period.

### *3.2.1 Application of Static Compression*

Select tissue constructs were grown in culture in DMEM supplemented with 10% heat-inactivated FBS, 1% antibiotic-antimycotic, and 0.2% ascorbic acid for 7 days to allow for some tissue growth, then stainless steel support disks were placed underneath each insert and stainless steel weights eliciting a force of 17 mN or 32 mN were placed on top of tissues. The cultures underwent static compression sessions for 3 hours per day, 5 days per week, for 3 weeks. Control tissues were cultured in absence of weights throughout the culture period.

### *3.2.2 Administration of Exogenous Inorganic PolyP and Phosphate*

Select tissue constructs were also grown in DMEM supplemented with 10% heat-inactivated FBS, 1% antibiotic-antimycotic, and 0.2% ascorbic acid for 4 days. On day 1 and 3 of culture, tissue constructs were treated with 1 mM of polyP or 1 mM of Pi suspended in the media composition above. Control tissues were cultured with no exposure to polyP or Pi. Cell viability under each condition was assessed 24-hours after the last media change.

## 3.3 Biochemical Composition of Cartilage Constructs

### *3.3.1 Water Content of 3D Cartilage Tissue Constructs*

In vitro-formed cartilage tissues were harvested and washed in phosphate buffered saline (PBS). Excess liquid was removed by gently applying absorbent paper on the tissues and the tissue wet weight measured using an electrical balance (AB204-S/FACT; Mettler Toledo). The tissues were then frozen at -80°C, lyophilized (FreeZone Plus 6; Labconco) over a 24-hour period and weighed again to determine the dry weight. Water content was calculated as a percentage of wet weight based on the difference between the wet and dry weights.

### *3.3.2 Papain Digestion*

In vitro-formed tissue samples were digested with 40 µg/mL papain (Sigma-Aldrich) in a buffer containing 5 mM cysteine HCl and 5 mM EDTA at pH = 6.2 for 48 hours at 65°C. Papain digests were kept at -20°C until further analysis.

### *3.3.3 DNA Content*

DNA content of the papain digests was measured using the Quant-IT PicoGreen assay kit (Invitrogen) according to the manufacturer's instructions and a Synergy H1 plate reader (Biotek). Fluorescence was measured at excitation and emission wavelengths of 480 and 520 nm, respectively. Lambda DNA was utilized to generate a standard curve and used to calculate the amount of DNA in the samples.

### *3.3.4 Sulfated Glycosaminoglycan Content*

Sulfated glycosaminoglycan (GAG) content of the papain digests was measured using a 1,9-dimethylmethylene blue (DMMB) binding assay [143]. The papain digests were diluted appropriately using PBS and 10 µL of diluted sample was mixed with 200 µL DMMB solution (16 µg/mL DMMB in a buffer containing 40 mM glycine, 40 mM NaCl at pH = 1.5). Of note,

DMMB was first dissolved at 1.6 mg/mL in 95% ethanol, prior to addition to the buffer. Chondroitin sulfate was utilized to generate a standard curve. Absorbance was read at 525 and 595 nm using a Synergy H1 plate reader, and the ratio of the two readings was used to determine the amount of sulfated GAG in each sample. Sulfated GAG content was normalized per mg of dry weight or to DNA content and expressed as µg/mg of dry weight and µg/µg DNA, respectively.

### *3.3.5 Collagen Content*

The collagen content of the papain digests was quantified by measuring the hydroxyproline content [144]. Papain digests were aliquoted in Pyrex tubes in volumes of 100 µL and subjected to acid hydrolysis by adding an equal volume of 6N HCl and incubating at 110°C for 18 hours. The hydroxylates were cooled, centrifuged, and neutralized by adding 100 µL of 5.7N NaOH. Samples were diluted with distilled water and 120 µL aliquots were prepared for each sample. To each aliquot, 60 µL of 0.05N Chloramine T was added and incubated at room temperature for 20 minutes, followed by 60 uL of 3.15N perchloric acid and an incubation at room temperature for 5 minutes. Lastly, 60 uL of 0.2 g/mL Ehrlich's reagent in 2-methoxyethanol was added and the solution incubated at 60°C for 20 minutes. The resulting samples cooled and the colour change was quantified by measuring the absorbance at 560 nm with a Synergy H1 plate reader. L-hydroxyproline was utilized to generate a standard curve and estimate the amount of collagen in the samples. Collagen content was normalized per mg of dry weight or to DNA content expressed as µg/mg of dry weight and µg/µg DNA, respectively.

## 3.4 Histology

Histology was performed by the Louise Pelletier Histology Core Facility at the University of Ottawa. In vitro-formed tissue samples were fixed in 10% formalin for 72 hours at room

temperature and transferred into 70% ethanol. The tissues were then embedded in paraffin and then sectioned into 4 µm thick sections. Sections were dewaxed in xylene and subsequently rehydrated by replacing xylene with ethanol and ethanol with distilled water. Sections were then stained with Hematoxylin and Eosin (H&E) , Alcian blue (AB), and Picosirius Red (SR). The tissues samples were observed using an Axio Scan.Z1 microscope with a Plan-Apochromat 20X objective lens and a brightfield channel.

## 3.5 Quantification of Metabolites in Cartilage Tissue and Culture Media

### *3.5.1 Glucose Content in Culture Media*

Media samples were collected at the time points of 3 hours, 6 hours, 24 hours, 48 hours, and 72 hours from the last media change on day 14 of culture and kept at -20°C until analysis. The glucose content was measured using a spectrophotometric hexokinase (HK) assay [145]. Media samples were diluted with PBS and 20 µL aliquots were mixed with 100 µL HK assay reagent (1.12x Tris $MgCl_2$ at pH = 7.5, 50 U/mL hexokinase, 50 U/mL glucose-6-phosphate dehydrogenase, 20 mg/mL NAD, and 44 mg/mL ATP). The solutions were incubated for 15 minutes at room temperature and the absorbance was read at 340 nm with a Synergy H1 plate reader. DMEM was diluted in 1x PBS was used to generate a standard curve and calculate the g/L glucose content in the samples. The glucose consumption rate over the 72 hours after a media change was calculated by normalizing the glucose consumed over time by the DNA content and expressed as ug/ ug DNA/hr.

### *3.5.2 Lactate Content in Culture Media*

The levels of lactate were also measured in media samples collected as detailed in 3.5.1. A colorimetric L-Lactate Assay Kit (Sigma) was used to measure the lactate concentration in the samples based on the principle that lactate dehydrogenase oxidation of lactate produces NADH,

which in turn reduces MTT into formazan, according to the manufacturer's instructions. Samples were diluted using distilled water and a 16 µL aliquot was mixed with 64 µL of reaction mix. The absorbance was immediately read at 565 nm with a Synergy H1 plate reader (initial absorbance) and left to incubate at room temperature for 20 minutes. After incubation, the plate was read again at 565 nm to measure the final absorbance. A standard curve was prepared by diluting 1 mM L-lactate in DMEM. The difference between the initial and final absorbance readings was used to calculate the lactate concentration in the media samples. The lactate concentration was expressed as mM and the lactate released from the tissues was expressed as mmol/well. Lactate content was also assessed as a ratio of glucose consumed and is expressed as mmol lactate/mmol glucose.

*3.5.3 PolyP Content in Cartilage Tissues and Culture Media*

Quantification of polyP was performed with modifications to the protocol by Lee et al. (2018) [126]. In vitro-formed tissue samples were harvested and digested in 1 mg/mL proteinase K in a buffer containing 10 mM EDTA and 10 mM Tris at pH = 8, with 10 µL of proteinase K solution added per mg of tissue wet weight. Media samples were also digested in a 1:1 ratio (v/v) in 2 mg/mL proteinase K in a buffer solution with 20 mM EDTA and 20 mM Tris at pH = 8. Both the tissue and media samples were digested for 2 hours at 56°C to release the polyP. Each sample was mixed well then divided into two 85 µL aliquots. To one of the two aliquots, 7 nmol of polyP was added (85 µL 50 µM polyP; 'spiked'), while the second aliquots received 85 µL of distilled water ('non-spiked'). Samples were then incubated for another 2 hours at 56°C. Following incubation, the digests were combined with 280 µL of binding buffer solution (5 M guanidine thiocyanate, 0.9 M sodium acetate, 25 mM EDTA, 1% β-mercaptoethanol, 50 mM Tris, pH = 6.8) and incubated at room temperature for 10 minutes. Subsequently, 280 µL of 100% ethanol was added and the

mixture was incubated at room temperature for 3 minutes. The samples were loaded onto silica spin columns (Epoch Life Science) to adsorb the polyP. The columns were then washed once with 550 µL wash buffer I (1.0 M guanidine thiocyanate in 80% ethanol), twice with 550 µL and 300 µL wash buffer II (150 mM sodium chloride and 10 mM Tris in 80% ethanol pH 7.5) and eluted with 180 µL elution buffer (10 mM Tris pH 7.2). The eluent was digested with 10 U DNase I (Millipore Signma) and 2.5 U RNase A (Millipore Sigma) in a nuclease buffer (100 µM calcium chloride; 1 mM magnesium chloride; 50 µg/mL bovine serum albumin; 10 mM Tris, pH 7.5) to remove unwanted fluorescence from nucleic acids. Tris solution (3 M, pH = 7.5) was subsequently added to achieve a final concentration of 500 mM in each sample to eliminate the unwanted fluorescence contributed by chondroitin sulfate. Aliquots of 20 µL were mixed with 50 µL of DAPI (50 µg/mL) and incubated at room temperature for 5 minutes. PolyP was quantified by measuring the fluorescence with a Synergy H1 plate reader at excitation and emission wavelengths of 415 nm and 558 nm, respectively. A polyP standard curve was generated (1-80 µM) to determine the concentration of polyP in nmol/construct, nmol/µg DNA, nmol/µg sGAG and nmol/mg of wet weight for the tissue samples and nmol/mL for media samples.

### *3.5.4 Cell Viability in Cartilage Tissues*

Cell viability was evaluated on a fluorescent and colorimetric basis using the Alamar Blue assay. Fresh media corresponding to each of the conditions outline in 3.2.2 was prepared and supplemented with 10% Alamar Blue cell viability reagent. To the outside of each insert, 500 µL of the media with Alamar Blue was added and an additional 500 µL was dispensed inside of the insert. A blank for each media condition, which are inserts with no cells, are exposed to Alamar Blue in the same manner as the samples. All the samples and blanks were incubated at 37ºC for 1 hour, where the spent media inside and outside of the insert was collected and thoroughly mixed.

Once the samples were collected, 100 µL was dispensed in triplicates in a black 96-well plate to measure fluorescence which as read at excitation and emission wavelengths of 560 nm and 590 nm, respectively using a Synergy H1 plate reader. The remaining spent media for each condition was loaded in 100 µL triplicates onto a clear 96-well plate to measure absorbance at 570 nm and 600 nm using a Synergy H1 plate reader. Background fluorescence and absorbance were removed by subtracting the values from the samples by the blanks. The fluorescence readings and the ratio of the two absorbance readings were used to determine the percent cell viability compared to controls.

## 4 Statistical Analysis

Experiments were conducted at least two times with cells extracted from different animals. Statistical significance between the means of three or more groups was evaluated using one-way analysis of variance (ANOVA) with Tukey's Post hoc test for pairwise comparisons ($p \leq 0.05$). Two-way and three-way ANOVAs were used to evaluate the statistical significance of two variables, three variables, two-way interactions, and three-way interactions on the outcomes. To assess the statistical significance of experiments with two groups, t-tests were conducted ($p \leq 0.05$). Data are represented as means ± standard deviation.

# RESULTS AND DISCUSSION:

## 5.1 Effect of media and media supplement on endogenous polyP accumulation

In order to gain an understanding of the metabolic behaviour of polyP in chondrocytes, we must first determine whether chondrocytes can independently produce the molecule or if it is uptaken through its environment. To investigate this question, we needed to create a culture environment where polyP is and is not present and quantify the accumulation of polyP in the tissue and changes in its levels in the media. In this study, we utilized fetal bovine serum (FBS) as our polyP-containing supplement and insulin-transferrin-selenium (ITS) as our non-polyP-containing supplement, both of which are commonly used medium supplements for chondrocyte cultures. Additionally, DMEM and Ham's F12 were both compared to investigate the impact of the base medium on endogenous polyP production and determine if media composition (Appendix I) could impact polyP metabolism in chondrocytes.

To test the effect of different media and supplement combinations, we measured the levels of polyP in the tissue constructs and spent media 72 hours after the last media change on day 14 across the four conditions detailed in the methods, namely DMEM/FBS, DMEM/ITS, F12/FBS, and F12/ITS. Among the conditions, tissue constructs grown in DMEM/FBS had the highest levels of polyP followed by DMEM/ITS, F12/FBS, and F12/ITS (Figure 5A). Significant differences compared to DMEM/FBS were observed for the F12/FBS ($p<0.05$) and F12/ITS ($p<0.01$) conditions. A three-way ANOVA was conducted to determine the impact of media, media supplements, sets (with each set representing three independent tissue replicates prepared with cells from a distinct cell extraction), two-way interactions, and three-way interactions on endogenous polyP production. Media ($p<0.001$), media supplements ($p<0.001$), and sets ($p<0.001$) independently have a significant impact on polyP accumulation.

PolyP was also quantified in the media to determine if a portion of the synthesized polyP from tissue constructs is released. No significant differences in the levels of polyP were detected between conditions (Figure 5B). A three-way ANOVA determined that independently, media ($p<0.05$) contributes significantly to polyP release. Additionally, the two-way interaction between the media and sets ($p<0.05$) and the three-way interaction between media, media supplements, and sets ($p<0.01$) significantly influences polyP retention in the tissue.

The ability of chondrocytes to independently synthesize polyP is not well understood. However, detectable levels of polyP quantified in the conditions supplemented with ITS suggests that chondrocytes can produce polyP, as it is not supplied from the environment under these conditions. Once we established chondrocyte's ability to independently produce polyP, we wanted to understand the impact of different types of cell culture mediums such as DMEM and Ham's F12 on polyP levels. The influence of culture medium could be significant due to the differences in cell growth in tissues formed under each condition and/or their differing tissue compositions, which could affect retention rather than synthesis. Although DMEM and Ham's F12 are both widely used in cell culture practice, they have distinct formulations that can influence cell metabolism and behavior. DMEM is enriched with glucose, amino acids, and vitamins, making it suitable for a broad range of cell types, especially those requiring higher glucose levels for optimal growth. Specifically, the 4.5 g/L glucose concentration can support high energy demands by converting glucose into ATP through glycolysis, where the subsequent ATP can be potentially used to synthesize and accumulate polyP as an energy reserve [146]. In contrast, Ham's F12 medium includes a more diverse array of components such as additional trace elements like zinc and thymidine that are not found in DMEM [147]. This complexity allows Ham's F12 to support the growth of more fastidious cell types, potentially affecting polyP

metabolism differently by providing a more complex nutrient environment than DMEM. These differences between Ham's F12 and DMEM underline the importance of selecting the appropriate medium based on the specific needs of the cell type and the metabolic pathways under investigation, especially when studying polyP dynamics and its role in cellular processes.

The use of serums in cell culture provides distinct nutrients, growth factors, and hormones, that may influence the metabolism of polyP. FBS is a rich source of growth factors and hormones that can influence and stimulate cellular activity differently compared to ITS which has a minimal composition of insulin, transferrin, and selenium. Studies investigating the influence of serums on metabolic pathways can provide us with indirect evidence of their impact on polyP metabolism. For example, it has been found that FBS can contain 300-1300 pmol/L of ATP [148], and when these levels are introduced to the culture media could serve as a reservoir for polyP production. On the other hand, the supplementation of ITS introduces insulin into the culture medium, which may alter glucose metabolism differently, leading to variations in ATP levels and subsequent polyP levels.

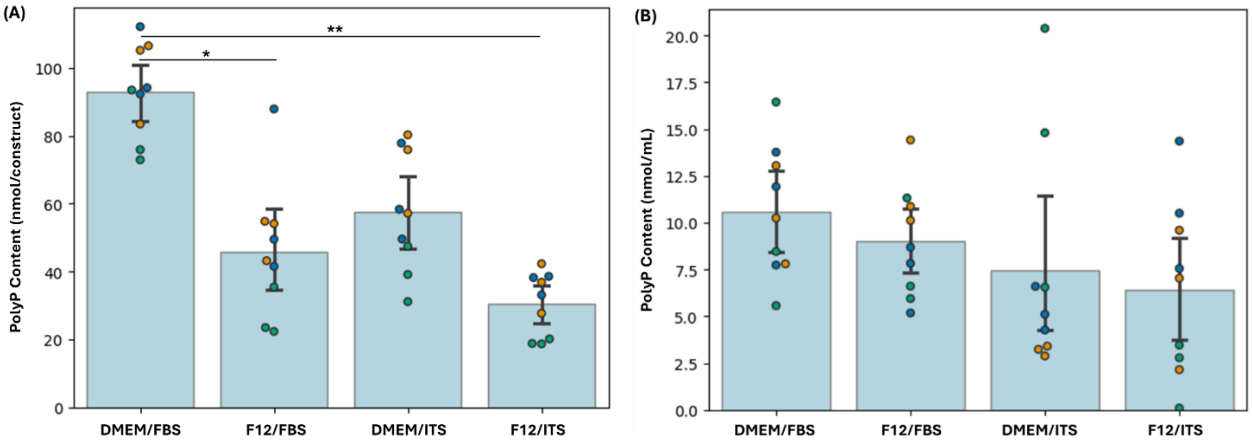


**Figure 5. (A)** Total polyP content in cartilage constructs and **(B)** media on day 14 72 hours after media change. Experiments were repeated 3 times with cells isolated from different animals and are represented by data points in different colours. Data are represented as mean ± SD. Statistically significant differences between the groups is denoted by * ($p<0.05$) and ** ($p<0.01$).

To standardize and reduce the variability between each experiment repeat and address the potential for the effects observed above to be caused by the number of cells in each tissue and by matrix retention, polyP levels were normalized to wet weight, DNA, and sGAG content (Figure 6). When normalized to wet weight (Figure 6A), polyP levels among the four conditions followed a similar trend reported in Figure 5A, with only a significant difference between the DMEM/FBS and F12/ITS groups ($p<0.05$). However, when normalized to sGAG, we observe a significant increase in polyP to sGAG ratio in the FBS conditions compared to the ITS conditions (Figure 6C). A three-way ANOVA validated that the media supplement has the most significant impact ($p<0.001$) on the polyP to sGAG fraction, however, the two-way interactions between media and media supplement ($p<0.05$) as well as media and sets ($p<0.05$) also contribute to the patterns observed.

These results demonstrate that the amount of polyP produced in relation to cell growth can be influenced by the media composition. Above, we discussed how components such as glucose and

ATP could indirectly impact polyP accumulation. The choice of media and media supplement could influence the nutrient availability in the culture medium, and subsequently promote pathways that favour cell division or proteoglycan synthesis. Figure 6B demonstrates that polyP is synthesized at ratios greater than 1 across all four conditions. Interestingly, the polyP to DNA ratios in the DMEM conditions are 25% greater than the F12 conditions, suggesting the polyP production per cell is influenced by media type. These elevated ratios may be attributed to the differences in glucose concentration between DMEM and F12, as the concentration in DMEM is 2.5 times greater than F12. This difference could provide chondrocytes with more substrate to produce greater concentrations of ATP, which could be subsequently used to accumulate more polyP in tissue constructs grown in DMEM as opposed to F12. Regarding the polyP to sGAG ratios, we observe a 2-3 times elevation in the conditions supplemented with FBS compared to ITS. FBS has been found to suppress TGF-β1 [149] which is one of the crucial growth factors responsible for ECM production. This activity suggests that sGAG levels in the conditions supplemented with FBS would likely be lower than the ITS conditions, and when normalized to the amount of polyP would result in higher ratios of polyP to sGAG. This effect of media supplements on ECM synthesis could explain the differences seen in the polyP to sGAG ratios and that there may not be a link between ECM and polyP synthesis.

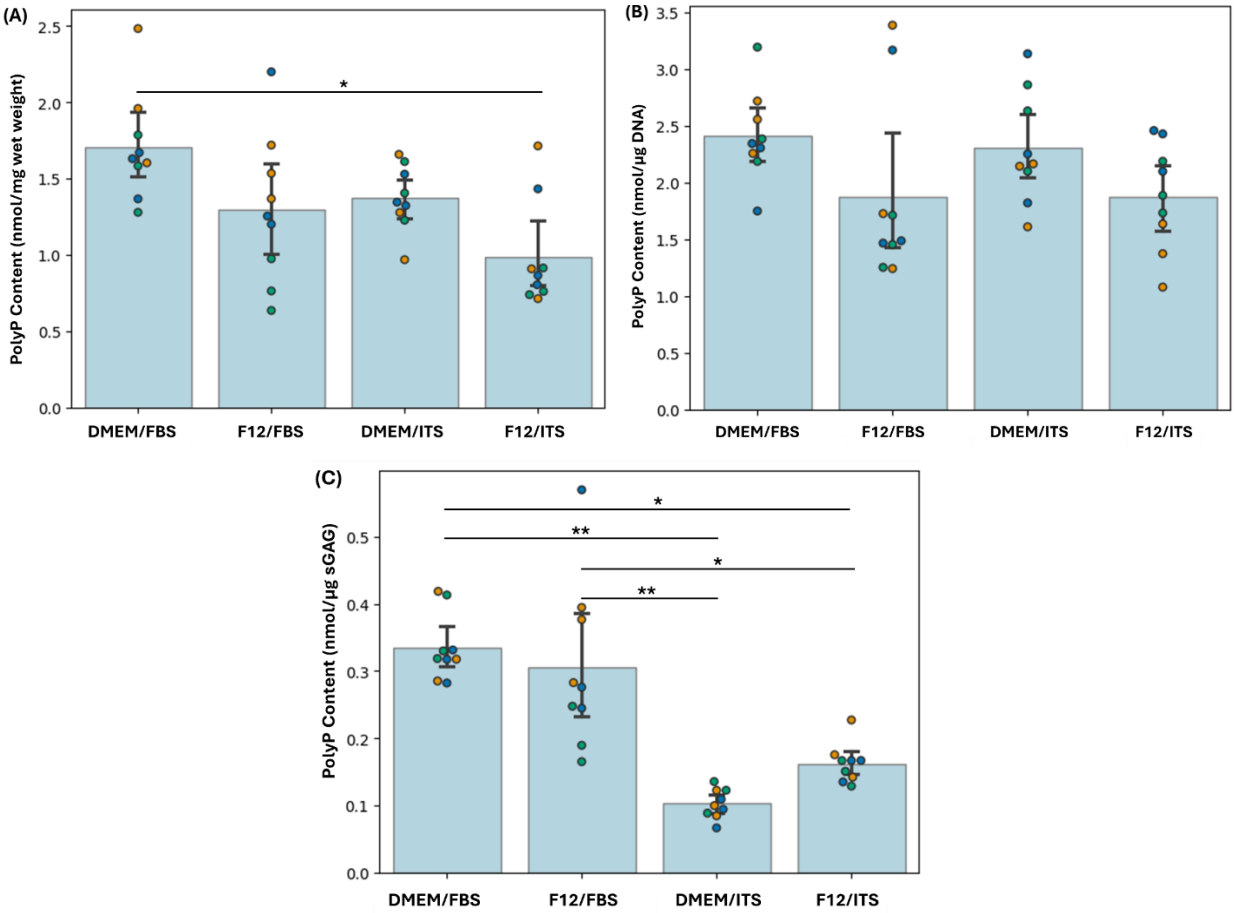


**Figure 6. (A)** Total polyP content of cartilage constructs normalized to wet weight, **(B)** DNA, and **(C)** sGAG on day 14 72 hours after media change. Experiments were repeated 3 times with cells isolated from different animals and are represented by data points in different colours. Data are represented as mean ± SD. Statistically significant differences between the groups is denoted by * ($p<0.05$) and ** ($p<0.01$).

To better understand the trends from the normalized polyP data, we evaluated how the media conditions impact the levels of DNA and sGAG independently, as well as the ratio of sGAG to DNA. Looking at the DNA levels (Figure 7A), we see a significant decline in the F12/ITS condition compared to the DMEM/FBS condition ($p<0.05$), while DNA content between F12/FBS and DMEM/ITS is intermediate and comparable. Independently, media ($p<0.001$), media supplements ($p<0.001$), and sets ($p<0.001$) have a significant effect on the levels of DNA.

Regarding sGAG content (Figure 7B), all the conditions compared to the DMEM/ITS group are significantly lower. Media ($p<0.001$), media supplements ($p<0.001$), sets ($p<0.001$), and all two-way interactions such as media:media supplements ($p<0.001$); media:sets ($p<0.01$); media supplements:sets ($p<0.01$) have a significant impact on sGAG production. When we take the ratio of sGAG to DNA (Figure 7C), the ITS conditions, namely, the DMEM/ITS group is significantly higher compared to three other conditions of F12/ITS ($p<0.01$), DMEM/FBS ($p<0.01$), and F12/FBS ($p<0.001$). Statistically analyses indicate that media ($p<0.001$), media supplements ($p<0.001$), and the interaction between the two factors have a significant effect ($p<0.001$) on the amount of sGAG produced per cell.

As discussed above, the differences in nutrient composition of DMEM and Ham's F12 can lead to variations in cellular activity such as cell proliferation and ECM production. DMEM can provide ample energy for cell growth and division, potentially resulting in higher DNA synthesis rates compared to media with lower glucose concentrations or different formulations like Ham's F12. However, studies have demonstrated that high glucose levels can evoke inflammatory responses that can subsequently impede chondrocyte proliferation [150, 151]. This suggests that glucose may promote rapid cell division in the beginning by supplying the cells with an abundant substrate for ATP production. However, over time, advanced glycation end-products (AGEs) which are proteins or lipids that become glycated because of high glucose exposure can arise and trigger various cellular changes such as inflammation, ECM degradation, and chondrocyte apoptosis [151, 152].

Glucose metabolism also plays an active role in GAG formation. Glucose is converted to glucose-6-phosphate then to glucose-1-phosphate, which combines with uridine triphosphate (UTP) to form uridine diphosphate-glucose (UDP-glucose). UDP-glucose is converted further

into UDP-glucuronic acid which is the precursor for the synthesis of GAGs [153]. Since glucose metabolism and GAG production are linked, the glucose concentration will likely have a direct impact on the amount of GAG the chondrocytes produce. It is assumed that the higher the glucose concentration the more sGAG will be produced per cell, which aligns with the results presented in Figure 7C with the DMEM/ITS condition having the highest ratio of sGAG secreted per cell. Interestingly, literature has shown excessive levels of glucose depleting GAG concentrations [154, 155].

Another media component that is attributed to chondrocyte proliferation and matrix synthesis is glutamine. In a study conducted by Stegen et al. [156], they determined that glutamine-derived aspartate is crucial for DNA replication and protein synthesis in chondrocytes. Since the concentration of glutamine is four times higher in DMEM than in Ham's F12 [157, 158], it is possible that the combination of elevated glutamine and glucose levels in DMEM influenced both the rate of cell proliferation and sGAG production.

Regarding the influence of additives such as FBS and ITS, there have been various comparative studies looking at their influence on cell proliferation and ECM synthesis. Lui et al. [159] found that ITS can support DNA synthesis and cell growth effectively but could not achieve the same level of proliferation as FBS. A potential explanation for this may be that FBS is rich in nutrients, growth factors, and hormones which support cell growth and proliferation, leading to increased levels of DNA.

Looking at the sGAG content (Figure 7B) and sGAG to DNA ratio (Figure 7C), we see a significant elevation in the DMEM/ITS condition compared to other medium conditions suggesting composition of DMEM and ITS plays an important role in promoting GAG synthesis. Above, we discussed the potential media components of DMEM that could be involved in

promoting GAG production such as glucose and glutamine which have greater concentrations than Ham's F12. The influence of additives on GAG production could be explained by a study conducted by Bilgen et al. [149] which observed significantly lower GAG amounts and GAG to DNA ratios in cells cultured in 10% FBS compared to 1% ITS, which is consistent with the results we obtained. They found that FBS suppressed the activity of TGF-β1 which is responsible for stimulating chondrocyte proliferation and ECM formation [160]. This depletion in TGF-β1 could be a possible justification for the depletion in the GAG and GAG to DNA ratio in the FBS condition. On the other hand, ITS has been found to upregulated TGF-β1 [161] activity which could explain the 2-3 fold GAG increase in the DMEM/ITS condition compared to the other media combinations.

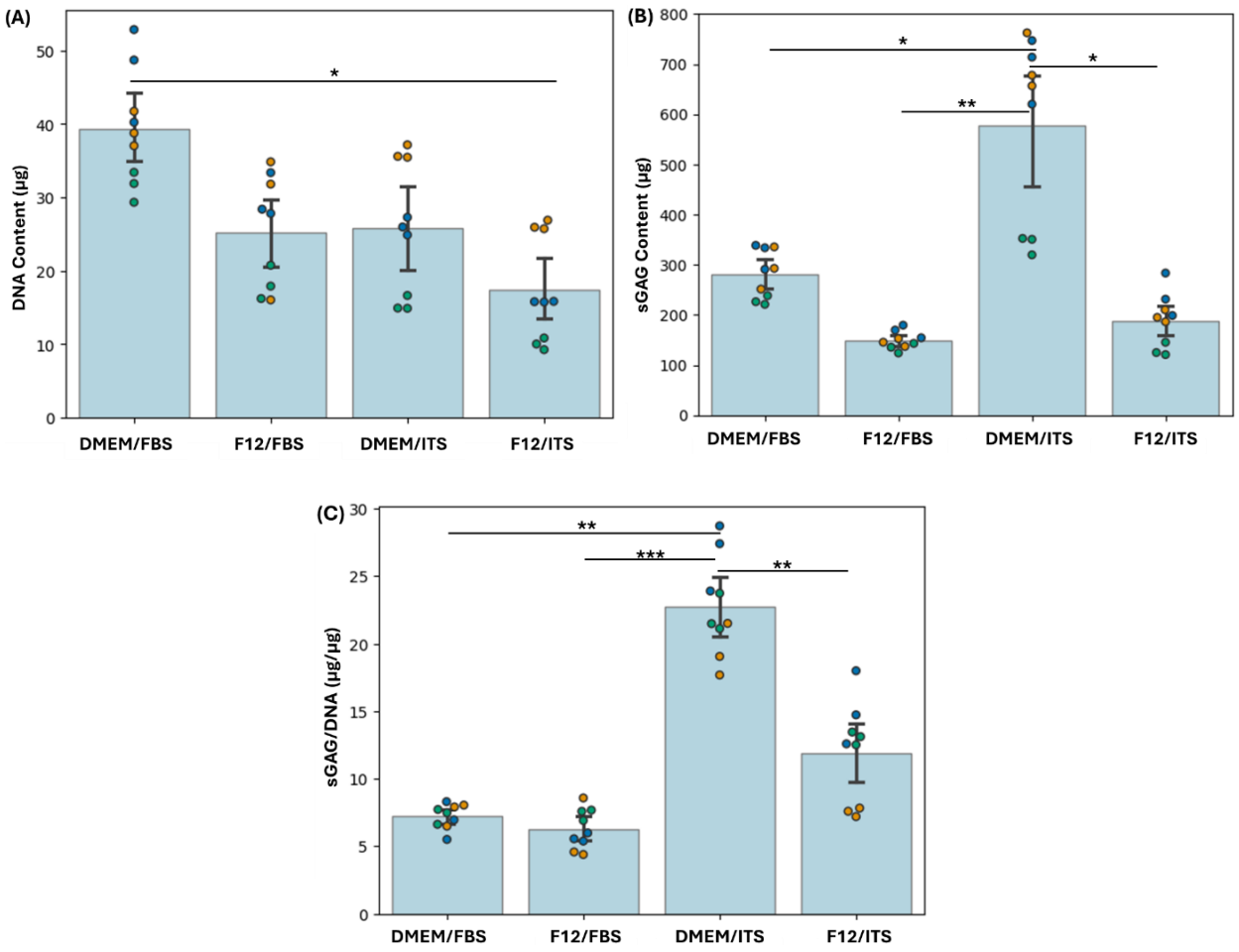


**Figure 7. (A)** DNA content, **(B)** sGAG content, and **(C)** sGAG to DNA ratio of constructs on day 14 72 hours after media change. Experiments were repeated 3 times with cells isolated from different animals and are represented by data points in different colours. Data are represented as mean ± SD. Statistically significant differences between the groups is denoted by * ($p<0.05$), ** ($p<0.01$), and *** ($p<0.001$).

Histological assessment of the tissue constructs was conducted to visualize the morphological differences between the conditions. The tissues were harvested on day 14 and stained with Picrosirius red (SR), Hematoxylin and Eosin (H&E), and Alcian blue (AB) to detect the collagen, nuclei and ECM, and sGAG, respectively (Figure 8). The relative thickness of the tissue constructs was similar across all conditions, however, there are variations in staining

intensity. H&E staining had the highest intensity in the DMEM/FBS condition followed by F12/FBS and DMEM/ITS; which have similar staining intensities, and F12/ITS conditions. These qualitative observations support the quantitative findings in Figure 7A. Moreover, tissues grown in the ITS conditions have a more uniform distribution than tissues grown in FBS. Interestingly, the AB staining intensity appears to be the most abundant in the F12/FBS condition, although quantitatively the DMEM/ITS condition was recorded to have the greatest sGAG content. This discrepancy between the quantitative and qualitative findings may be due to the non-uniform distribution of sGAG localized in the histology image. The section taken may illustrate a greater concentration of sGAG; however, it may not be representative of the whole tissue, therefore resulting in variations between the qualitative and quantitative evaluations.

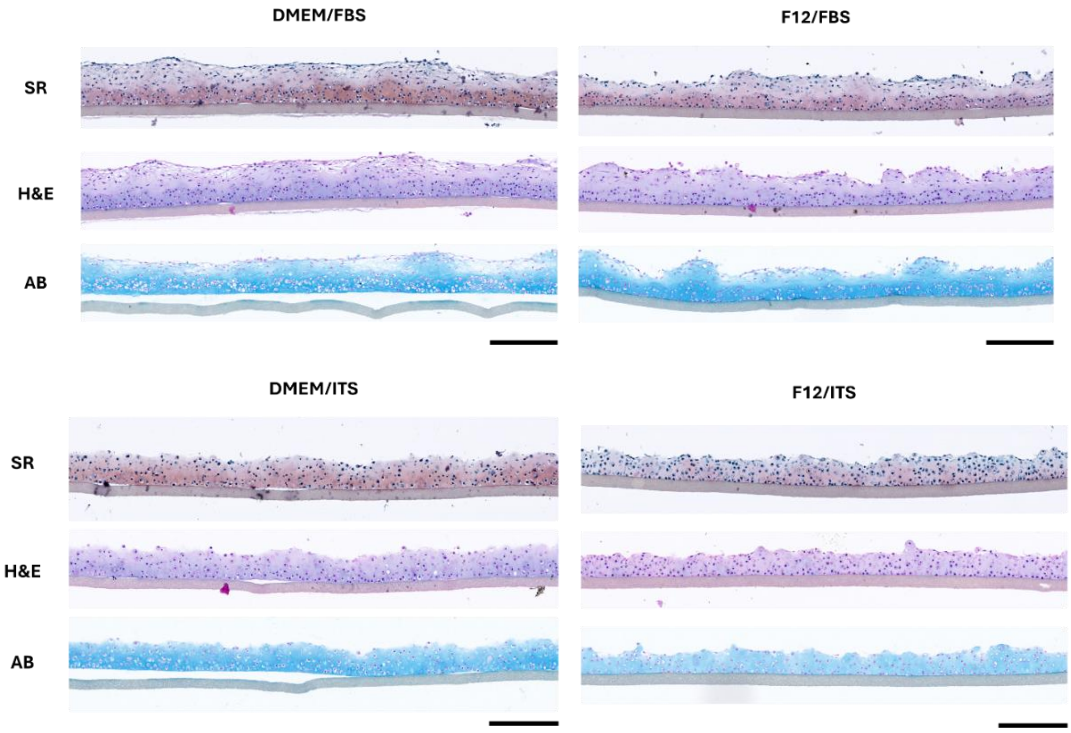


**Figure 8.** Histological sections of cartilage constructs grown in DMEM/FBS, F12/FBS, DMEM/ITS, and F12/ITS stained with Sirius Red (SR), Hematoxylin and Eosin (H&E), and Alcian Blue (AB) on day 14. Scale bar = 200 µm.

Due to the unexpected result of elevated sGAG levels in the DMEM/ITS condition, we wanted to investigate if a potential trend existed between the conditions, wet weight, and amount of polyP accumulated in the tissue constructs. This hypothesis is motivated by a previous study conducted by St-Pierre et al. [7], where the exogenous administration of polyP resulted in a stimulatory effect on matrix accumulation, indicating increased production of polyP could increase sGAG levels and in turn the weight of the tissue. When we plotted the wet weight against the amount of polyP per tissue construct, we generally see a positive correlation between the two variables (Figure 9). Among the conditions, DMEM/ITS has the strongest linear relationship ($R^2 = 0.855$), followed by F12/FBS ($R^2 = 0.553$), F12/ITS ($R^2 = 0.505$), and DMEM/FBS ($R^2 = 0.210$).

Tissue wet weight is often associated with the level of GAG in the tissue as its highly negative charge has a strong tendency to attract water into the matrix. In Figure 7B, we see DMEM/ITS had the highest levels of sGAG; however, the spread of the tissue wet weights in Figure 9 are variable. The DMEM/FBS had the second highest levels of sGAG, but the tissue wet weights across the experimental repeats are consistently high. Variations in the wet weights suggests that GAG content may not be the only factor attributing to water retention in the tissue constructs. Another justification that could explain the wet weights differences between the four conditions is the level of polyP found in the tissue constructs. PolyP is a negatively charged biopolymer [163] that could attract water into the matrix, similar to sGAG. The DMEM/ITS samples displayed the strongest correlation between polyP amount and wet weight with an $R^2 = 0.855$, suggesting polyP could be influencing the water retention in the tissue. However, this hypothesis cannot account for the three other conditions as their $R^2$ values are less than 0.6.

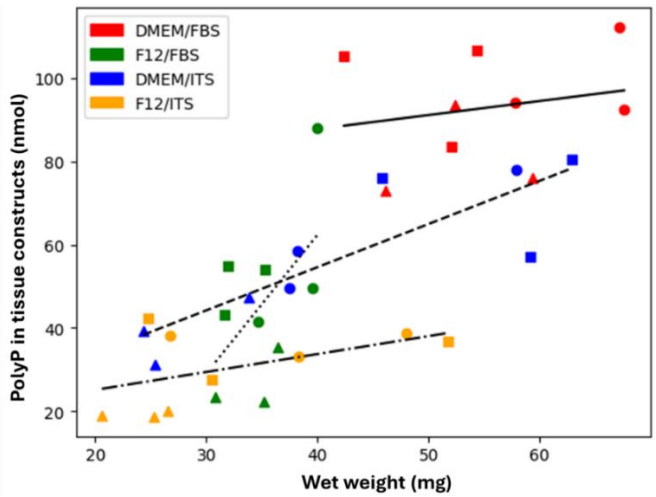


**Figure 9.** Correlation between total polyP in constructs and wet weight grown of four different medium conditions represented by different colours. Experiments were repeated 3 times with cells isolated from different animals. Each repeat is represented by a different shape ○ set 1; □ set 2; △ set 3. DMEM/FBS correlation (——); F12/FBS correlation (⋯⋯ ); DMEM/ITS correlation (-----); and F12/ITS correlation (– · –)

### 5.2 Glucose consumption, lactate release, and polyP release over time

One of the main objects of this project is to assess the changes in polyP production over time. To explore this question, it was crucial to monitor the changes in concentration over a time course of 72 hours at the timepoints of 0 hours, 3 hours, 6 hours, 24 hours, 48 hours, and 72 hours, representing the maximum period between two media changes. Since polyP is a bioenergetic molecule we wanted to assess the relationship between polyP and other metabolic molecules such as glucose and lactate. Glucose is a common energy source for cells to utilize to produce ATP via glycolysis. Lactate, often thought of as a waste product of glycolysis, also serves as an energy reserve that can be broken down by LDH to produce pyruvate to be used in the TCA cycle. We first investigated the concentration changes of glucose and found a steady level throughout 0 to 6 hours (Figure 10). However, we begin to see a depletion of glucose

content at 24 hours with significant decreases at 48 hours ($p<0.01$) and 72 hours ($p<0.001$). A two-way ANOVA found that independently, time ($p<0.001$) and the biological differences between the cells of each experimental repeat ($p<0.001$) were statistically significant in impacting the glucose concentration in the medium. In Figure 11, we can see that the rate of glucose consumed is the highest at the 3-hour mark at 6.84 µg of glucose per µg of DNA per hour, which is statistically greater than the rate of consumption of the later timepoints. From our statistical analyses, time ($p<0.001$) and biological differences between experimental repeats ($p<0.001$) are significant factors for glucose consumed per DNA per hour.

As mentioned above, there are minimal changes to the glucose concentration in the medium for the first 6 hours after a media change which is likely attributed to the chondrocytes adjusting to their new nutrient environment. However, we witness a significant depletion of glucose concentration 48 hours onwards, which may be the result of a greater lapse of time between the 6-hour and 48-hour timepoints compared to the 0-hour and 24-hour timepoints. We observe that the 3-hour mark has the greatest glucose consumption rate over the time course which may be due to the cells exhibiting high metabolic activity in the short-term. This may be attributed to the chondrocytes utilizing glucose in multiple pathways. Glucose is involved in energy storage and production pathways such as glycogen synthesis, glycolysis, and OXPHOS, as well as pathways that support cell proliferation and ECM synthesis via pentose phosphate pathway (PPP) and GAG synthesis pathway, respectively [164].

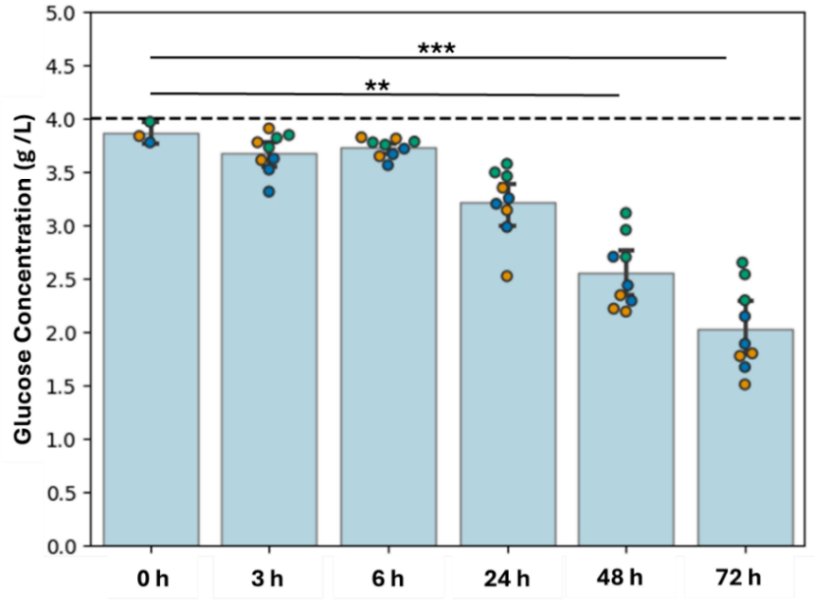


**Figure 10.** Glucose concentration in media incubated with high density chondrocyte culture 0, 3, 6, 24, 48, and 72 hours after media change on day 14 of culture period. Experiments were repeated 3 times with cells isolated from different animals and are represented by data points in different colours. Mean glucose concentration of fresh medium (----). Data are represented as mean ± SD. Statistically significant decrease in glucose concentration compared to 0 h is denoted by ** ($p<0.01$) and *** ($p<0.001$).

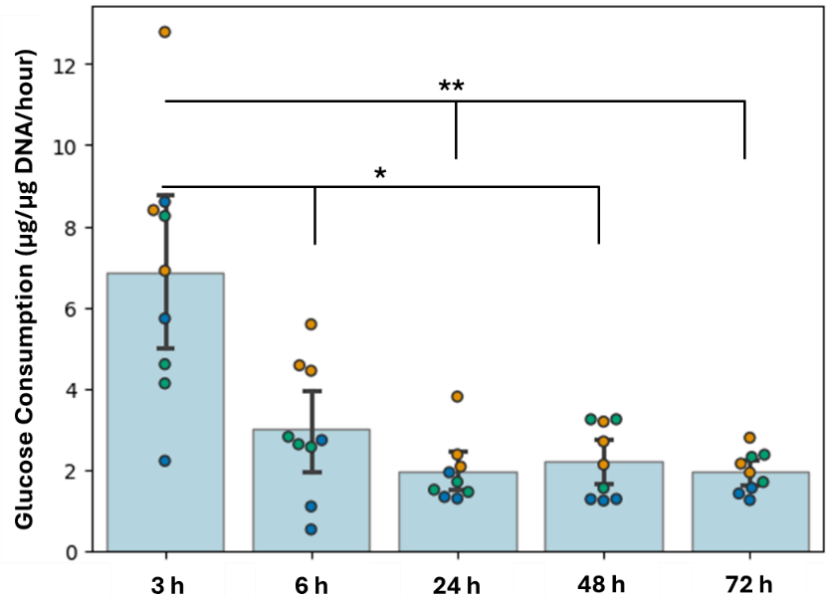


**Figure 11.** Glucose consumption rate of constructs 3, 6, 24, 48, and 72 hours after media change on day 14 of culture period. Experiments were repeated 3 times with cells isolated from different animals and are represented by data points in different colours. Data are represented as mean ± SD. Statistically significant differences in glucose consumption compared to 3 h is denoted by * ($p<0.05$) and ** ($p<0.01$).

Lactate is a metabolic byproduct of the glycolysis pathway where the resulting pyruvate is converted to lactate via the oxidation of NADH to $NAD^+$ and $H^+$. The production of lactate indicates that pyruvate did not enter the TCA cycle and supports the notion that chondrocytes primarily rely on glycolysis for energy production and not OXPHOS [165]. Figure 12A illustrates the changes in lactate concentration over 72 hours, with significant increases from earlier timepoints compared to the later timepoints. In particular, at the 48- and 72-hour mark, the concentration of lactate is significantly greater compared to the 3-hour ($p<0.05$, $p<0.01$) and 6-hour ($p<0.05$, $p<0.01$) timepoints. Two-way ANOVAs determined that time ($p<0.001$) and biological differences between sets ($p<0.001$) have a statistically significant effect on both the lactate concentration and amount of lactate produced per well.

The steady elevation of lactate and depletion of glucose supports the notion that chondrocytes are utilizing glucose via anaerobic glycolysis to produce and accumulate lactate in the medium [165]. As mentioned above, the earlier timepoints of 3 and 6 hours have a greater rate of glucose consumption compared to the later timepoints; however, the lactate levels are at the lowest at these two time periods. It is likely that the chondrocytes are adjusting to their replenished nutrient environment and potentially utilizing the glucose to support metabolic pathways where lactate is not a byproduct resulting in low lactate levels in the medium for the first 6 hours of the time course. However, in the later timepoints of 24 hours and onwards, glucose could be utilized in the PPP to support cell proliferation and glycolysis to generate ATP to support an elevated chondrocyte population. Both the PPP and glycolysis pathway produce lactate as a byproduct, and the combined lactate release from both pathways could explain the significant elevation of lactate 24 hours onwards [166]. Of note, greater lactate concentrations can create acidic culture conditions which can be harmful for the chondrocytes causing them to inhibit cell proliferation and matrix accumulation [167]. These increasing stress conditions could impact the metabolic activity of chondrocytes to shift to pathways that protect against environmental stresses.

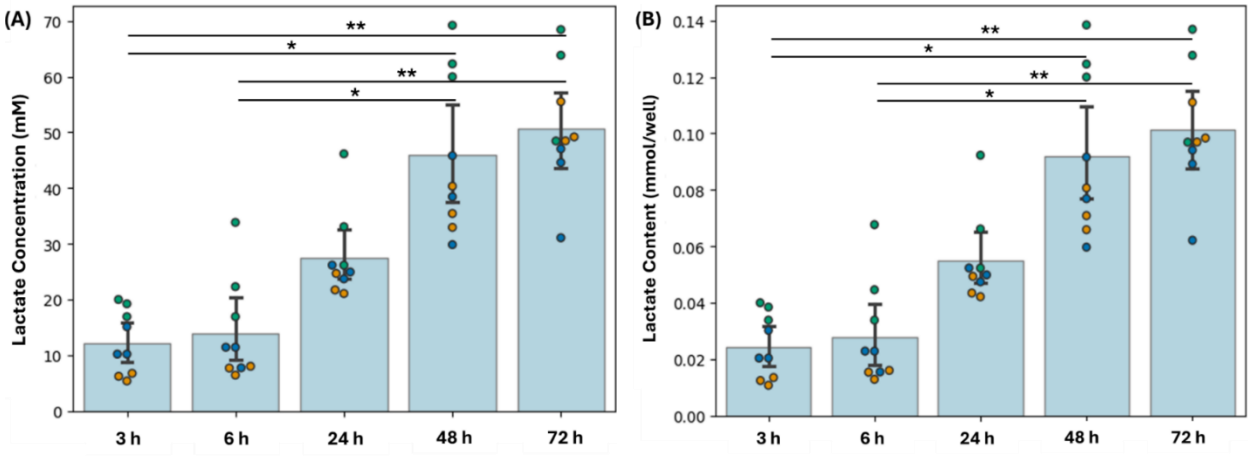


**Figure 12**. **(A)** Lactate concentration and **(B)** total lactate content in media incubated with high density chondrocyte culture 3, 6, 24, 48, and 72 hours after media change on day 14 of culture period. Experiments were repeated 3 times with cells isolated from different animals and are represented by data points in different colours. Data are represented as mean ± SD. Statistically significant increase in lactate concentration and content between conditions is denoted by * ($p<0.05$) and ** ($p<0.01$).

To gain further insight into the energetic changes of the chondrocytes in relation to time, we investigated the amount of lactate produced per glucose consumed. In the early stages, the ratio of lactate in the medium to glucose consumed is steady up to hour 6 (Figure 13) with values under 1. However, for the timepoints of 24 hours and onwards, the amount of lactate released surpasses the glucose content with ratios 2–4 fold greater than the 3- and 6-hour mark. A potential explanation for such high lactate to glucose ratios at the later timepoints, is that the medium used for this study contains pyruvate and glutamine which can both be converted to lactate. The pyruvate in the medium can be converted into lactate through glycolysis and this may have influenced the lactate content in the spent medium, and in turn, the yield of lactate release to glucose consumed ratio. Although the impact of glutamine on lactate levels is not fully understood in mammalian cells, there is strong evidence that lactate is a byproduct of glutamine

metabolism [168, 169, 170]. Additionally, the chondrocytes could be using other carbon sources such as glycogen, the storage form of glucose, which can undergo glycolysis and produce lactate [171]. Until we determine how pyruvate and glutamine influence lactate content in the media, we cannot speculate that most of the glucose is being converted to lactate through anaerobic glycolysis [172]. Another explanation of why such high lactate to glucose ratios were measured may be attributed to the chondrocyte phenotype. Rajpurohit et al. [173] found higher ratios of lactate to glucose in hypertrophic chondrocytes than proliferating chondrocytes. These elevated ratios may give us insight into the phenotypic changes that may be occurring in the chondrocytes in relation to dynamic metabolic environment.

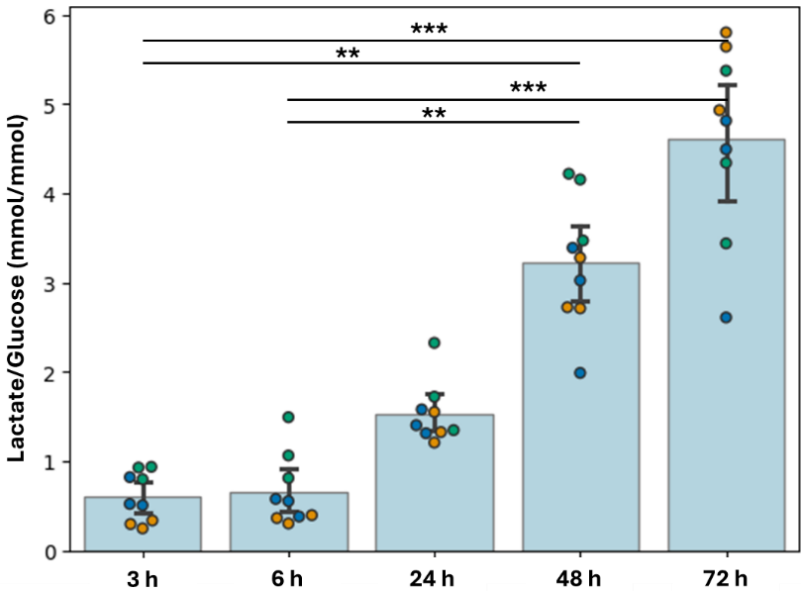


**Figure 13**. Total lactate to glucose ratio in media incubated with high density chondrocyte culture 3, 6, 24, 48, and 72 hours after media change on day 14 of culture period. Experiments were repeated 3 times with cells isolated from different animals and are represented by data points in different colours. Data are represented as mean ± SD. Statistically significant differences between conditions is denoted by ** ($p<0.01$) and *** ($p<0.001$).

After witnessing the glucose consumption and lactate release trends over the 72-hour period, we wanted to investigate how the polyP levels in the tissue constructs and spent medium align with the activity of these biomolecules. Looking at the polyP content in the tissue (Figure 14A) and medium (Figure 14B), we see a steady increase from 3 hours to 72 hours, with no statistically significant differences among the timepoints. A three-way ANOVA determined that glucose ($p<0.01$), lactate ($p<0.001$), experimental repeats ($p<0.05$) and the three-way interaction between these factors ($p<0.05$) have a statistically significant effect on the chondrocytes producing polyP. However, for the polyP released into the medium, the three-way interaction between glucose, lactate, and experimental repeats ($p<0.05$) was found to be the only significant influence.

Although there is minimal research looking into tracking the metabolic changes of polyP in mammalian cells, we can derive some hypotheses on what may be occurring based on existing literature. It is well documented that prokaryotes accumulate polyP as a stress response to environmental changes such as nutrient depletion [96], elevation of oxidative species [97], and pH fluctuations [174]. With this abundance of evidence of polyP's role as protective stress mechanism, it suggests that this function could be potentially conserved in mammalian cells as well. Xie et al. [175] demonstrated that in response to cisplatin-induced stress, polyP accumulation occurred in the nucleolus in mammalian cells. The increasing polyP levels in both the tissue and media suggests there could be a positive correlation with elevated lactate content, which creates an increasingly acidic environment, inducing protective stress mechanisms in the chondrocytes. Chronic accumulation of polyP in the nucleolus has been contributed to pathological conditions by disrupting RNA polymerase I activity [175, 176].

Glucose and lactate levels coincided with changes in polyP levels in both tissue and media

independently, however, their influence was not statistical significance on the cumulative polyP (Figure 14C). The impact of a media change could possibly influence the amount of polyP measured in both the tissue and medium by releasing the polyP accumulated in the tissue into the medium. This disturbance in changing the medium could lead to lower levels in the tissue and higher levels in the medium, which can overall skew the total polyP quantified in each compartment. However, when we take the sum of the polyP present in the tissue constructs and medium, we observe relatively stable levels suggesting that disturbances in changing the medium do not have major effects on the cumulative polyP. All in all, despite the substantial changes in the concentration of glucose and lactate, the levels of polyP appear fairly stable, suggesting that there is no relationship between polyP accumulation and glucose depletion and lactate elevation.

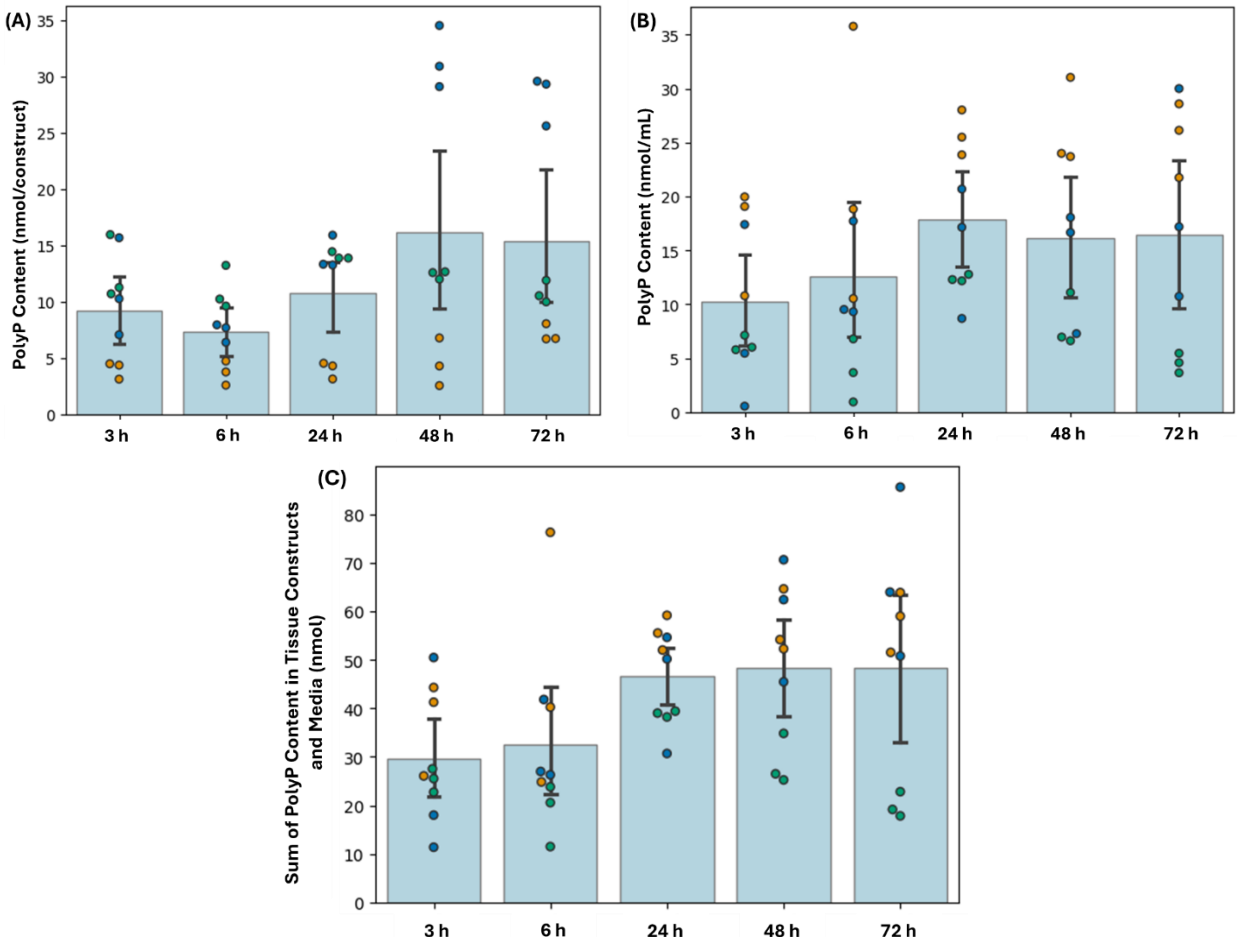


**Figure 14. (A)** Total polyP content in cartilage constructs, **(B)** media, and **(C)** constructs and media combined incubated with high density chondrocyte culture 3, 6, 24, 48, and 72 hours after media change on day 14 of culture. Experiments were repeated 3 times with cells isolated from different animals and are represented by data points in different colours. Data are represented as mean ± SD.

### 5.3 Effect of exogenous polyP on the metabolic activity of cartilage constructs

After gaining insight into the chondrocytes' ability to produce and accumulate polyP in response to various media and media supplement combinations and time, we wanted to investigate how chondrocytes would respond to exogenous administration of polyP. The exogenous administration of polyP to cultures of chondrocytes allows us to artificially

manipulate the levels of this biomolecule in our cultures and has shown to stimulate cartilage matrix accumulation, while intra-articular injection in a guinea pig model of OA protects the cartilage from some degenerative changes [7, 8]. These results show the potential of polyP to be a chondroprotective treatment for OA, however, changes to the metabolic activity of chondrocytes in response to these protective mechanisms have yet to be thoroughly investigated. This is interesting given the potential bioenergetic roles ascribed to the molecules in different organisms and mammalian tissues. To gain an understanding of the metabolic changes the chondrocytes may experience because of polyP exposure, we examined the differences in glucose and lactate levels in chondrocytes cultured with no inorganic phosphate (Pi) or polyP as a control, 1 mM Pi, and 1 mM polyP.

Taking a look at the glucose concentrations in spent media of the three conditions (Figure 15A), we observe no significant difference between the groups as the final glucose concentrations were relatively stable between the control, Pi, and polyP conditions at 2.41 g/L, 2.15 g/L, and 2.27 g/L, respectively. Although there were no detectable differences in the glucose concentration and consumption rate (Figure 15B) between the conditions, a two-way ANOVA found that the results of both studies were significantly influenced by the biological differences between the cells of each experimental repeat ($p<0.05$).

Regarding the lactate concentration (Figure 15C) and content per well (Figure 15D) secreted by the chondrocytes, we observed no significant differences among the control, Pi, and polyP conditions. Interestingly, similar to the glucose results, a two-way ANOVA found that the biological differences between the three sets of cells had a significant influence on lactate production ($p<0.001$). When we examine the lactate to glucose ratio (Figure 15E) we see that the lactate to glucose ratios is elevated in both the Pi and polyP groups, with no significant

differences were found between the three conditions. However, differences between the cells in each experimental repeat were found to have a significant impact on these ratios ($p<0.05$).

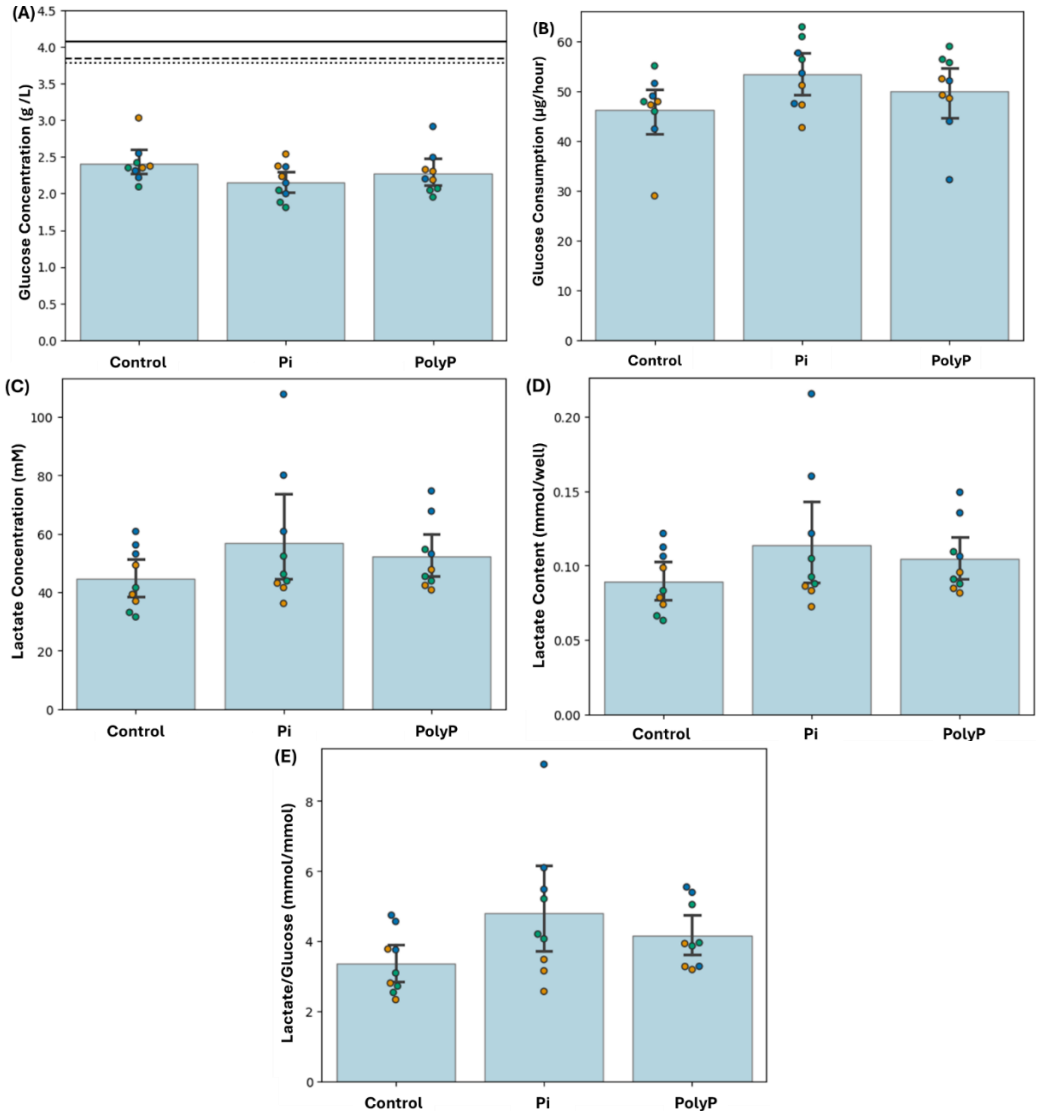


**Figure 15. (A)** Glucose concentration, **(B)** glucose consumption, **(C)** lactate concentration, **(D)** total lactate content, and **(E)** lactate to glucose ratio of cartilage constructs on day 14 72 hours after media change. Experiments were repeated 3 times with cells isolated from different animals and are represented by data points in different colours. Pi = inorganic phosphate; PolyP = polyphosphate. Initial glucose concentration of control (——), Pi (·····), and PolyP (- - - -). Data are represented as mean ± SD.

Examining the glucose and lactate results above, we observe a mild elevation in the glucose consumption rate and lactate production for the Pi condition suggesting that it may be supporting greater cellular activity compared to the control and polyP conditions. To gain further insight into how these conditions may influence the cellular activity of the chondrocytes, we investigated the potential differences in metabolic activity between conditions. We utilized the Alamar blue assay which measures the number of living and metabolically active cells via fluorescence readings. Metabolic activity was measured as a percentage in comparison to control, and when we examine the fluorescence results (Figure 16) we see that the metabolic activity of the Pi condition is 5.4% greater than the control while the polyP condition is 4.5% lower than the control. A one-way ANOVA determined that no significant differences are observed between the conditions. However, a two-way ANOVA found that the differences between the cells from the first and second set of experiments ($p<0.001$), the culture conditions ($p<0.05$), and interaction between the two factors ($p<0.01$) have a significant impact on metabolic activity.

This investigation was conducted because spent media pH is affected by polyP with pH being visibly lower in polyP treated cells at some point in the culture period. This effect is eventually reversed after a longer culture period, which is likely due to the eventual effects of polyP on proliferation. The timing of these changes is cell source dependent making it difficult to choose an appropriate time point for polyP treatment. Further, there is no guarantee that these pH variations will be reflected in glucose, lactate or metabolic activity levels. Thus, to properly design our experiments, we must take a step back to understand how our system varies with time.

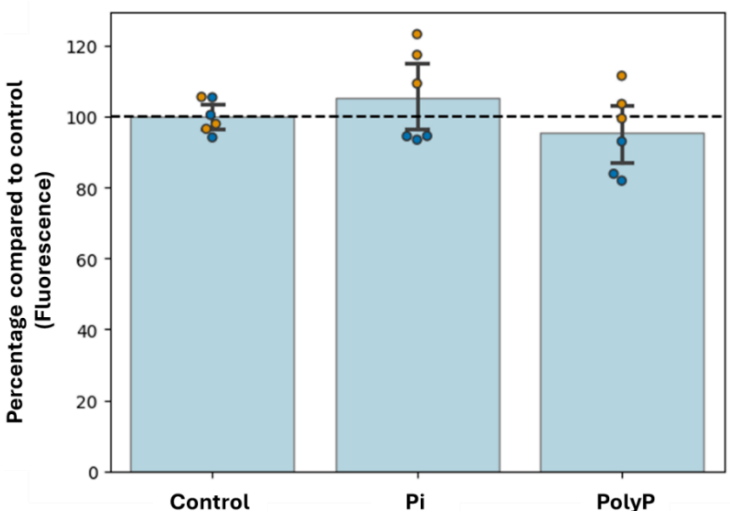


**Figure 16.** Fluorescence readings of the cell viability of chondrocyte constructs on day 15 24 hours after the last media change. Experiments were repeated 2 times with cells isolated from different animals and are represented by data points in different colours. Pi = inorganic phosphate; PolyP = polyphosphate. Data are represented as mean ± SD.

### 5.4 Biochemical composition of static compressed cartilage constructs

One of the primary functions of articular cartilage is to absorb and distribute the mechanical loads of the joints during physical activity. Articular cartilage undergoes various types of mechanical forces such as compression, shear stress, and tensile stress. It is important to understand how these forces impact the biochemical composition and metabolic activity of the chondrocytes to understand the pathological impact it may have on OA. Static compression has been associated with catabolic activity, which can potentially lead to pathological changes in cartilage tissue [177, 178]. We investigated how chondrocytes would respond to being subjected to 17 mN and 32 mN of static compressive force sessions of 3 hours/day 5 days/week for 3 weeks. During the beginning phases of this study, we found that the ages of the cow in which cells were extracted from played a role in skewing our findings and their impact was considered for our analyses.

Firstly, we investigated how the application of 17 mN and 32 mN of force would impact cell proliferation by measuring the level of DNA in the tissue constructs. The DNA was normalized to the dry weight and the controls to enhance comparability between the conditions despite age-related differences among the cells. In Figure 17A, we observe that the DNA per milligram of dry weight is slightly elevated in the 17 mN and 32 mN conditions compared to the control with no significant differences between the groups. When standardized to the controls (Figure 17B), the rate of proliferation of the chondrocytes subjected to 17 mN and 32 mN of force are quantified to be 10% higher compared to the control. The results of this study align with Ryan et al. [179] findings which demonstrate that static mechanical compression induces chondrocyte proliferation via the activation of extracellular signal-regulated kinase 1/2 (ERK 1/2). ERK 1/2 belongs to the mitogen-activated protein kinase (MAPK) family and has various roles in chondrocyte proliferation [179] and differentiation [180, 181]. The mechanical stimulation of the chondrocytes can trigger the activation of mechanoreceptors to initiate the MAPK-ERK signaling cascade and activate ERK 1/2 [182]. Once activated ERK 1/2 is translocated to the nucleus [183] to phosphorylate transcription factors such as c-FOS that regulate the expression of the gene cyclin D1 which is involved in cell proliferation [184]. The regulation of the MAPK-ERK pathway can also be modulated by TGF-β [185, 186], which is often released in response to mechanical stimulation and further enhances ERK-mediated proliferation [160].

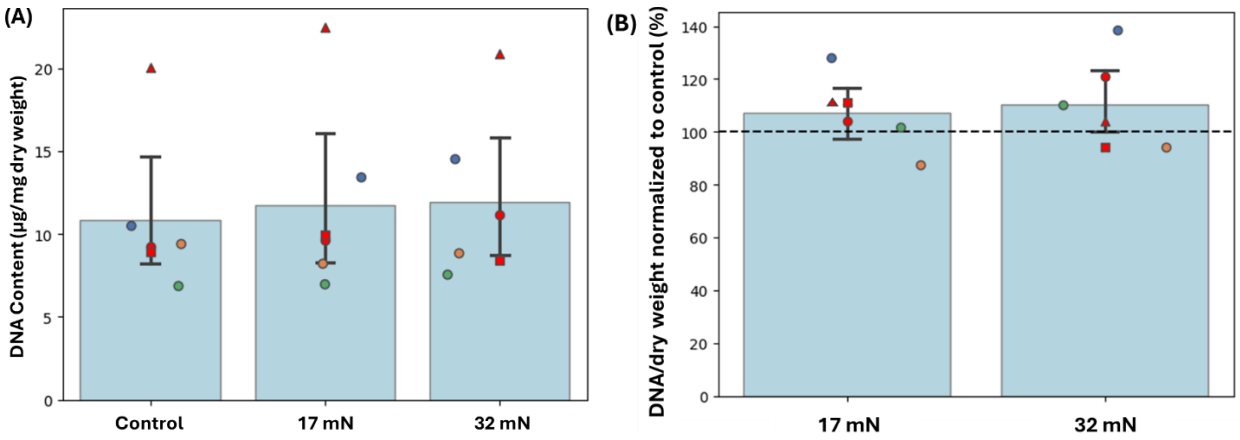


**Figure 17.** DNA content of cartilage constructs **(A)** normalized to dry weight and **(B)** to the DNA to dry weight fraction normalized to control at day 28 in culture. Experiments were repeated 6 times with cells isolated from different animals of various ages. Veal (16 – 18 weeks); young – set 1 (1 – 2 years); young – set 2 (1 – 2 years); young – set 3 (1 – 2 years); adult (2 – 4 years); old (5 – 8 years). Data are represented as mean ± SD.

With the slight elevation of cell proliferation in response to compressive forces, we wanted to investigate if the mechanical cues applied could impact ECM accumulation in the cultures. Sulfated glycosaminoglycans (sGAG) are one of the major components of the ECM and are responsible for imparting a swelling pressure within the matrix to provide compressive strength to the cartilage. When compressive forces are applied to the tissue constructs, we see a steady depletion in sGAG content when normalized to the dry weight (Figure 18A) and the controls (Figure 18B), with no significant differences between the groups. Additionally, we examined the ratio of sGAG secreted per molecule DNA (Figure 18C) and found declining trends with no significant differences between the conditions. However, when we normalized the sGAG to DNA ratio to the controls (Figure 18D) we see a significant difference in the 32 mN condition when compared to the control ($p<0.05$).

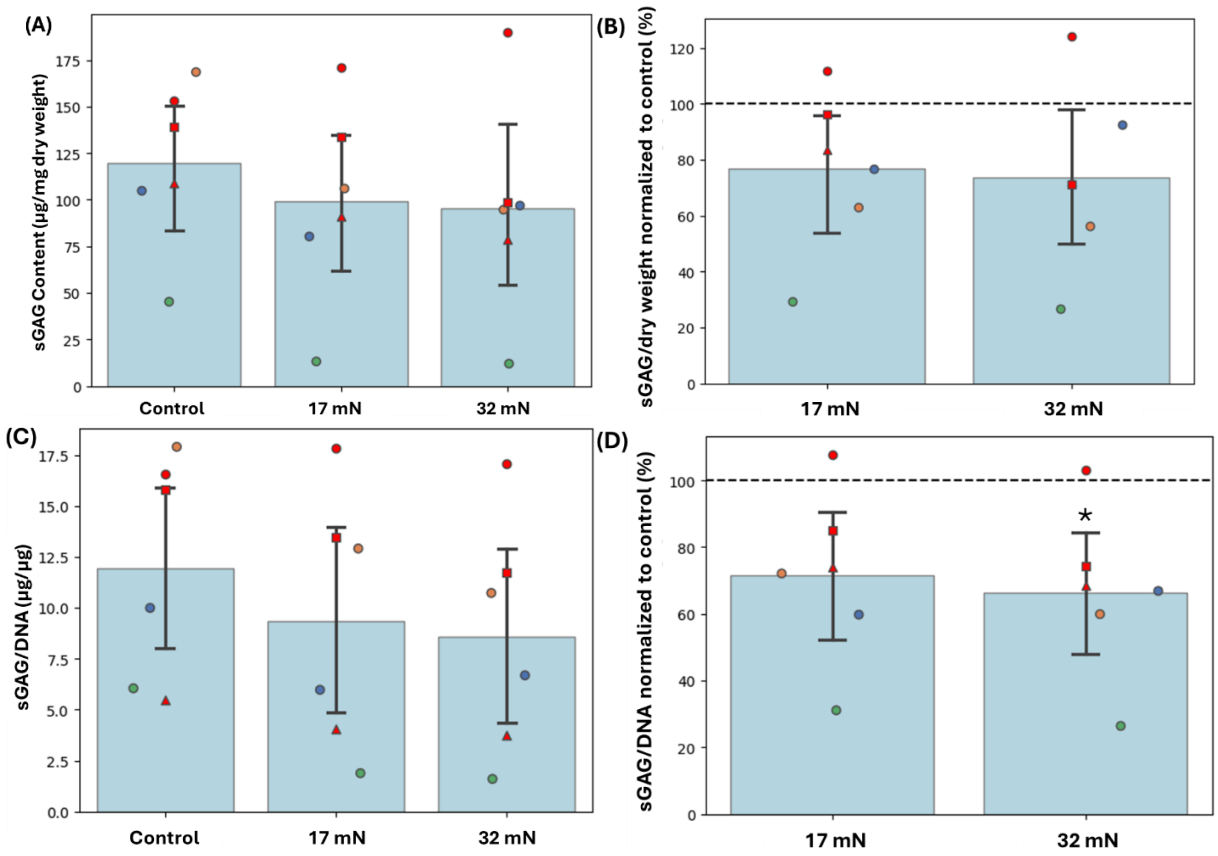


**Figure 18. (A)** Total sGAG content of cartilage constructs normalized to dry weight, **(B)** sGAG to dry weight ratio normalized to control, **(C)** sGAG to DNA fraction, and **(D)** sGAG to DNA fraction normalized to control for day 28. Experiments were repeated 6 times with cells isolated from different animals of various ages. ● Veal (16 – 18 weeks); ● young – set 1 (1 – 2 years); ▲ young – set 2 (1 – 2 years); ■ young – set 3 (1 – 2 years); ● adult (2 – 4 years); ● old (5 – 8 years). Data are represented as mean ± SD. Statistically significant differences between the groups compared to the control is denoted by * ($p<0.05$).

Collagen is another component of the ECM responsible for providing tensile strength to the cartilage. After witnessing a decline in sGAG in relation to the application of compressive forces, we wanted to see if these forces would also elicit a negative impact on collagen levels. Surprisingly, when collagen is normalized to the tissue dry weight (Figure 19A) and the controls

(Figure 19B), the levels are stable across all the conditions. However, when we take the collagen to DNA ratio (Figure 19C) and its normalization to the control (Figure 19D) there appears to be a decrease in collagen content in the 17 mN and 32 mN conditions with no significant differences between the groups.

It is well established that static compression of chondrocytes increases matrix catabolism, whereas certain protocols of dynamic compression enhance matrix synthesis [187, 188, 189, 190]. Mechanical loading of cartilage in the form of compression, tension and shear stress is linked to regulating MMPs, ADAMTS, and Wnt5a expression [191, 192, 193]. Specifically, mechanical overloading has been shown to upregulate MMP-1, MMP-3, MMP-13, ADAMTS-5 and Wnt5a which cumulatively promotes ECM degradation [191, 192]. Huang et al. [194] found that the overexpression of Wnt5a was able to suppress the transcription of the aggrecan gene (ACAN), while promoting the expression MMP-1, MMP-3, and MMP-13 [194, 195] Suppression of ACAN transcription along with elevated levels of MMP-3 and ADAMTS-5 would not only reduce the amount proteoglycans synthesized in ECM, but also promote the breakdown of existing proteoglycans. The combined effects of ACAN, MMP-3, and ADAMTS-5 could explain the 23.29 – 26.19% depletion of sGAG content in the cartilage constructs subjected to 17 mN and 32 mN of compressive force (Figure 18B). Moreover, the elevated levels of MMP-1 and MMP-13 could enhance the degradation of collagen type II in the ECM which is reflected in the 8.85 and 9.64% decrease in the 32 mN and 17 mN respectively. (Figure 19B). Another effect of Wnt5a signaling is the subsequent activation of ERK, which discussed above, induces cell proliferation in chondrocytes. This could explain why the ratio of sGAG to DNA (Figure 18D) and collagen to DNA (Figure 19D) may be lower than expected when normalized to the control.

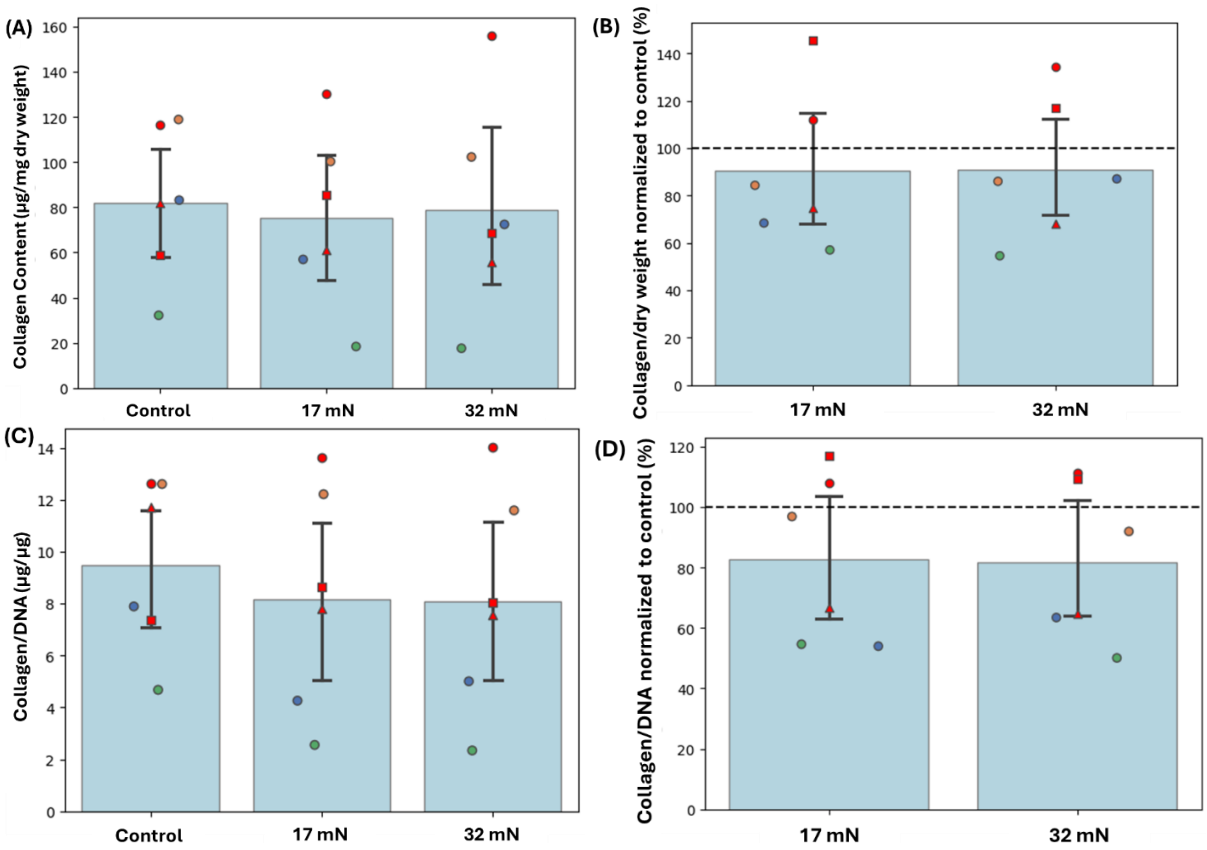


**Figure 19. (A)** Total collagen content of cartilage constructs normalized to dry weight, **(B)** collagen to dry weight ratio normalized to control, **(C)** collagen to DNA ratio, and **(D)** collagen to DNA ratio normalized to control for day 28. Experiments were repeated 6 times with cells isolated from different animals of various ages. ● Veal (16 – 18 weeks); ● young – set 1 (1 – 2 years); ▲ young – set 2 (1 – 2 years); ■ young – set 3 (1 – 2 years); ● adult (2 – 4 years); ● old (5 – 8 years). Data are represented as mean ± SD.

In native cartilage, the fluid phase can account for 60 to 80% of the tissue weight [20] and plays a role interacting with the proteoglycans and collagens from the matrix to influence the mechanical properties of the tissue [12]. The water content of our in vitro formed cartilage constructs ranged from 85-94% with no significant differences observed between the conditions and the age of the cells (Figure 20). The elevated water content in our 3D constructs compared to native cartilage suggests matrix differences that facilitate a greater retention of water. This may

be the result of the relatively low collagen to sGAG ratio within in vitro-formed constructs compared to the native cartilage tissue [196]. These differences in matrix composition can lead to variations in the mechanical properties of the tissue. Additionally, the minimal differences in the water content between the different conditions and age groups may be due to the lack of differences in the collagen content as water is required for the triple helix configuration of collagen [197] and can be potentially entrapped in or reconfigured around the fibrils [198].

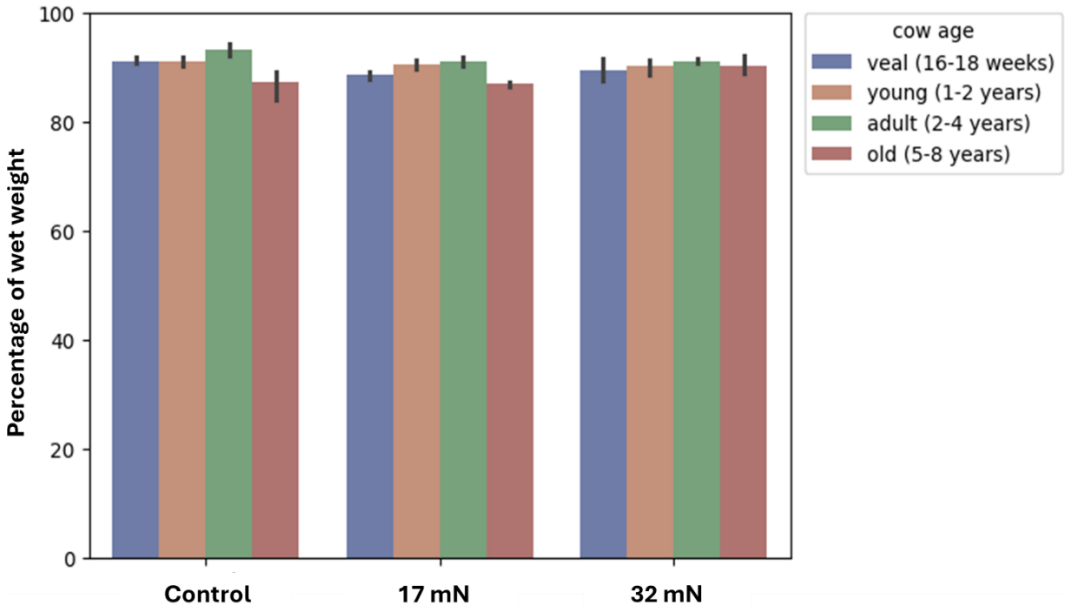


**Figure 20.** Percentage of wet weight of cartilage constructs for day 28. Experiments were repeated 6 times with cells isolated from different animals of various ages. Age ranges are represented by data points in different colours and repeat experiments within an age range is represented by different shapes. Data are represented as mean ± SD.

Histological assessment of the tissue constructs was conducted to visualize the morphological differences between the conditions. The tissues were harvested on day 28 and stained with Sirius red, Hematoxylin and Eosin, and Alcian blue to detect the collagen, nuclei and ECM, and sGAG respectively (Figure 21). The relative thickness and staining intensity of the tissues showcase similar levels of cells and collagen across all the conditions and supports

the quantitative findings of the DNA and collagen assays. However, when we look at the conditions stained in Alcian blue, the 17 mN and 32 mN conditions appear to be richer in proteoglycans compared to the controls which is contradictory to our findings. This may be due to the biological differences attributed to the bovine specimen the cells were extracted from, as these histological sections were taken from the first set of the young age category which exhibits a steady incline in sGAG content as more compressive force is elicited. Contradictory quantitative and qualitative results suggests that careful documentation of biological factors such as age and sex that could attribute to differences in the data should be taken into account to elucidate their impact. These histological results would have to be reproduced with cells from different animals.

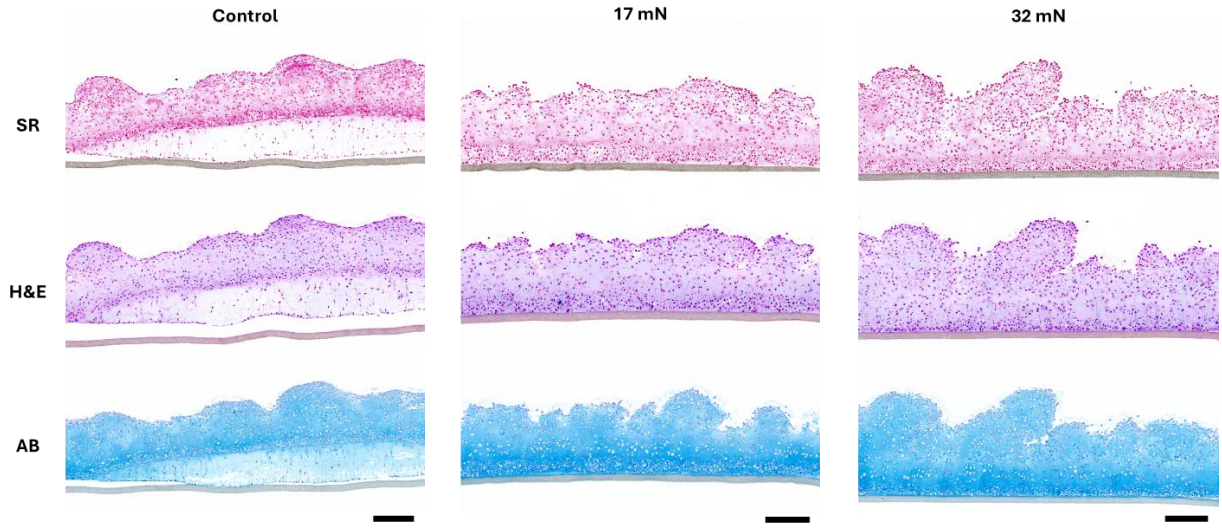


**Figure 21.** Histological sections of cartilage constructs subjected to no force (control), 17 mN of force, 32 mN of force stained with Sirius Red (SR), Hematoxylin and Eosin (H&E), and Alcian Blue (AB) on day 28. Scale bar = 200 µm.

## 5.5 Glucose consumption, lactate release, and endogenous polyP release

After observing the biochemical composition of the constructs, we wanted to assess the metabolic activity of the tissue when they are subjected to 17 mN and 32 mN of compressive force. Firstly, we examined the glucose concentration across the three conditions and found no significant differences between the groups (Figure 22A). Seeing these stable trends in the glucose concentration, we presume that the lactate levels would follow a similar pattern based on the assumption that pyruvate, the end product of glycolysis, is converted to lactate in a 1:2 ratio through the activity of lactate dehydrogenase [199]. The lactate concentration (Figure 22B) and amount per well (Figure 22C) are stable throughout the control and the two compression conditions with no significant differences between the groups. These steady levels of glucose and lactate suggest that the glucose consumption and lactate production rate is occurring at similar rates across the conditions. To determine if this assumption is true, we looked at the lactate to glucose ratio (Figure 22D) and found that the rate of conversion is similar throughout the groups. Interestingly, the ratio is slightly larger than the expected 1:2 conversion of pyruvate to lactate. This is likely attributed to the presence of the medium components of pyruvate and glutamine which has been implicated to be converted into lactate through anaerobic glycolysis and glutamine metabolism, respectively.

The stability of the metabolic activity across all three conditions suggests that constructs undergoing 17 mN and 32 mN of compressive force eventually reach a state of equilibrium within the 72-hour period after the last compression session before sample harvest. Salinas et al. [200] was able to demonstrate that shorter compression times of 15- or 30-minutes could increase glycolysis activity while simultaneously depleting the metabolites involved in collagen and proteoglycan synthesis. Elevated levels of glucose, pyruvate, and lactate were recorded

during the first 15 minutes of compression, however, the concentration of all three metabolites began to deplete at the 30-minute mark. This demonstrates that static compression may have a short-term effect on metabolic activity which subsequently stabilizes the longer the compression sessions. Shorter compression sessions may need to be conducted to verify the potential short-term effects of static compression on metabolic activity.

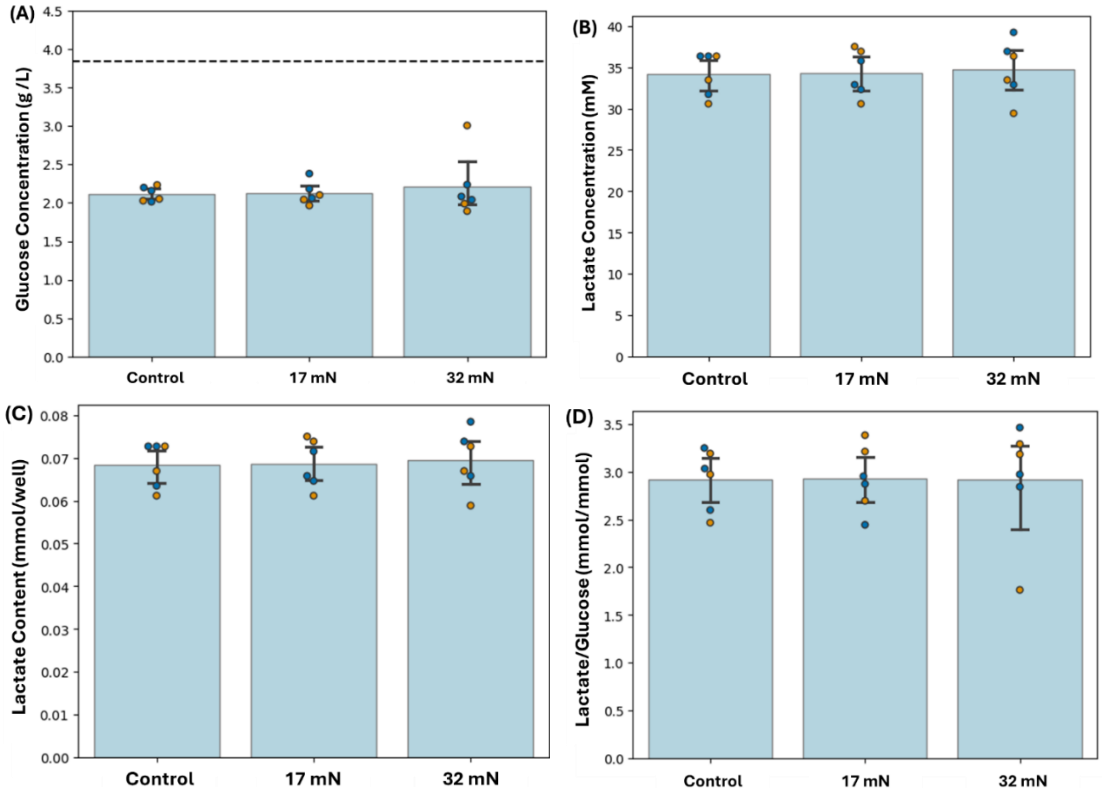


**Figure 22**. **(A)** Glucose concentration, **(B)** lactate concentration, **(C)** total lactate content, and **(D)** lactate to glucose ratio in media incubated with high density chondrocytes subjected to various magnitudes of force on day 28 of culture. Experiments were repeated 2 times with cells isolated from different animals and are represented by data points in different colours. Data are represented as mean ± SD.

After observing the steady levels of glucose and lactate across the conditions, we wanted to assess if the levels of polyP would follow the same trend. No significant differences were

observed between the control, 17 mN, and 32 mN conditions when we examine the total amount of polyP per construct (Figure 23A) and polyP normalized to wet weight (Figure 23B). To reduce the variability attributed to the biological differences between the cells, we normalized polyP levels to the amount of DNA produced (Figure 23C). The ratio of polyP to DNA is similar across the groups with no significant differences between them. To determine the amount of polyP released from the tissue constructs, we measured the polyP content in the spent medium. In Figure 23D, we observe similar levels in the control and 32 mN conditions while the levels in the 17 mN condition is two times lower in comparison, with no significant difference between the groups.

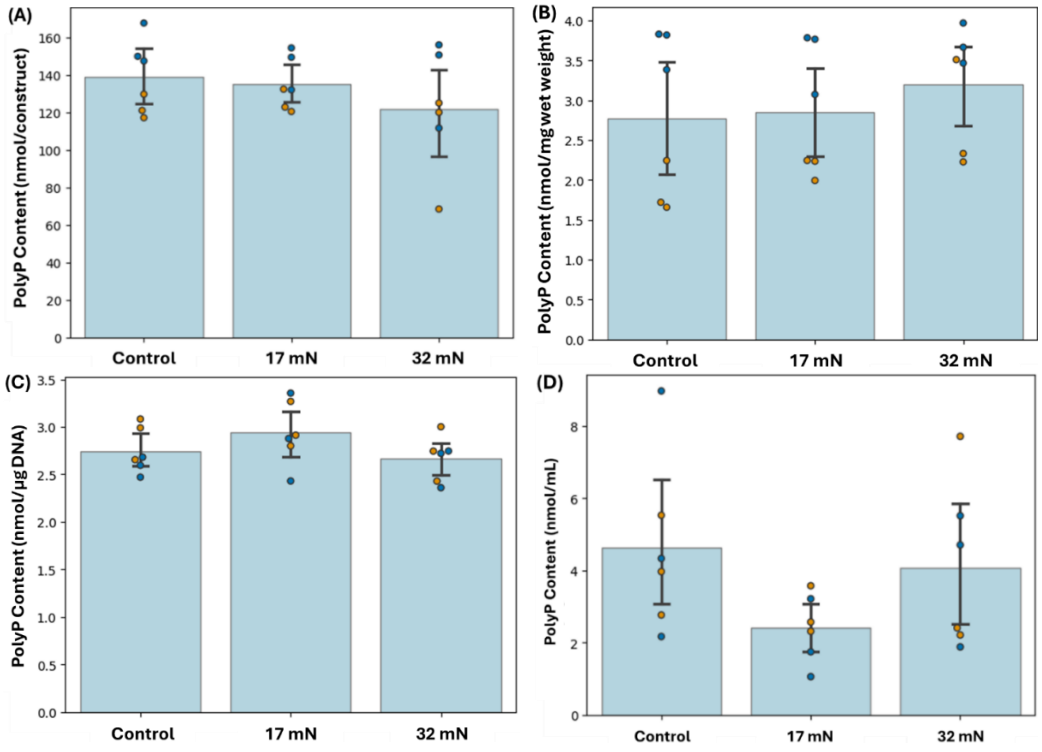


**Figure 23. (A)** Total polyP content of cartilage constructs, **(B)** total polyP normalized to wet weight, and **(C)** total polyP normalized to DNA, **(D)** total polyP content in media on day 28 of culture. Experiments were repeated 2 times with cells isolated from different animals and are represented by data points in different colours. Data are represented as mean ± SD.

In our work, we provided mechanical cues to our constructs which did not affect polyP levels in cultures. Samples were harvested 72-hours after the last compression session which may have given the chondrocytes time to reach a state of equilibrium comparable to the controls. Static mechanical forces have shown to affect various cellular processes, but the specific impact on polyP in chondrocytes remains unexplored, however, some indirect evidence suggested that mechanical stimuli could potentially influence polyP levels. It is well established that during periods of stress, organisms such as bacteria and yeast, elevate polyP synthesis in response [97, 103, 201]. Since excessive biomechanical forces often induce a stress response in cells, it is plausible that polyP synthesis could be modulated as part of a cellular adaptation to mechanical stress in chondrocytes. Additionally, polyP is known to interact with various signaling pathways that respond to stress, including those associated with oxidative stress [97, 202] and energy metabolism [103]. Since chondrocytes exposed to static compressive forces have shown to adjust their energy metabolism during short-term exposure it is possible that changes in metabolic pathways due to biomechanical forces could indirectly alter polyP production. While direct evidence of static compressive forces influencing polyP production is limited, there is potential for mechanical stress to affect polyP levels through cellular stress responses and metabolic adjustments. However, targeted research is needed to fully elucidate this relationship.

# CONCLUDING STATEMENTS

## 6.1 Effect of media and media supplements on polyP accumulation in cartilage constructs

For this project, we were interested in understanding the production and metabolism of polyP in chondrocytes and its relationship with other metabolites. We first assessed the ability of the chondrocytes to independently produce polyP by culturing them in media conditions where exogenous polyP was not present (i.e. media supplemented with ITS) compared to conditions where exogenous polyP was present, albeit at low concentrations (i.e. media supplemented with FBS). Detectable levels of polyP in tissue constructs and in spent media were measured in culture conditions comprising media supplemented with ITS, demonstrating that chondrocytes can independently produce polyP without the presence of exogenous polyP in culture. Next, we examined the relationship between polyP and environmental conditions provided by different culture media. Although significant differences in the levels of polyP between the constructs cultured in DMEM and Ham's F12 were detected, additional experiment replication might be required to validate these findings. To further investigate this question, we tracked changes in the concentration of key bioenergetic molecules such as glucose and lactate over a 72-hour period to assess potential relationships that may exist between polyP metabolism and glycolysis. The inverse relationship between the glucose consumption and lactate production over the 72-hour period suggests chondrocytes are undergoing anaerobic glycolysis by shunting the conversion of pyruvate to lactate. PolyP content exhibited a mild upward trend and may suggest polyP accumulation positively correlates with increasing stress conditions associated with lactate buildup. Having said this, changes in polyP levels were much more limited, therefore, it is also possible that there is no correlation between polyP and lactate levels. The changes in polyP levels could reflect an effort to replenish stores lost during media changes. Lastly, we investigate

the impact of exogenous polyP treatment on the metabolic activity of tissue constructs by assessing the changes in glucose consumption and lactate production. The administration of exogenous polyP did not elicit significant differences compared to the controls and Pi conditions, suggesting that polyP may not have an active role in influencing the glycolysis pathway. However, when we examine the metabolic activity of the cells through the Alamar blue assay, we observe elevated activity in constructs cultured in Pi while constructs cultured in polyP had a mild depletion compared to the controls. No significant differences were observed between the control, Pi, and polyP cultures; however, normalizing the metabolic activity to cell numbers could reveal differences. Additionally, these effects may be time dependent so careful consideration of the timeframe cultures are exposed to Pi and polyP, and the timepoint for sample harvest should be considered for repeat experiments. Overall, these findings suggest that the exogenous administration of polyP may affect metabolic pathways that are not directly associated with glycolysis.

### 6.2 Effect of media and media supplements on ECM accumulation in cartilage constructs

Media and media supplement composition are important considerations for cell culture work as the variations in nutrient availability and concentration can impact the cellular behavior of chondrocyte constructs and ECM accumulation. We hypothesized that combination of DMEM and FBS would promote cell proliferation, ECM synthesis, and polyP accumulation due to the higher concentration of nutrients and growth factors in both components compared to Ham's F12 and ITS. Chondrocytes cultured in a combination of DMEM and FBS, had the greatest cell proliferation and polyP accumulation across all experimental conditions. The sGAG content was recorded to be highest in the DMEM and ITS condition, however, histological assessment did not validate this finding. These findings highlight the importance of carefully selecting and

assessing the components in media and media supplements to gain an understanding of how various components could influence subsequent outcomes.

### 6.3 Effect of static compression on cartilage constructs

Static compression was used to simulate the impact of excessive mechanical loading on cartilage constructs in a sterile and prolonged manner. Compressive forces elicited a minimal decrease in cell proliferation and collagen synthesis, however, the sGAG content depleted significantly as more force was applied to the constructs. These findings are supported by previous studies conducted by Ryan et al. [179] and Timmermans et al. [192] that investigated the impact of static loading on chondrocyte proliferation and ECM synthesis, respectively. The impact of static compression on metabolic processes appears to be minimal as the glucose and lactate content in the media and polyP content in the tissues were stable across all experimental conditions. Stability in the glucose and lactate content in the media, and polyP levels in the tissue, may be due to the chondrocytes reaching a state of equilibrium within the 72-hour period before sample harvest such that the concentration of metabolites would be similar to the controls.

### 6.4 Future Work

This thesis has provided insight into how polyP metabolism can be modulated by various environmental factors; however, much remains incompletely understood about this inorganic biopolymer and its roles in cartilage biology. In the future, there will be various steps necessary to gain a comprehensive picture of polyP metabolism in chondrocytes. To develop a deeper understanding of the molecules involved in modulating polyP levels, gene expression and immunoassays of the proteins involved in polyP metabolism should be conducted to determine how the rates of polyP synthesis and breakdown differ across various conditions. There is limited knowledge of the mammalian enzymes responsible for the synthesis of polyP and this can be

further complicated by identifying the factors that can impact endogenous polyP levels. However, for initial investigation, monitoring the expression of polyphosphatases could provide insights into the dynamics of polyP metabolism.

In addition to investigating the endogenous processes involved in polyP metabolism in chondrocytes, further work should be undertaken to understand the impact of exogenous polyP administration on metabolic processes. Although the impact of exogenous polyP was examined to have a minimal impact on glucose consumption and lactate release, it should be noted that pH differences were observed in the spent media suggesting variations in metabolic activity between the conditions. Media samples were collected 72 hours after the last media change for metabolite quantifications; however, qualitative pH differences were observed 48 hours from the previous media change suggesting there may be time-dependent effects of exogenous polyP administration on chondrocyte metabolism. To gain a deeper understanding of the timeframe exogenous polyP administration has on pH and possibly metabolism, a timepoints study should be conducted to examine the potential variations of metabolites over a fixed period of 72 hours.

Another avenue to explore is the effect of polyP administration on metabolic pathways such as the TCA cycle. Although minimal differences were observed when we quantified glucose and lactate levels it is possible that polyP could influence other pathways such as the TCA cycle which could attribute to bioenergetic variations that could explain the differences in cell viability. To elucidate if polyP is involved in the TCA cycle, quantification of metabolites such as acetyl coenzyme A could be done to assess the influence polyP may have on aerobic glycolysis in chondrocytes. This work should be done through an exhaustive non-supervised metabolomics study to increase the probability of identifying relevant changes.

In regard to gaining a comprehensive understanding of the influence of static compression on chondrocyte metabolism, shorter periods of loading should be investigated to elucidate the potential short-term effects on metabolism. Stable trends observed in the glucose and lactate content between the conditions suggests the chondrocytes reach a form of equilibrium within the 72-hour period before sample harvest. To gauge whether this assumption is true, a time course evaluation should be conducted to determine the crucial timepoints chondrocytes adjust their metabolism in response to static mechanical loading. Additionally, the minimal differences in the glucose and lactate content across the experimental conditions suggests that static compression may have a minimal impact on the glycolysis pathway. Quantification of metabolites from other bioenergetic pathways such as the TCA cycle and pentose phosphate pathway should be done to get a thorough understanding of the impact static loading has on chondrocyte metabolism.

## REFERENCES

[1] Arthritis Society. (n.d.). *The Truth about Arthritis - Prevalence & Impact*. https://arthritis.ca/about-arthritis/what-is-arthritis/the-truth-about-arthritis

[2] Arthritis Society. (n.d.-a). *Arthritis Facts, Figures and Statistics*. https://arthritis.ca/about-arthritis/what-is-arthritis/arthritis-facts-and-figures

[3] Chen, D., Shen, J., Zhao, W., Wang, T., Han, L., Hamilton, J. L., & Im, H.-J. (2017). Osteoarthritis: Toward a comprehensive understanding of pathological mechanism. *Bone Research*, *5*(1), 16044. https://doi.org/10.1038/boneres.2016.44

[4] Sophia Fox, A. J., Bedi, A., & Rodeo, S. A. (2009). The Basic Science of Articular Cartilage: Structure, Composition, and Function. *Sports Health: A Multidisciplinary Approach*, *1*(6), 461–468. https://doi.org/10.1177/1941738109350438

[5] Rönn, K., Reischl, N., Gautier, E., & Jacobi, M. (2011). Current Surgical Treatment of Knee Osteoarthritis. *Arthritis*, *2011*, 1–9. https://doi.org/10.1155/2011/454873

[6] Wang, L., Yan, J., Wise, M. J., Liu, Q., Asenso, J., Huang, Y., Dai, S., Liu, Z., Du, Y., & Tang, D. (2018). Distribution Patterns of Polyphosphate Metabolism Pathway and Its Relationships With Bacterial Durability and Virulence. *Frontiers in Microbiology*, *9*, 782. https://doi.org/10.3389/fmicb.2018.00782

[7] St-Pierre, J.-P., Wang, Q., Li, S. Q., Pilliar, R. M., & Kandel, R. A. (2012). Inorganic Polyphosphate Stimulates Cartilage Tissue Formation. *Tissue Engineering Part A*, *18*(11–12), 1282–1292. https://doi.org/10.1089/ten.tea.2011.0356

[8] St-Pierre J., De Croos J., Theodoropoulos J., Willett T., Pilliar R., Grynpas M., Kandel R. Inorganic Polyphosphate exhibits chondroprotective effects in a guinea pig model of osteoarthritis. World Congress of the International Cartilage Research Society, Macau, China, 2018.

[9] Patel, J. M., Wise, B. C., Bonnevie, E. D., & Mauck, R. L. (2019). A Systematic Review and Guide to Mechanical Testing for Articular Cartilage Tissue Engineering. *Tissue Engineering Part C: Methods*, *25*(10), 593–608. https://doi.org/10.1089/ten.tec.2019.0116

[10] S., N., A., D., & Carlos, J. (2012). Mechanical Behavior of Articular Cartilage. In T. Goswami (Ed.), *Injury and Skeletal Biomechanics*. InTech. https://doi.org/10.5772/48323

[11] Bhosale, A. M., & Richardson, J. B. (2008). Articular cartilage: Structure, injuries and review of management. *British Medical Bulletin*, *87*(1), 77–95. https://doi.org/10.1093/bmb/ldn025

[12] Buckwalter, J. A., Mankin, H. J., & Grodzinsky, A. J. (2005). Articular cartilage and osteoarthritis. *Instructional Course Lectures*, *54*, 465–480.

[13] Nahian, A., & Sapra, A. (2024). Histology, Chondrocytes. In *StatPearls*. StatPearls Publishing. http://www.ncbi.nlm.nih.gov/books/NBK557576/

[14] Shoulders, M. D., & Raines, R. T. (2009). Collagen Structure and Stability. *Annual Review of Biochemistry*, *78*(1), 929–958. https://doi.org/10.1146/annurev.biochem.77.032207.120833

[15] Han, E., Chen, S. S., Klisch, S. M., & Sah, R. L. (2011). Contribution of Proteoglycan Osmotic Swelling Pressure to the Compressive Properties of Articular Cartilage. *Biophysical Journal*, *101*(4), 916–924. https://doi.org/10.1016/j.bpj.2011.07.006

[16] Pullig, O., Weseloh, G., & Swoboda, B. (1999). Expression of type VI collagen in normal and osteoarthritic human cartilage. *Osteoarthritis and Cartilage*, *7*(2), 191–202. https://doi.org/10.1053/joca.1998.0208

[17] Zelenski, N. A., Leddy, H. A., Sanchez-Adams, J., Zhang, J., Bonaldo, P., Liedtke, W., & Guilak, F. (2015). Type VI Collagen Regulates Pericellular Matrix Properties, Chondrocyte Swelling, and Mechanotransduction in Mouse Articular Cartilage. *Arthritis & Rheumatology (Hoboken, N.J.)*, *67*(5), 1286–1294. https://doi.org/10.1002/art.39034

[18] Alcaide-Ruggiero, L., Molina-Hernández, V., Granados, M. M., & Domínguez, J. M. (2021). Main and Minor Types of Collagens in the Articular Cartilage: The Role of Collagens in Repair Tissue Evaluation in Chondral Defects. *International Journal of Molecular Sciences*, *22*(24), 13329. https://doi.org/10.3390/ijms222413329

[19] Shen, G. (2005). The role of type X collagen in facilitating and regulating endochondral ossification of articular cartilage. *Orthodontics & Craniofacial Research*, *8*(1), 11–17. https://doi.org/10.1111/j.1601-6343.2004.00308.x

[20] Eschweiler, J., Horn, N., Rath, B., Betsch, M., Baroncini, A., Tingart, M., & Migliorini, F. (2021). The Biomechanics of Cartilage—An Overview. *Life*, *11*(4), 302. https://doi.org/10.3390/life11040302

[21] Mansour, J. M. (2003). Biomechanics of cartilage. *Kinesiology: the mechanics and pathomechanics of human movement*, *2*, 66-79.

[22] Kazemi, M., & Williams, J. L. (2021). Properties of Cartilage–Subchondral Bone Junctions: A Narrative Review with Specific Focus on the Growth Plate. *CARTILAGE*, *13*(2_suppl), 16S-33S. https://doi.org/10.1177/1947603520924776

[23] Wang, W., Ye, R., Xie, W., Zhang, Y., An, S., Li, Y., & Zhou, Y. (2022). Roles of the calcified cartilage layer and its tissue engineering reconstruction in osteoarthritis treatment. *Frontiers in Bioengineering and Biotechnology*, *10*, 911281. https://doi.org/10.3389/fbioe.2022.911281

[24] Eggli, P. S., Herrmann, W., Hunziker, E. B., & Schenk, R. K. (1985). Matrix compartments in the growth plate of the proximal tibia of rats. *The Anatomical Record*, *211*(3), 246–257. https://doi.org/10.1002/ar.1092110304

[25] Guilak, F., Alexopoulos, L. G., Upton, M. L., Youn, I., Choi, J. B., Cao, L., Setton, L. A., & Haider, M. A. (2006). The Pericellular Matrix as a Transducer of Biomechanical and Biochemical Signals in Articular Cartilage. *Annals of the New York Academy of Sciences*, *1068*(1), 498–512. https://doi.org/10.1196/annals.1346.011

[26] Szirmai, J. A. (1969). Aging of Connective and Skeletal Tissue. *Structure of Cartilage*, 163-200.

[27] Thorp, H., Kim, K., Kondo, M., Maak, T., Grainger, D. W., & Okano, T. (2021). Trends in Articular Cartilage Tissue Engineering: 3D Mesenchymal Stem Cell Sheets as Candidates for Engineered Hyaline-Like Cartilage. *Cells*, *10*(3), 643. https://doi.org/10.3390/cells10030643

[28] Li, G., Yin, J., Gao, J., Cheng, T. S., Pavlos, N. J., Zhang, C., & Zheng, M. H. (2013). Subchondral bone in osteoarthritis: Insight into risk factors and microstructural changes. *Arthritis Research & Therapy*, *15*(6), 223. https://doi.org/10.1186/ar4405

[29] Sanchez-Lopez, E., Coras, R., Torres, A., Lane, N. E., & Guma, M. (2022). Synovial inflammation in osteoarthritis progression. *Nature Reviews. Rheumatology*, *18*(5), 258–275. https://doi.org/10.1038/s41584-022-00749-9

[30] Chen, D., Shen, J., Zhao, W., Wang, T., Han, L., Hamilton, J. L., & Im, H.-J. (2017). Osteoarthritis: Toward a comprehensive understanding of pathological

[31] Arden, N., & Nevitt, M. (2006). Osteoarthritis: Epidemiology. *Best Practice & Research Clinical Rheumatology*, *20*(1), 3–25. https://doi.org/10.1016/j.berh.2005.09.007

[32] Molnar, V., Matišić, V., Kodvanj, I., Bjelica, R., Jeleč, Ž., Hudetz, D., Rod, E., Čukelj, F., Vrdoljak, T., Vidović, D., Starešinić, M., Sabalić, S., Dobričić, B., Petrović, T., Antičević, D., Borić, I., Košir, R., Zmrzljak, U. P., & Primorac, D. (2021). Cytokines and Chemokines Involved in Osteoarthritis Pathogenesis. *International Journal of Molecular Sciences*, *22*(17), 9208. https://doi.org/10.3390/ijms22179208

[33] Mehana, E.-S. E., Khafaga, A. F., & El-Blehi, S. S. (2019). The role of matrix metalloproteinases in osteoarthritis pathogenesis: An updated review. *Life Sciences*, *234*, 116786. https://doi.org/10.1016/j.lfs.2019.116786

[34] Akkiraju, H., & Nohe, A. (2015). Role of Chondrocytes in Cartilage Formation, Progression of Osteoarthritis and Cartilage Regeneration. *Journal of Developmental Biology*, *3*(4), 177–192. https://doi.org/10.3390/jdb3040177

[35] Mukherjee, A., & Das, B. (2024). The role of inflammatory mediators and matrix metalloproteinases (MMPs) in the progression of osteoarthritis. *Biomaterials and Biosystems*, *13*, 100090. https://doi.org/10.1016/j.bbiosy.2024.100090

[36] Loeser, R. F. (2008). Molecular mechanisms of cartilage destruction in osteoarthritis. *J Musculoskelet Neuronal Interact*, *8*(4), 303-306.

[37] Man, G. S., & Mologhianu, G. (2014). Osteoarthritis pathogenesis—A complex process that involves the entire joint. *Journal of Medicine and Life, 7*(1), 37–41.

[38] Elahi, S. A., Castro-Viñuelas, R., Tanska, P., Korhonen, R. K., Lories, R., Famaey, N., & Jonkers, I. (2023). Contribution of collagen degradation and proteoglycan depletion to cartilage degeneration in primary and secondary osteoarthritis: An in silico study. *Osteoarthritis and Cartilage, 31*(6), 741–752. https://doi.org/10.1016/j.joca.2023.01.004

[39] Sun, D., Liu, X., Xu, L., Meng, Y., Kang, H., & Li, Z. (2022). Advances in the Treatment of Partial-Thickness Cartilage Defect. *International Journal of Nanomedicine, 17*, 6275–6287. https://doi.org/10.2147/IJN.S382737

[40] Hunziker, E. B. (1999). Articular cartilage repair: Are the intrinsic biological constraints undermining this process insuperable? *Osteoarthritis and Cartilage, 7*(1), 15–28. https://doi.org/10.1053/joca.1998.0159

[41] Allaeys, C., Arnout, N., Van Onsem, S., Govaers, K., & Victor, J. (2020). Conservative treatment of knee osteoarthritis. *Acta Orthop Belg*, *86*(3), 412-421.

[42] King, L. K., March, L., & Anandacoomarasamy, A. (2013). Obesity & osteoarthritis. *The Indian Journal of Medical Research*, *138*(2), 185–193.

[43] Kong, H., Wang, X.-Q., & Zhang, X.-A. (2022). Exercise for Osteoarthritis: A Literature Review of Pathology and Mechanism. *Frontiers in Aging Neuroscience, 14*, 854026. https://doi.org/10.3389/fnagi.2022.854026

[44] Vincent, K. R., & Vincent, H. K. (2012). Resistance exercise for knee osteoarthritis. *PM & R: The Journal of Injury, Function, and Rehabilitation*, *4*(5 Suppl), S45-52. https://doi.org/10.1016/j.pmrj.2012.01.019

[45] Khosravi, M., Babaee, T., Daryabor, A., & Jalali, M. (2022). Effect of knee braces and insoles on clinical outcomes of individuals with medial knee osteoarthritis: A systematic review and meta-analysis. *Assistive Technology*, *34*(5), 501–517. https://doi.org/10.1080/10400435.2021.1880495

[46] Martin, C. L., & Browne, J. A. (2019). Intra-articular Corticosteroid Injections for Symptomatic Knee Osteoarthritis: What the Orthopaedic Provider Needs to Know. *Journal of the American Academy of Orthopaedic Surgeons*, *27*(17), e758–e766. https://doi.org/10.5435/JAAOS-D-18-00106

[47] Jüni, P., Hari, R., Rutjes, A. W., Fischer, R., Silletta, M. G., Reichenbach, S., & Da Costa, B. R. (2015). Intra-articular corticosteroid for knee osteoarthritis. *Cochrane Database of Systematic Reviews*, *2015*(11). https://doi.org/10.1002/14651858.CD005328.pub3

[48] Ayhan, E., Kesmezacar, H., & Akgun, I. (2014). Intraarticular injections (corticosteroid, hyaluronic acid, platelet rich plasma) for the knee osteoarthritis. *World Journal of Orthopedics*, *5*(3), 351–361. https://doi.org/10.5312/wjo.v5.i3.351

[49] Redondo, M. L., Waterman, B. R., Bert, J. M., & Cole, B. J. (2018). Marrow Stimulation and Augmentation. In J. Farr & A. H. Gomoll (Eds.), *Cartilage Restoration* (pp. 189–206). Springer International Publishing. https://doi.org/10.1007/978-3-319-77152-6_16

[50] Lv, Z., Cai, X., Bian, Y., Wei, Z., Zhu, W., Zhao, X., & Weng, X. (2023). Advances in Mesenchymal Stem Cell Therapy for Osteoarthritis: From Preclinical and Clinical Perspectives.

*Bioengineering (Basel, Switzerland)*, *10*(2), 195. https://doi.org/10.3390/bioengineering10020195

[51] Thoene, M., Bejer-Olenska, E., & Wojtkiewicz, J. (2023). The Current State of Osteoarthritis Treatment Options Using Stem Cells for Regenerative Therapy: A Review. *International Journal of Molecular Sciences*, *24*(10), 8925. https://doi.org/10.3390/ijms24108925

[52] Hoffman, J. K., Geraghty, S., & Protzman, N. M. (2015). Articular Cartilage Repair Using Marrow Stimulation Augmented with a Viable Chondral Allograft: 9-Month Postoperative Histological Evaluation. *Case Reports in Orthopedics*, *2015*, 1–10. https://doi.org/10.1155/2015/617365

[53] Hoemann, C. D., Guzmán-Morales, J., Picard, G., Chen, G., Veilleux, D., Chevrier, A., Sim, S., Garon, M., Quenneville, E., Lafantaisie-Favreau, C.-H., Buschmann, M. D., & Hurtig, M. B. (2020). Guided bone marrow stimulation for articular cartilage repair through a freeze-dried chitosan microparticle approach. *Materialia*, *9*, 100609. https://doi.org/10.1016/j.mtla.2020.100609

[54] Goyal, D., Keyhani, S., Lee, E. H., & Hui, J. H. P. (2013). Evidence-Based Status of Microfracture Technique: A Systematic Review of Level I and II Studies. *Arthroscopy: The Journal of Arthroscopic & Related Surgery*, *29*(9), 1579–1588. https://doi.org/10.1016/j.arthro.2013.05.027

[55] Brittberg, M. (2011). Autologous Chondrocyte Implantation. In *Cartilage Surgery* (pp. 139–146). Elsevier. https://doi.org/10.1016/B978-1-4377-0878-3.10014-2

[56] Batty, L., Dance, S., Bajaj, S., & Cole, B. J. (2011). Autologous chondrocyte implantation: An overview of technique and outcomes. *ANZ Journal of Surgery*, *81*(1–2), 18–25. https://doi.org/10.1111/j.1445-2197.2010.05495.x

[57] Pareek, A., Carey, J. L., Reardon, P. J., Peterson, L., Stuart, M. J., & Krych, A. J. (2016). Long-Term Outcomes after Autologous Chondrocyte Implantation: A Systematic Review at Mean Follow-Up of 11.4 Years. *Cartilage*, *7*(4), 298–308. https://doi.org/10.1177/1947603516630786

[58] Robinson, A., Lindsay, A., Vidal, A., & Frank, R. M. (2020). Osteochondral Autograft Transfer (OATS). *Operative Techniques in Sports Medicine*, *28*(4), 150781. https://doi.org/10.1016/j.otsm.2020.150781

[59] Branam GM, Saber AY. Osteochondral Autograft Transplantation. [Updated 2023 Jul 25]. In: StatPearls [Internet]. Treasure Island (FL): StatPearls Publishing; 2024 Jan-. Available from: https://www.ncbi.nlm.nih.gov/books/NBK560655/

[60] Kadakia, A., & Fuchs, D. (2015). Osteochondral allograft transplantation in the ankle: A review of current practice. *Orthopedic Research and Reviews*, 95. https://doi.org/10.2147/ORR.S54379

[61] Brach Del Prever, E. M., Costa, L., Piconi, C., Baricco, M., & Massè, A. (2016). Biomaterials for Total Joint Replacements. In D. G. Poitout (Ed.), *Biomechanics and Biomaterials in Orthopedics* (pp. 59–70). Springer London. https://doi.org/10.1007/978-1-84882-664-9_5

[62] Orbell, S., Espley, A., Johnston, M., & Rowley, D. (1998). Health benefits of joint replacement surgery for patients with osteoarthritis: Prospective evaluation using independent

assessments in Scotland. *Journal of Epidemiology & Community Health*, *52*(9), 564–570. https://doi.org/10.1136/jech.52.9.564

[63] Xiang, S., Zhao, Y., Li, Z., Feng, B., & Weng, X. (2019). Clinical outcomes of ceramic femoral prosthesis in total knee arthroplasty: A systematic review. *Journal of Orthopaedic Surgery and Research*, *14*(1), 57. https://doi.org/10.1186/s13018-019-1090-4

[64] Hörlesberger, N., Smolle, M. A., Leitner, L., Hauer, G., Leithner, A., & Sadoghi, P. (2023). Long-term clinical and radiological outcome of a cementless titanium-coated total knee arthroplasty system. *Archives of Orthopaedic and Trauma Surgery*, *144*(2), 847–853. https://doi.org/10.1007/s00402-023-05091-7

[65] Portillo, M. E., Salvadó, M., Alier, A., Sorli, L., Martínez, S., Horcajada, J. P., & Puig, L. (2013). Prosthesis failure within 2 years of implantation is highly predictive of infection. *Clinical Orthopaedics and Related Research*, *471*(11), 3672–3678. https://doi.org/10.1007/s11999-013-3200-7

[66] Varacallo M, Luo TD, Mabrouk A, *et al.* Total Knee Arthroplasty Techniques. [Updated 2024 May 6]. In: StatPearls [Internet]. Treasure Island (FL): StatPearls Publishing; 2024 Jan-. Available from: https://www.ncbi.nlm.nih.gov/books/NBK499896/

[67] Mody, B. S., & Mody, K. (2014). Arthroplasty in young adults: Options, techniques, trends, and results. *Current Reviews in Musculoskeletal Medicine*, *7*(2), 131–135. https://doi.org/10.1007/s12178-014-9213-3

[68] Csobonyeiova, M., Polak, S., Nicodemou, A., Zamborsky, R., & Danisovic, L. (2021). iPSCs in Modeling and Therapy of Osteoarthritis. *Biomedicines*, *9*(2), 186. https://doi.org/10.3390/biomedicines9020186

[69] Toh, W. S., Spector, M., Lee, E. H., & Cao, T. (2011). Biomaterial-Mediated Delivery of Microenvironmental Cues for Repair and Regeneration of Articular Cartilage. *Molecular Pharmaceutics*, *8*(4), 994–1001. https://doi.org/10.1021/mp100437a

[70] Raina, D. B., Qayoom, I., Larsson, D., Zheng, M. H., Kumar, A., Isaksson, H., Lidgren, L., & Tägil, M. (2019). Guided tissue engineering for healing of cancellous and cortical bone using a combination of biomaterial based scaffolding and local bone active molecule delivery. *Biomaterials*, *188*, 38–49. https://doi.org/10.1016/j.biomaterials.2018.10.004

[71] Liang, J., Liu, P., Yang, X., Liu, L., Zhang, Y., Wang, Q., & Zhao, H. (2023). Biomaterial-based scaffolds in promotion of cartilage regeneration: Recent advances and emerging applications. *Journal of Orthopaedic Translation*, *41*, 54–62. https://doi.org/10.1016/j.jot.2023.08.006

[72] Wu, X., Fan, X., Crawford, R., Xiao, Y., & Prasadam, I. (2022). The Metabolic Landscape in Osteoarthritis. *Aging and Disease*, *13*(4), 1166. https://doi.org/10.14336/AD.2021.1228

[73] Riddle, R. C., & Clemens, T. L. (2017). Bone Cell Bioenergetics and Skeletal Energy Homeostasis. *Physiological Reviews*, *97*(2), 667–698. https://doi.org/10.1152/physrev.00022.2016

[74] Wang, C., Silverman, R. M., Shen, J., & O'Keefe, R. J. (2018). Distinct metabolic programs induced by TGF-β1 and BMP2 in human articular chondrocytes with osteoarthritis. *Journal of Orthopaedic Translation*, *12*, 66–73. https://doi.org/10.1016/j.jot.2017.12.004

[75] Qu, J., Lu, D., Guo, H., Miao, W., Wu, G., & Zhou, M. (2016). PFKFB 3 modulates glycolytic metabolism and alleviates endoplasmic reticulum stress in human osteoarthritis

cartilage. *Clinical and Experimental Pharmacology and Physiology*, *43*(3), 312–318. https://doi.org/10.1111/1440-1681.12537

[76] Jiang, D., Guo, J., Liu, Y., Li, W., & Lu, D. (2024). Glycolysis: An emerging regulator of osteoarthritis. *Frontiers in Immunology*, *14*, 1327852. https://doi.org/10.3389/fimmu.2023.1327852

[77] Yang, X., Chen, W., Zhao, X., Chen, L., Li, W., Ran, J., & Wu, L. (2018). Pyruvate Kinase M2 Modulates the Glycolysis of Chondrocyte and Extracellular Matrix in Osteoarthritis. *DNA and Cell Biology*, *37*(3), 271–277. https://doi.org/10.1089/dna.2017.4048

[78] High, R. A., Ji, Y., Ma, Y.-J., Tang, Q., Murphy, M. E., Du, J., & Chang, E. Y. (2019). In vivo assessment of extracellular pH of joint tissues using acidoCEST-UTE MRI. *Quantitative Imaging in Medicine and Surgery*, *9*(10), 1664–1673. https://doi.org/10.21037/qims.2019.08.11

[79] Arra, M., Swarnkar, G., Ke, K., Otero, J. E., Ying, J., Duan, X., Maruyama, T., Rai, M. F., O'Keefe, R. J., Mbalaviele, G., Shen, J., & Abu-Amer, Y. (2020). LDHA-mediated ROS generation in chondrocytes is a potential therapeutic target for osteoarthritis. *Nature Communications*, *11*(1), 3427. https://doi.org/10.1038/s41467-020-17242-0

[80] Haseeb, A., Makki, M. S., & Haqqi, T. M. (2014). Modulation of Ten-Eleven Translocation 1 (TET1), Isocitrate Dehydrogenase (IDH) Expression, α-Ketoglutarate (α-KG), and DNA Hydroxymethylation Levels by Interleukin-1β in Primary Human Chondrocytes. *Journal of Biological Chemistry*, *289*(10), 6877–6885. https://doi.org/10.1074/jbc.M113.512269

[81] Liu, L., Zhang, W., Liu, T., Tan, Y., Chen, C., Zhao, J., Geng, H., & Ma, C. (2023). The physiological metabolite α-ketoglutarate ameliorates osteoarthritis by regulating mitophagy and oxidative stress. *Redox Biology*, *62*, 102663. https://doi.org/10.1016/j.redox.2023.102663

[82] Zheng, L., Zhang, Z., Sheng, P., & Mobasheri, A. (2021). The role of metabolism in chondrocyte dysfunction and the progression of osteoarthritis. *Ageing Research Reviews*, *66*, 101249. https://doi.org/10.1016/j.arr.2020.101249

[83] Orang, A. V., Petersen, J., McKinnon, R. A., & Michael, M. Z. (2019). Micromanaging aerobic respiration and glycolysis in cancer cells. *Molecular Metabolism*, *23*, 98–126. https://doi.org/10.1016/j.molmet.2019.01.014

[84] Melkonian EA, Schury MP. Biochemistry, Anaerobic Glycolysis. [Updated 2023 Jul 31]. In: StatPearls [Internet]. Treasure Island (FL): StatPearls Publishing; 2024 Jan-. Available from: https://www.ncbi.nlm.nih.gov/books/NBK546695/

[85] Bar-Even, A., Flamholz, A., Noor, E., & Milo, R. (2012). Rethinking glycolysis: On the biochemical logic of metabolic pathways. *Nature Chemical Biology*, *8*(6), 509–517. https://doi.org/10.1038/nchembio.971

[86] Denkert, C., Budczies, J., Weichert, W., Wohlgemuth, G., Scholz, M., Kind, T., Niesporek, S., Noske, A., Buckendahl, A., Dietel, M., & Fiehn, O. (2008). Metabolite profiling of human colon carcinoma – deregulation of TCA cycle and amino acid turnover. *Molecular Cancer*, *7*(1), 72. https://doi.org/10.1186/1476-4598-7-72

[87] Martínez-Reyes, I., & Chandel, N. S. (2020). Mitochondrial TCA cycle metabolites control physiology and disease. *Nature Communications*, *11*(1), 102. https://doi.org/10.1038/s41467-019-13668-3

[88] Blanco, F. J., Rego, I., & Ruiz-Romero, C. (2011). The role of mitochondria in osteoarthritis. *Nature Reviews Rheumatology*, *7*(3), 161–169. https://doi.org/10.1038/nrrheum.2010.213

[89] Liu, H., Li, Z., Cao, Y., Cui, Y., Yang, X., Meng, Z., & Wang, R. (2019). Effect of chondrocyte mitochondrial dysfunction on cartilage degeneration: A possible pathway for osteoarthritis pathology at the subcellular level. *Molecular Medicine Reports*. https://doi.org/10.3892/mmr.2019.10559

[90] Zorova, L. D., Popkov, V. A., Plotnikov, E. Y., Silachev, D. N., Pevzner, I. B., Jankauskas, S. S., Babenko, V. A., Zorov, S. D., Balakireva, A. V., Juhaszova, M., Sollott, S. J., & Zorov, D. B. (2018). Mitochondrial membrane potential. *Analytical Biochemistry*, *552*, 50–59. https://doi.org/10.1016/j.ab.2017.07.009

[91] Christ, J. J., Willbold, S., & Blank, L. M. (2019). Polyphosphate Chain Length Determination in the Range of Two to Several Hundred P-Subunits with a New Enzyme Assay and $^{31}$ P NMR. *Analytical Chemistry*, *91*(12), 7654–7661. https://doi.org/10.1021/acs.analchem.9b00567

[92] Yeon, J. H., Mazinani, N., Schlappi, T. S., Chan, K. Y. T., Baylis, J. R., Smith, S. A., Donovan, A. J., Kudela, D., Stucky, G. D., Liu, Y., Morrissey, J. H., & Kastrup, C. J. (2017). Localization of Short-Chain Polyphosphate Enhances its Ability to Clot Flowing Blood Plasma. *Scientific Reports*, *7*(1), 42119. https://doi.org/10.1038/srep42119

[93] Kornberg, A., Rao, N. N., & Ault-Riché, D. (1999). Inorganic Polyphosphate: A Molecule of Many Functions. *Annual Review of Biochemistry*, *68*(1), 89–125. https://doi.org/10.1146/annurev.biochem.68.1.89

[94] Ault-Riché, D., Fraley, C. D., Tzeng, C.-M., & Kornberg, A. (1998). Novel Assay Reveals Multiple Pathways Regulating Stress-Induced Accumulations of Inorganic Polyphosphate in

*Escherichia coli*. *Journal of Bacteriology*, *180*(7), 1841–1847. https://doi.org/10.1128/JB.180.7.1841-1847.1998

[95] Magkiriadou, S., Stepp, W. L., Newman, D. K., Manley, S., & Racki, L. R. (2024). Polyphosphate affects cytoplasmic and chromosomal dynamics in nitrogen-starved *Pseudomonas aeruginosa*. *Proceedings of the National Academy of Sciences*, *121*(15), e2313004121. https://doi.org/10.1073/pnas.2313004121

[96] Racki, L. R., Tocheva, E. I., Dieterle, M. G., Sullivan, M. C., Jensen, G. J., & Newman, D. K. (2017). Polyphosphate granule biogenesis is temporally and functionally tied to cell cycle exit during starvation in *Pseudomonas aeruginosa*. *Proceedings of the National Academy of Sciences*, *114*(12). https://doi.org/10.1073/pnas.1615575114

[97] Gray, M. J., & Jakob, U. (2015). Oxidative stress protection by polyphosphate—New roles for an old player. *Current Opinion in Microbiology*, *24*, 1–6. https://doi.org/10.1016/j.mib.2014.12.004

[98] McGrath, J. W., & Quinn, J. P. (2000). Intracellular accumulation of polyphosphate by the yeast Candida humicola G-1 in response to acid pH. *Applied and Environmental Microbiology*, *66*(9), 4068–4073. https://doi.org/10.1128/AEM.66.9.4068-4073.2000

[99] Baev, A. Y., Negoda, A., & Abramov, A. Y. (2017). Modulation of mitochondrial ion transport by inorganic polyphosphate—Essential role in mitochondrial permeability transition pore. *Journal of Bioenergetics and Biomembranes*, *49*(1), 49–55. https://doi.org/10.1007/s10863-016-9650-3

[100] Solesio, M. E., Xie, L., McIntyre, B., Ellenberger, M., Mitaishvili, E., Bhadra-Lobo, S., Bettcher, L. F., Bazil, J. N., Raftery, D., Jakob, U., & Pavlov, E. V. (2021). Depletion of

mitochondrial inorganic polyphosphate (polyP) in mammalian cells causes metabolic shift from oxidative phosphorylation to glycolysis. *The Biochemical Journal*, *478*(8), 1631–1646. https://doi.org/10.1042/BCJ20200975

[101] Seidlmayer, L. K., & Dedkova, E. N. (2016). Inorganic Polyphosphates in the Mitochondria of Mammalian Cells. In T. Kulakovskaya, E. Pavlov, & E. N. Dedkova (Eds.), *Inorganic Polyphosphates in Eukaryotic Cells* (pp. 91–114). Springer International Publishing. https://doi.org/10.1007/978-3-319-41073-9_7

[102] Domingues, G., Moraes, J., Fonseca, R. N. D., & Campos, E. (2023). Inorganic polyphosphate's role in energy production and mitochondrial permeability transition pore opening in tick mitochondria. *Archives of Insect Biochemistry and Physiology*, *114*(1), e22029. https://doi.org/10.1002/arch.22029

[103] Kus, F., Smolenski, R. T., & Tomczyk, M. (2022). Inorganic Polyphosphate—Regulator of Cellular Metabolism in Homeostasis and Disease. *Biomedicines*, *10*(4), 913. https://doi.org/10.3390/biomedicines10040913

[104] Rao, N. N., & Kornberg, A. (1999). Inorganic Polyphosphate Regulates Responses of Escherichia coli to Nutritional Stringencies, Environmental Stresses and Survival in the Stationary Phase. In H. C. Schröder & W. E. G. Müller (Eds.), *Inorganic Polyphosphates* (Vol. 23, pp. 183–195). Springer Berlin Heidelberg. https://doi.org/10.1007/978-3-642-58444-2_9

[105] Achbergerová, L., & Nahálka, J. (2011). Polyphosphate—An ancient energy source and active metabolic regulator. *Microbial Cell Factories*, *10*, 63. https://doi.org/10.1186/1475-2859-10-63

[106] Wang, L., Yan, J., Wise, M. J., Liu, Q., Asenso, J., Huang, Y., Dai, S., Liu, Z., Du, Y., & Tang, D. (2018). Distribution Patterns of Polyphosphate Metabolism Pathway and Its Relationships With Bacterial Durability and Virulence. *Frontiers in Microbiology*, *9*, 782. https://doi.org/10.3389/fmicb.2018.00782

[107] Tomashevsky, A., Kulakovskaya, E., Trilisenko, L., Kulakovskiy, I. V., Kulakovskaya, T., Fedorov, A., & Eldarov, M. (2021). VTC4 Polyphosphate Polymerase Knockout Increases Stress Resistance of Saccharomyces cerevisiae Cells. *Biology*, *10*(6), 487. https://doi.org/10.3390/biology10060487

[108] Gerasimaitė, R., Sharma, S., Desfougères, Y., Schmidt, A., & Mayer, A. (2014). Coupled synthesis and translocation restrains polyphosphate to acidocalcisome-like vacuoles and prevents its toxicity. *Journal of Cell Science*, jcs.159772. https://doi.org/10.1242/jcs.159772

[109] Liu, W., Wang, J., Comte-Miserez, V., Zhang, M., Yu, X., Chen, Q., Jessen, H. J., Mayer, A., Wu, S., & Ye, S. (2023). Cryo-EM structure of the polyphosphate polymerase VTC reveals coupling of polymer synthesis to membrane transit. *The EMBO Journal*, *42*(10), e113320. https://doi.org/10.15252/embj.2022113320

[110] Wild, R., Gerasimaite, R., Jung, J.-Y., Truffault, V., Pavlovic, I., Schmidt, A., Saiardi, A., Jessen, H. J., Poirier, Y., Hothorn, M., & Mayer, A. (2016). Control of eukaryotic phosphate homeostasis by inositol polyphosphate sensor domains. *Science*, *352*(6288), 986–990. https://doi.org/10.1126/science.aad9858

[111] Morrissey, J. H., Choi, S. H., & Smith, S. A. (2012). Polyphosphate: An ancient molecule that links platelets, coagulation, and inflammation. *Blood*, *119*(25), 5972–5979. https://doi.org/10.1182/blood-2012-03-306605

[112] Malde, A., Gangaiah, D., Chandrashekhar, K., Pina-Mimbela, R., Torrelles, J. B., & Rajashekara, G. (2014). Functional characterization of exopolyphosphatase/guanosine pentaphosphate phosphohydrolase (PPX/GPPA) of Campylobacter jejuni. *Virulence*, *5*(4), 521–533. https://doi.org/10.4161/viru.28311

[113] Paula, F. S., Chin, J. P., Schnürer, A., Müller, B., Manesiotis, P., Waters, N., Macintosh, K. A., Quinn, J. P., Connolly, J., Abram, F., McGrath, J. W., & O'Flaherty, V. (2019). The potential for polyphosphate metabolism in Archaea and anaerobic polyphosphate formation in Methanosarcina mazei. *Scientific Reports*, *9*(1), 17101. https://doi.org/10.1038/s41598-019-53168-4

[114] Wurst, H., Shiba, T., & Kornberg, A. (1995). The gene for a major exopolyphosphatase of Saccharomyces cerevisiae. *Journal of Bacteriology*, *177*(4), 898–906. https://doi.org/10.1128/jb.177.4.898-906.1995

[115] Sethuraman, A., Rao, N. N., & Kornberg, A. (2001). The endopolyphosphatase gene: Essential in *Saccharomyces cerevisiae*. *Proceedings of the National Academy of Sciences*, *98*(15), 8542–8547. https://doi.org/10.1073/pnas.151269398

[116] Andreeva, N., Trilisenko, L., Eldarov, M., & Kulakovskaya, T. (2015). Polyphosphatase PPN1 of Saccharomyces cerevisiae: Switching of exopolyphosphatase and endopolyphosphatase activities. *PloS One*, *10*(3), e0119594. https://doi.org/10.1371/journal.pone.0119594

[117] Andreeva, N., Ledova, L., Ryazanova, L., Tomashevsky, A., Kulakovskaya, T., & Eldarov, M. (2019). Ppn2 endopolyphosphatase overexpressed in Saccharomyces cerevisiae: Comparison with Ppn1, Ppx1, and Ddp1 polyphosphatases. *Biochimie*, *163*, 101–107. https://doi.org/10.1016/j.biochi.2019.06.001

[118] Kumble, K. D., & Kornberg, A. (1996). Endopolyphosphatases for Long Chain Inorganic Polyphosphate in Yeast and Mammals. *Journal of Biological Chemistry*, *271*(43), 27146–27151. https://doi.org/10.1074/jbc.271.43.27146

[119] Akiyama, M., Crooke, E., & Kornberg, A. (1993). An exopolyphosphatase of Escherichia coli. The enzyme and its ppx gene in a polyphosphate operon. *The Journal of Biological Chemistry*, *268*(1), 633–639.

[120] Kulakovskaya, T. V., Andreeva, N. A., Ledova, L. A., Ryazanova, L. P., Trilisenko, L. V., & Eldarov, M. A. (2021). Enzymes of Polyphosphate Metabolism in Yeast: Properties, Functions, Practical Significance. *Biochemistry (Moscow)*, *86*(S1), S96–S108. https://doi.org/10.1134/S0006297921140078

[121] Müller, W. E. G., Wang, S., Neufurth, M., Schröder, H. C., & Wang, X. (2023). Physiological Polyphosphate: A New Molecular Paradigm in Biomedical and Biocomputational Applications for Human Therapy. In I. Rojas, O. Valenzuela, F. Rojas Ruiz, L. J. Herrera, & F. Ortuño (Eds.), *Bioinformatics and Biomedical Engineering* (Vol. 13919, pp. 542–559). Springer Nature Switzerland. https://doi.org/10.1007/978-3-031-34953-9_42

[122] Mikami, Y., Tsuda, H., Akiyama, Y., Honda, M., Shimizu, N., Suzuki, N., & Komiyama, K. (2016). Alkaline phosphatase determines polyphosphate-induced mineralization in a cell-type independent manner. *Journal of Bone and Mineral Metabolism*, *34*(6), 627–637. https://doi.org/10.1007/s00774-015-0719-6

[123] Sharma, U., Pal, D., & Prasad, R. (2014). Alkaline phosphatase: An overview. *Indian Journal of Clinical Biochemistry: IJCB*, *29*(3), 269–278. https://doi.org/10.1007/s12291-013-0408-y

[124] Bondy-Chorney, E., Abramchuk, I., Nasser, R., Holinier, C., Denoncourt, A., Baijal, K., McCarthy, L., Khacho, M., Lavallée-Adam, M., & Downey, M. (2020). A Broad Response to Intracellular Long-Chain Polyphosphate in Human Cells. *Cell Reports*, *33*(4), 108318. https://doi.org/10.1016/j.celrep.2020.108318

[125] Christ, J. J., Willbold, S., & Blank, L. M. (2020). Methods for the Analysis of Polyphosphate in the Life Sciences. *Analytical Chemistry*, *92*(6), 4167–4176. https://doi.org/10.1021/acs.analchem.9b05144

[126] Lee, W. D., Gawri, R., Shiba, T., Ji, A.-R., Stanford, W. L., & Kandel, R. A. (2018). Simple Silica Column–Based Method to Quantify Inorganic Polyphosphates in Cartilage and Other Tissues. *CARTILAGE*, *9*(4), 417–427. https://doi.org/10.1177/1947603517690856

[127] Beauvoit, B., Rigoulet, M., Guerin, B., & Canioni, P. (1989). Polyphosphates as a source of high energy phosphates in yeast mitochondria: A $^{31}$ P NMR study. *FEBS Letters*, *252*(1–2), 17–21. https://doi.org/10.1016/0014-5793(89)80882-8

[128] Castro, C. D., Meehan, A. J., Koretsky, A. P., & Domach, M. M. (1995). In situ 31P nuclear magnetic resonance for observation of polyphosphate and catabolite responses of chemostat-cultivated Saccharomyces cerevisiae after alkalinization. *Applied and Environmental Microbiology*, *61*(12), 4448–4453. https://doi.org/10.1128/aem.61.12.4448-4453.1995

[129] Bru, S., Jimenez, J., Canadell, D., Arino, J., & Clotet, J. (2017). Improvement of biochemical methods of polyP quantification. *Microbial Cell*, *4*(1), 6–15. https://doi.org/10.15698/mic2017.01.551

[130] Ohtomo, R., Sekiguchi, Y., Kojima, T., & Saito, M. (2008). Different chain length specificity among three polyphosphate quantification methods. *Analytical Biochemistry*, *383*(2), 210–216. https://doi.org/10.1016/j.ab.2008.08.002

[131] Gerhardt, P. (Ed.). (1994). *Methods for general and molecular bacteriology*. American Society for Microbiology.

[132] Eikelboom, D., & van Buijsen, H. (Ed.) (1981). *Microscopic Sludge Investigation Manual*, (pp. 45). TNO Research Institute for Environmental Hygiene: Delft, The Netherlands.

[133] Loosdrecht, M. C. M. van, Nielsen, P. H., Lopez-Vazquez, C. M., & Brdjanovic, D. (Eds.). (2016). *Experimental methods in wastewater treatment*. (pp. 274). IWA Publishing.

[134] Gomes, F. M., Ramos, I. B., Wendt, C., Girard-Dias, W., De Souza, W., Machado, E. A., & Miranda, K. (2013). New insights into the in situ microscopic visualization and quantification of inorganic polyphosphate stores by 4’,6-diamidino-2-phenylindole (DAPI)-staining. *European Journal of Histochemistry*, *57*(4), 34. https://doi.org/10.4081/ejh.2013.e34

[135] Allan, R. A., & Miller, J. J. (1980). Influence of *S* -adenosylmethionine on DAPI-induced fluorescence of polyphosphate in the yeast vacuole. *Canadian Journal of Microbiology*, *26*(8), 912–920. https://doi.org/10.1139/m80-158

[136] Smith, S. A., & Morrissey, J. H. (2007). Sensitive fluorescence detection of polyphosphate in polyacrylamide gels using 4′,6-diamidino-2-phenylindol. *ELECTROPHORESIS*, *28*(19), 3461–3465. https://doi.org/10.1002/elps.200700041

[137] Angelova, P. R., Agrawalla, B. K., Elustondo, P. A., Gordon, J., Shiba, T., Abramov, A. Y., Chang, Y.-T., & Pavlov, E. V. (2014). In Situ Investigation of Mammalian Inorganic

Polyphosphate Localization Using Novel Selective Fluorescent Probes JC-D7 and JC-D8. *ACS Chemical Biology*, *9*(9), 2101–2110. https://doi.org/10.1021/cb5000696

[138] De Jager, H.-J., & Heyns, A. M. (1998). Study of the Hydrolysis of Sodium Polyphosphate in Water Using Raman Spectroscopy. *Applied Spectroscopy*, *52*(6), 808–814. https://doi.org/10.1366/0003702981944535

[139] Majed, N., Matthäus, C., Diem, M., & Gu, A. Z. (2009). Evaluation of Intracellular Polyphosphate Dynamics in Enhanced Biological Phosphorus Removal Process using Raman Microscopy. *Environmental Science & Technology*, *43*(14), 5436–5442. https://doi.org/10.1021/es900251n

[140] Moudříková, Š., Sadowsky, A., Metzger, S., Nedbal, L., Mettler-Altmann, T., & Mojzeš, P. (2017). Quantification of Polyphosphate in Microalgae by Raman Microscopy and by a Reference Enzymatic Assay. *Analytical Chemistry*, *89*(22), 12006–12013. https://doi.org/10.1021/acs.analchem.7b02393

[141] Moudříková, Š., Mojzeš, P., Zachleder, V., Pfaff, C., Behrendt, D., & Nedbal, L. (2016). Raman and fluorescence microscopy sensing energy-transducing and energy-storing structures in microalgae. *Algal Research*, *16*, 224–232. https://doi.org/10.1016/j.algal.2016.03.016

[142] Smith, S. A., Wang, Y., & Morrissey, J. H. (2018). DNA ladders can be used to size polyphosphate resolved by polyacrylamide gel electrophoresis. *ELECTROPHORESIS*, *39*(19), 2454–2459. https://doi.org/10.1002/elps.201800227

[143] Goldberg, R. L., & Kolibas, L. M. (1990). An Improved Method for Determining Proteoglycans Synthesized by Chondrocytes in Culture. *Connective Tissue Research*, *24*(3–4), 265–275. https://doi.org/10.3109/03008209009152154

[144] Berg, R. A. (1982). [17] Determination of 3- and 4-hydroxyproline. In *Methods in Enzymology* (Vol. 82, pp. 372–398). Elsevier. https://doi.org/10.1016/0076-6879(82)82074-0

[145] Cheng, Y.-S., Seibert, O., Klöting, N., Dietrich, A., Straßburger, K., Fernández-Veledo, S., Vendrell, J. J., Zorzano, A., Blüher, M., Herzig, S., Berriel Diaz, M., & Teleman, A. A. (2015). PPP2R5C Couples Hepatic Glucose and Lipid Homeostasis. *PLOS Genetics*, *11*(10), e1005561. https://doi.org/10.1371/journal.pgen.1005561

[146] Ushiki, T., Mochizuki, T., Suzuki, K., Kamimura, M., Ishiguro, H., Suwabe, T., & Kawase, T. (2022). Modulation of ATP Production Influences Inorganic Polyphosphate Levels in Non-Athletes' Platelets at the Resting State. *International Journal of Molecular Sciences*, *23*(19), 11293. https://doi.org/10.3390/ijms231911293

[147] *Dulbecco's Modified Eagle Medium F12 (DMEM F12) | Thermo Fisher Scientific - IE*. (n.d.). https://www.thermofisher.com/ca/en/home/life-science/cell-culture/mammalian-cell-culture/cell-culture-media/dmem-f12.html#:~:text=DMEM%20alone%20is%20rich%20in,more%20standard%20basal%20media%20formulations.

[148] Vultaggio-Poma, V., Scussel Bergamin, L., Falzoni, S., Tarantini, M., Giuliani, A. L., Sandonà, D., Polverino De Laureto, P., & Di Virgilio, F. (2024). Fetal bovine serum contains biologically available ATP. *Purinergic Signalling*, *20*(1), 83–89. https://doi.org/10.1007/s11302-023-09941-2

[149] Bilgen, B., Orsini, E., Aaron, R. K., & Ciombor, D. McK. (2007). FBS suppresses TGF-β1-induced chondrogenesis in synoviocyte pellet cultures while dexamethasone and dynamic

stimuli are beneficial. *Journal of Tissue Engineering and Regenerative Medicine*, *1*(6), 436–442. https://doi.org/10.1002/term.56

[150] Pi, P., Zeng, L., Zeng, Z., Zong, K., Han, B., Bai, X., & Wang, Y. (2024). The role of targeting glucose metabolism in chondrocytes in the pathogenesis and therapeutic mechanisms of osteoarthritis: A narrative review. *Frontiers in Endocrinology*, *15*, 1319827. https://doi.org/10.3389/fendo.2024.1319827

[151] Li, Q., Wen, Y., Wang, L., Chen, B., Chen, J., Wang, H., & Chen, L. (2021). Hyperglycemia-induced accumulation of advanced glycosylation end products in fibroblast-like synoviocytes promotes knee osteoarthritis. *Experimental & Molecular Medicine*, *53*(11), 1735–1747. https://doi.org/10.1038/s12276-021-00697-6

[152] He, C.-P., Chen, C., Jiang, X.-C., Li, H., Zhu, L.-X., Wang, P.-X., & Xiao, T. (2022). The role of AGEs in pathogenesis of cartilage destruction in osteoarthritis. *Bone & Joint Research*, *11*(5), 292–300. https://doi.org/10.1302/2046-3758.115.BJR-2021-0334.R1

[153] Oyinlade, O., Wei, S., Lal, B., Laterra, J., Zhu, H., Goodwin, C. R., Wang, S., Ma, D., Wan, J., & Xia, S. (2018). Targeting UDP-α-d-glucose 6-dehydrogenase inhibits glioblastoma growth and migration. *Oncogene*, *37*(20), 2615–2629. https://doi.org/10.1038/s41388-018-0138-y

[154] Kelley, K. M., Johnson, T. R., Ilan, J., & Moskowitz, R. W. (1999). Glucose regulation of the IGF response system in chondrocytes: Induction of an IGF-I-resistant state. *American Journal of Physiology-Regulatory, Integrative and Comparative Physiology*, *276*(4), R1164–R1171. https://doi.org/10.1152/ajpregu.1999.276.4.R1164

[155] Leonard, C. M., Bergman, M., Frenz, D. A., Macreery, L. A., & Newman, S. A. (1989). Abnormal ambient glucose levels inhibit proteoglycan core protein gene expression and reduce proteoglycan accumulation during chondrogenesis: Possible mechanism for teratogenic effects of maternal diabetes. *Proceedings of the National Academy of Sciences*, *86*(24), 10113–10117. https://doi.org/10.1073/pnas.86.24.10113

[156] Stegen, S., Rinaldi, G., Loopmans, S., Stockmans, I., Moermans, K., Thienpont, B., Fendt, S.-M., Carmeliet, P., & Carmeliet, G. (2020). Glutamine Metabolism Controls Chondrocyte Identity and Function. *Developmental Cell*, *53*(5), 530-544.e8. https://doi.org/10.1016/j.devcel.2020.05.001

[157] *Ham's F-12 Nutrient Mix | Thermo Fisher Scientific - IE*. (n.d.). https://www.thermofisher.com/ca/en/home/technical-resources/media-formulation.64.html

[158] *DMEM, high glucose | Thermo Fisher Scientific - IE*. (n.d.). https://www.thermofisher.com/ca/en/home/technical-resources/media-formulation.8.html

[159] Liu, X., Liu, J., Kang, N., Yan, L., Wang, Q., Fu, X., Zhang, Y., Xiao, R., & Cao, Y. (2014). Role of Insulin-Transferrin-Selenium in Auricular Chondrocyte Proliferation and Engineered Cartilage Formation in Vitro. *International Journal of Molecular Sciences*, *15*(1), 1525–1537. https://doi.org/10.3390/ijms15011525

[160] Li, T.-F. (2005). TGF-b signaling in chondrocytes. *Frontiers in Bioscience*, *10*(1–3), 681. https://doi.org/10.2741/1563

[161] Liu, X., Zhang, T., Wang, R., Shi, P., Pan, B., & Pang, X. (2019). Insulin-Transferrin-Selenium as a Novel Serum-free Media Supplement for the Culture of Human Amnion Mesenchymal Stem Cells. *Annals of Clinical and Laboratory Science*, *49*(1), 63–71.

[162] Ladner, Y. D., Alini, M., & Armiento, A. R. (2023). The Dimethylmethylene Blue Assay (DMMB) for the Quantification of Sulfated Glycosaminoglycans. In M. J. Stoddart, E. Della Bella, & A. R. Armiento (Eds.), *Cartilage Tissue Engineering* (Vol. 2598, pp. 115–121). Springer US. https://doi.org/10.1007/978-1-0716-2839-3_9

[163] Garcés, P., Amaro, A., Montecino, M., & Van Zundert, B. (2024). Inorganic polyphosphate: From basic research to diagnostic and therapeutic opportunities in ALS/FTD. *Biochemical Society Transactions*, *52*(1), 123–135. https://doi.org/10.1042/BST20230257

[164] Hollander, J. M., & Zeng, L. (2019). The Emerging Role of Glucose Metabolism in Cartilage Development. *Current Osteoporosis Reports*, *17*(2), 59–69. https://doi.org/10.1007/s11914-019-00506-0

[165] Lee, R. B., Wilkins, R. J., Razaq, S., & Urban, J. P. G. (2002). The effect of mechanical stress on cartilage energy metabolism. *Biorheology*, *39*(1–2), 133–143.

[166] Lee, M. H., Malloy, C. R., Corbin, I. R., Li, J., & Jin, E. S. (2019). Assessing the pentose phosphate pathway using [2, 3- $^{13}C_2$ ]glucose. *NMR in Biomedicine*, *32*(6), e4096. https://doi.org/10.1002/nbm.4096

[167] Adam, M. S., Zhuang, H., Ren, X., Zhang, Y., & Zhou, P. (2024). The metabolic characteristics and changes of chondrocytes in vivo and in vitro in osteoarthritis. *Frontiers in Endocrinology*, *15*, 1393550. https://doi.org/10.3389/fendo.2024.1393550

[168] Zielke, H. R., Sumbilla, C. M., Sevdalian, D. A., Hawkins, R. L., & Ozand, P. T. (1980). Lactate: A major product of glutamine metabolism by human diploid fibroblasts. *Journal of Cellular Physiology*, *104*(3), 433–441. https://doi.org/10.1002/jcp.1041040316

[169] Reitzer, L. J., Wice, B. M., & Kennell, D. (1979). Evidence that glutamine, not sugar, is the major energy source for cultured HeLa cells. *The Journal of Biological Chemistry*, *254*(8), 2669–2676.

[170] Li, X., Yang, Y., Zhang, B., Lin, X., Fu, X., An, Y., Zou, Y., Wang, J.-X., Wang, Z., & Yu, T. (2022). Lactate metabolism in human health and disease. *Signal Transduction and Targeted Therapy*, *7*(1), 305. https://doi.org/10.1038/s41392-022-01151-3

[171] Calì, C., Tauffenberger, A., & Magistretti, P. (2019). The Strategic Location of Glycogen and Lactate: From Body Energy Reserve to Brain Plasticity. *Frontiers in Cellular Neuroscience*, *13*, 82. https://doi.org/10.3389/fncel.2019.00082

[172] Heywood, H. K., Bader, D. L., & Lee, D. A. (2006). Glucose Concentration and Medium Volume Influence Cell Viability and Glycosaminoglycan Synthesis in Chondrocyte-Seeded Alginate Constructs. *Tissue Engineering*, *12*(12), 3487–3496. https://doi.org/10.1089/ten.2006.12.3487

[173] Rajpurohit, R., Mansfield, K., Ohyama, K., Ewert, D., & Shapiro, I. M. (1999). Chondrocyte death is linked to development of a mitochondrial membrane permeability transition in the growth plate. *Journal of Cellular Physiology*, *179*(3), 287–296. https://doi.org/10.1002/(SICI)1097-4652(199906)179:3<287::AID-JCP6>3.0.CO;2-T

[174] A. Mullan, J. P. Quinn, & J. W. McGrath. (2002). Enhanced Phosphate Uptake and Polyphosphate Accumulation in Burkholderia cepacia Grown under Low-pH Conditions. *Microbial Ecology*, *44*(1), 69–77. http://www.jstor.org/stable/4287632

[175] Xie, L., Rajpurkar, A., Quarles, E., Taube, N., Rai, A. S., Erba, J., Sliwinski, B., Markowitz, M., Jakob, U., & Knoefler, D. (2019). Accumulation of Nucleolar Inorganic

Polyphosphate Is a Cellular Response to Cisplatin-Induced Apoptosis. *Frontiers in Oncology*, *9*, 1410. https://doi.org/10.3389/fonc.2019.01410

[176] Jimenez-Nunez, M. D., Moreno-Sanchez, D., Hernandez-Ruiz, L., Benitez-Rondan, A., Ramos-Amaya, A., Rodriguez-Bayona, B., Medina, F., Brieva, J. A., & Ruiz, F. A. (2012). Myeloma cells contain high levels of inorganic polyphosphate which is associated with nucleolar transcription. *Haematologica*, *97*(8), 1264–1271. https://doi.org/10.3324/haematol.2011.051409

[177] Leipzig, N. D., & Athanasiou, K. A. (2008). Static compression of single chondrocytes catabolically modifies single-cell gene expression. *Biophysical Journal*, *94*(6), 2412–2422. https://doi.org/10.1529/biophysj.107.114207

[178] Davisson, T., Kunig, S., Chen, A., Sah, R., & Ratcliffe, A. (2002). Static and dynamic compression modulate matrix metabolism in tissue engineered cartilage. *Journal of Orthopaedic Research*, *20*(4), 842–848. https://doi.org/10.1016/S0736-0266(01)00160-7

[179] Ryan, J. A., Eisner, E. A., DuRaine, G., You, Z., & Reddi, A. H. (2009). Mechanical compression of articular cartilage induces chondrocyte proliferation and inhibits proteoglycan synthesis by activation of the ERK pathway: Implications for tissue engineering and regenerative medicine. *Journal of Tissue Engineering and Regenerative Medicine*, *3*(2), 107–116. https://doi.org/10.1002/term.146

[180] Chen, Z., Yue, S. X., Zhou, G., Greenfield, E. M., & Murakami, S. (2015). ERK1 and ERK2 Regulate Chondrocyte Terminal Differentiation During Endochondral Bone Formation. *Journal of Bone and Mineral Research*, *30*(5), 765–774. https://doi.org/10.1002/jbmr.2409

[181] Wang, X., Xue, Y., Ye, W., Pang, J., Liu, Z., Cao, Y., Zheng, Y., & Ding, D. (2018). The MEK-ERK1/2 signaling pathway regulates hyaline cartilage formation and the redifferentiation

of dedifferentiated chondrocytes in vitro. *American Journal of Translational Research*, *10*(10), 3068–3085.

[182] Zhao, Z., Li, Y., Wang, M., Zhao, S., Zhao, Z., & Fang, J. (2020). Mechanotransduction pathways in the regulation of cartilage chondrocyte homoeostasis. *Journal of Cellular and Molecular Medicine*, *24*(10), 5408–5419. https://doi.org/10.1111/jcmm.15204

[183] Lu, N., & Malemud, C. J. (2019). Extracellular Signal-Regulated Kinase: A Regulator of Cell Growth, Inflammation, Chondrocyte and Bone Cell Receptor-Mediated Gene Expression. *International Journal of Molecular Sciences*, *20*(15), 3792. https://doi.org/10.3390/ijms20153792

[184] Abarrategi, A., Gambera, S., Alfranca, A., Rodriguez-Milla, M. A., Perez-Tavarez, R., Rouault-Pierre, K., Waclawiczek, A., Chakravarty, P., Mulero, F., Trigueros, C., Navarro, S., Bonnet, D., & García-Castro, J. (2018). C-Fos induces chondrogenic tumor formation in immortalized human mesenchymal progenitor cells. *Scientific Reports*, *8*(1), 15615. https://doi.org/10.1038/s41598-018-33689-0

[185] Zhen, G., Guo, Q., Li, Y., Wu, C., Zhu, S., Wang, R., Guo, X. E., Kim, B. C., Huang, J., Hu, Y., Dan, Y., Wan, M., Ha, T., An, S., & Cao, X. (2021). Mechanical stress determines the configuration of TGFβ activation in articular cartilage. *Nature Communications*, *12*(1), 1706. https://doi.org/10.1038/s41467-021-21948-0

[186] Li, Z., Kupcsik, L., Yao, S., Alini, M., & Stoddart, M. J. (2010). Mechanical load modulates chondrogenesis of human mesenchymal stem cells through the TGF-β pathway. *Journal of Cellular and Molecular Medicine, 14*(6a), 1338–1346. https://doi.org/10.1111/j.1582-4934.2009.00780.x

[187] Bougault, C., Paumier, A., Aubert-Foucher, E., & Mallein-Gerin, F. (2009). Investigating conversion of mechanical force into biochemical signaling in three-dimensional chondrocyte cultures. *Nature Protocols*, *4*(6), 928–938. https://doi.org/10.1038/nprot.2009.63

[188] Buschmann, M. D., Gluzband, Y. A., Grodzinsky, A. J., & Hunziker, E. B. (1995). Mechanical compression modulates matrix biosynthesis in chondrocyte/agarose culture. *Journal of Cell Science, 108*(4), 1497–1508. https://doi.org/10.1242/jcs.108.4.1497

[189] Jones, I. L., Klämfeldt, A., & Sandström, T. (1982). The effect of continuous mechanical pressure upon the turnover of articular cartilage proteoglycans in vitro. *Clinical Orthopaedics and Related Research, 165*, 283–289.

[190] Sah, R. L. -Y., Kim, Y., Doong, J. H., Grodzinsky, A. J., Plass, A. H. K., & Sandy, J. D. (1989). Biosynthetic response of cartilage explants to dynamic compression. *Journal of Orthopaedic Research, 7*(5), 619–636. https://doi.org/10.1002/jor.1100070502

[191] Young, D. A., Barter, M. J., & Wilkinson, D. J. (2019). Recent advances in understanding the regulation of metalloproteinases. *F1000Research, 8*, F1000 Faculty Rev-195. https://doi.org/10.12688/f1000research.17471.1

[192] Timmermans, R. G. M., Blom, A. B., Nelissen, R. G. H. H., Broekhuis, D., Van Der Kraan, P. M., Meulenbelt, I., Van Den Bosch, M. H. J., & Ramos, Y. F. M. (2024). Mechanical stress and inflammation have opposite effects on Wnt signaling in human chondrocytes. *Journal of Orthopaedic Research, 42*(2), 286–295. https://doi.org/10.1002/jor.25673

[193] Sun, H. B. (2010). Mechanical loading, cartilage degradation, and arthritis. *Annals of the New York Academy of Sciences, 1211*(1), 37–50. https://doi.org/10.1111/j.1749-6632.2010.05808.x

[194] Huang, G., Chubinskaya, S., Liao, W., & Loeser, R. F. (2017). Wnt5a induces catabolic signaling and matrix metalloproteinase production in human articular chondrocytes. *Osteoarthritis and Cartilage*, *25*(9), 1505–1515. https://doi.org/10.1016/j.joca.2017.05.018

[195] Malemud, C. J. (2015). Biologic basis of osteoarthritis: State of the evidence. *Current Opinion in Rheumatology*, *27*(3), 289–294. https://doi.org/10.1097/BOR.0000000000000162

[196] Han, E., Ge, C., Chen, A. C., Schumacher, B. L., & Sah, R. L. (2012). Compaction Enhances Extracellular Matrix Content and Mechanical Properties of Tissue-Engineered Cartilaginous Constructs. *Tissue Engineering Part A*, *18*(11–12), 1151–1160. https://doi.org/10.1089/ten.tea.2011.0300

[197] Cederlund, A. A., & Aspden, R. M. (2022). Walking on water: Revisiting the role of water in articular cartilage biomechanics in relation to tissue engineering and regenerative medicine. *Journal of the Royal Society, Interface*, *19*(193), 20220364. https://doi.org/10.1098/rsif.2022.0364

[198] Leo, L., Bridelli, M. G., & Polverini, E. (2021). Reversible processes in collagen dehydration: A molecular dynamics study. *Archives of Biochemistry and Biophysics*, *714*, 109079. https://doi.org/10.1016/j.abb.2021.109079

[199] Rabinowitz, J. D., & Enerbäck, S. (2020). Lactate: The ugly duckling of energy metabolism. *Nature Metabolism*, *2*(7), 566–571. https://doi.org/10.1038/s42255-020-0243-4

[200] Salinas, D., Minor, C. A., Carlson, R. P., McCutchen, C. N., Mumey, B. M., & June, R. K. (2017). Combining Targeted Metabolomic Data with a Model of Glucose Metabolism: Toward Progress in Chondrocyte Mechanotransduction. *PLOS ONE*, *12*(1), e0168326. https://doi.org/10.1371/journal.pone.0168326

[201] Kulakovskaya, T., Ryasanova, L., Dmitriev, V., & Zvonarev, A. (2016). The Role of Inorganic Polyphosphates in Stress Response and Regulation of Enzyme Activities in Yeast. In T. Kulakovskaya, E. Pavlov, & E. N. Dedkova (Eds.), *Inorganic Polyphosphates in Eukaryotic Cells* (pp. 3–14). Springer International Publishing. https://doi.org/10.1007/978-3-319-41073-9_1

[202] Trilisenko, L., Zvonarev, A., Valiakhmetov, A., Penin, A. A., Eliseeva, I. A., Ostroumov, V., Kulakovskiy, I. V., & Kulakovskaya, T. (2019). The Reduced Level of Inorganic Polyphosphate Mobilizes Antioxidant and Manganese-Resistance Systems in Saccharomyces cerevisiae. *Cells*, *8*(5), 461. https://doi.org/10.3390/cells8050461

## APPENDIX I – DMEM HIGH GLUCOSE AND HAM'S F12 MEDIA FORMULATION

| Components | Molecular Weight | Concentration (mg/L) | mM |
|---|---|---|---|
| Amino Acids | | | |
| Glycine | 75.0 | 30.0 | 0.4 |
| L-Arginine hydrochloride | 211.0 | 84.0 | 0.39810428 |
| L-Cystine 2HCl | 313.0 | 63.0 | 0.20127796 |
| L-Glutamine | 146.0 | 584.0 | 4.0 |
| L-Histidine hydrochloride-H2O | 210.0 | 42.0 | 0.2 |
| L-Isoleucine | 131.0 | 105.0 | 0.8015267 |
| L-Leucine | 131.0 | 105.0 | 0.8015267 |
| L-Lysine hydrochloride | 183.0 | 146.0 | 0.7978142 |
| L-Methionine | 149.0 | 30.0 | 0.20134228 |
| L-Phenylalanine | 165.0 | 66.0 | 0.4 |
| L-Serine | 105.0 | 42.0 | 0.4 |
| L-Threonine | 119.0 | 95.0 | 0.79831934 |
| L-Tryptophan | 204.0 | 16.0 | 0.078431375 |
| L-Tyrosine disodium salt dihydrate | 261.0 | 104.0 | 0.39846742 |
| L-Valine | 117.0 | 94.0 | 0.8034188 |
| Vitamins | | | |
| Choline chloride | 140.0 | 4.0 | 0.028571429 |
| D-Calcium pantothenate | 477.0 | 4.0 | 0.008385744 |
| Folic Acid | 441.0 | 4.0 | 0.009070295 |
| Niacinamide | 122.0 | 4.0 | 0.032786883 |
| Pyridoxine hydrochloride | 206.0 | 4.0 | 0.019417476 |
| Riboflavin | 376.0 | 0.4 | 0.0010638298 |
| Thiamine hydrochloride | 337.0 | 4.0 | 0.011869436 |
| i-Inositol | 180.0 | 7.2 | 0.04 |
| Inorganic Salts | | | |
| Calcium Chloride (CaCl2) (anhyd.) | 111.0 | 200.0 | 1.8018018 |
| Ferric Nitrate (Fe(NO3)3"9H2O) | 404.0 | 0.1 | 2.4752476E-4 |
| Magnesium Sulfate (MgSO4) (anhyd.) | 120.0 | 97.67 | 0.8139166 |
| Potassium Chloride (KCl) | 75.0 | 400.0 | 5.3333335 |

| | | | |
|---|---|---|---|
| Sodium Bicarbonate (NaHCO3) | 84.0 | 3700.0 | 44.04762 |
| Sodium Chloride (NaCl) | 58.0 | 6400.0 | 110.344826 |
| Sodium Phosphate monobasic (NaH2PO4-H2O) | 138.0 | 125.0 | 0.9057971 |
| Other Components | | | |
| D-Glucose (Dextrose) | 180.0 | 4500.0 | 25.0 |
| Phenol Red | 376.4 | 15.0 | 0.039851222 |
| Sodium Pyruvate | 110.0 | 110.0 | 1.0 |

**Table A1.** Media formulation for Gibco DMEM High Glucose.

| Components | Molecular Weight | Concentration (mg/L) | mM |
|---|---|---|---|
| Amino Acids | | | |
| Glycine | 75.0 | 7.5 | 0.1 |
| L-Alanine | 89.0 | 8.9 | 0.099999994 |
| L-Arginine hydrochloride | 211.0 | 211.0 | 1.0 |
| L-Asparagine-H2O | 150.0 | 15.01 | 0.10006667 |
| L-Aspartic acid | 133.0 | 13.3 | 0.1 |
| L-Cysteine hydrochloride-H2O | 176.0 | 35.12 | 0.19954544 |
| L-Glutamic Acid | 147.0 | 14.7 | 0.1 |
| L-Glutamine | 146.0 | 146.0 | 1.0 |
| L-Histidine hydrochloride-H2O | 210.0 | 21.0 | 0.1 |
| L-Isoleucine | 131.0 | 4.0 | 0.030534351 |
| L-Leucine | 131.0 | 13.1 | 0.1 |
| L-Lysine hydrochloride | 183.0 | 36.5 | 0.19945355 |
| L-Methionine | 149.0 | 4.5 | 0.030201342 |
| L-Phenylalanine | 165.0 | 5.0 | 0.030303031 |
| L-Proline | 115.0 | 34.5 | 0.3 |
| L-Serine | 105.0 | 10.5 | 0.1 |
| L-Threonine | 119.0 | 11.9 | 0.099999994 |
| L-Tryptophan | 204.0 | 2.04 | 0.01 |
| L-Tyrosine disodium salt dihydrate | 262.0 | 7.81 | 0.02980916 |
| L-Valine | 117.0 | 11.7 | 0.1 |
| Vitamins | | | |
| Biotin | 244.0 | 0.0073 | 2.9918034E-5 |
| Choline chloride | 140.0 | 14.0 | 0.1 |
| D-Calcium pantothenate | 477.0 | 0.5 | 0.001048218 |
| Folic Acid | 441.0 | 1.3 | 0.0029478457 |
| Niacinamide | 122.0 | 0.036 | 2.9508196E-4 |
| Pyridoxine hydrochloride | 206.0 | 0.06 | 2.9126214E-4 |
| Riboflavin | 376.0 | 0.037 | 9.8404256E-5 |
| Thiamine hydrochloride | 337.0 | 0.3 | 8.9020777E-4 |
| Vitamin B12 | 1355.0 | 1.4 | 0.0010332103 |
| i-Inositol | 180.0 | 18.0 | 0.1 |
| Inorganic Salts | | | |
| Calcium Chloride (CaCl2) (anhyd.) | 111.0 | 33.22 | 0.2992793 |

| | | | |
|---|---|---|---|
| Cupric sulfate (CuSO4-5H2O) | 250.0 | 0.0025 | 1.0E-5 |
| Ferric sulfate (FeSO4-7H2O) | 278.0 | 0.834 | 0.003 |
| Magnesium Chloride (anhydrous) | 95.0 | 57.22 | 0.6023158 |
| Potassium Chloride (KCl) | 75.0 | 223.6 | 2.9813335 |
| Sodium Bicarbonate (NaHCO3) | 84.0 | 1176.0 | 14.0 |
| Sodium Chloride (NaCl) | 58.0 | 7599.0 | 131.01724 |
| Sodium Phosphate dibasic (Na2HPO4) anhydrous | 142.0 | 142.0 | 1.0 |
| Zinc sulfate (ZnSO4-7H2O) | 288.0 | 0.863 | 0.0029965276 |
| Other Components | | | |
| D-Glucose (Dextrose) | 180.0 | 1802.0 | 10.011111 |
| Hypoxanthine Na | 159.0 | 4.77 | 0.03 |
| Linoleic Acid | 280.0 | 0.084 | 2.9999999E-4 |
| Lipoic Acid | 206.0 | 0.21 | 0.0010194174 |
| Phenol Red | 376.4 | 1.2 | 0.0031880978 |
| Putrescine 2HCl | 161.0 | 0.161 | 0.001 |
| Sodium Pyruvate | 110.0 | 110.0 | 1.0 |
| Thymidine | 242.0 | 0.7 | 0.002892562 |

**Table A2.** Media formulation for Gibco Ham's F12.

## APPENDIX II – POLYP DETECTION IN MEDIA SUPPLEMENTS

A common practice in cell culture work is the heat inactivation of FBS to inactive complement proteins in the serum. For our study looking at the impact of media supplements on polyP accumulation we wanted to investigate the impact of heat-inactivation on the polyP levels present in FBS. We compared the levels of polyP in FBS, 30 minutes heat-inactivated FBS, and 2 hours heat-inactivated FBS (Figure A1). There were no significant differences in the polyP levels between the conditions, however, there is a steady decrease in polyP as more time was applied to heat-inactive the FBS. With this information, non-heat inactivated FBS was used to assess its impact on polyP accumulation as we wished to introduce the full amount of polyP present in FBS for our cultures.

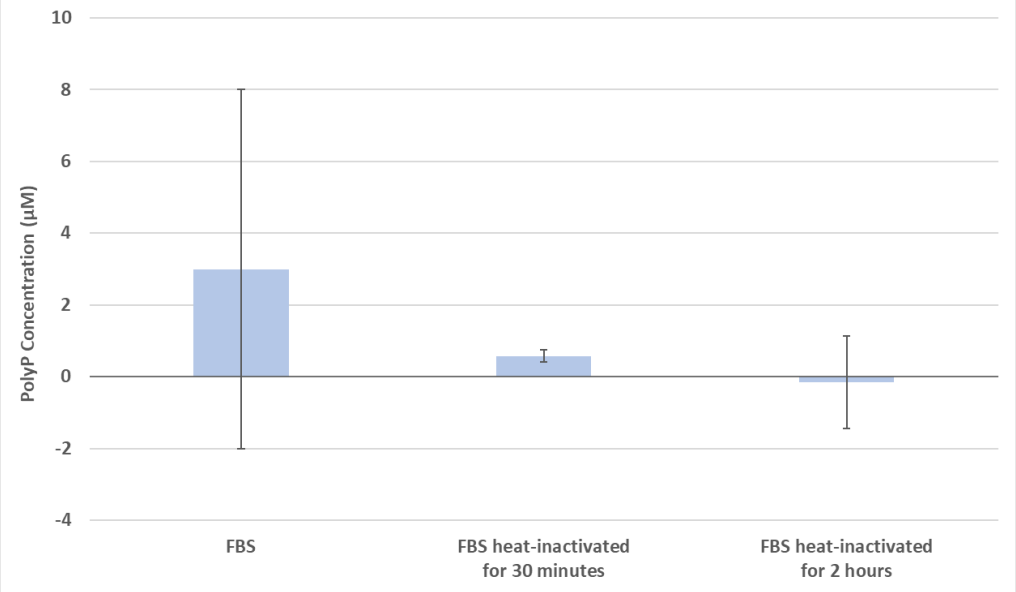


**Figure A1.** PolyP concentration in FBS, FBS heat-inactivated for 30 minutes, and FBS heat-inactivated for 2 hours. Data is represented as mean ± SD.

## APPENDIX III – POLYP ASSAY MODIFICATIONS

The protocol developed by Lee et al. [126] with modifications made by a previous student from the St-Pierre lab was used to quantify polyP levels. The original protocol consisted of making a standard curve with concentrations from 0 - 60 µM polyP. However, initial attempts to generate standard curves were repeatedly giving non-linear curves with $R^2$ < 99% (Figure A2.1A). These inconsistencies lead us to make an adjustment in technique to generate the standard curve via serial dilutions which gave rise to improved $R^2$ values but was still not sufficiently consistent (Figure A2.1B)

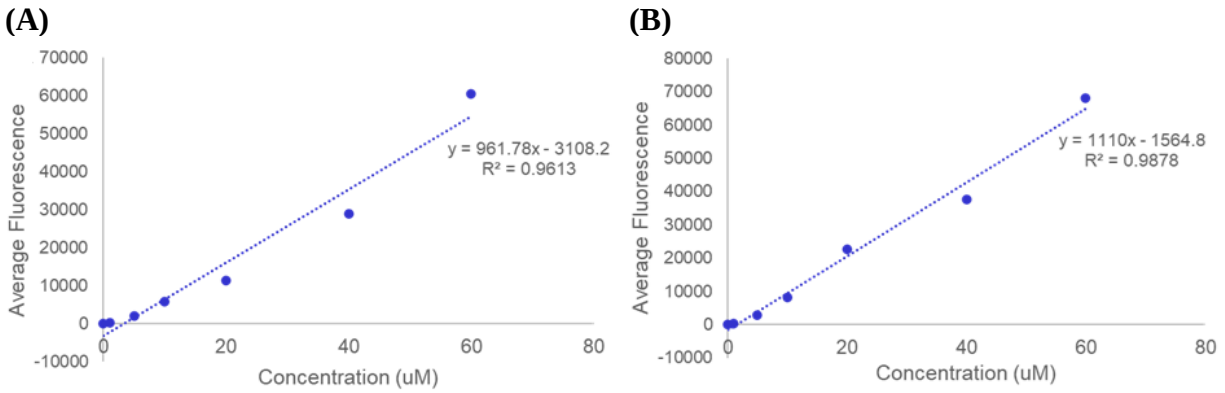


**Figure A2.1** Standard curves generated (A) not using and (B) using the serial dilution technique.

Although standard curves made via serial dilutions yielded better results, the polyP concentrations of 1 - 10 µM and 60 µM regularly showed fluctuations from expected results with an impact on the values obtained for the slope and intercept, resulting in inaccurate quantification for the samples. For example, a positive control with spiked with a known concentration of 7 nmol of polyP is read for every polyP assay to validate the accuracy of the readings. However, two readings using the same set of standards and positive controls can give drastically different results with the first read (Figure A2.2A) giving a value of 6.46 nmol and the second read (Figure A2.2B) giving a value of 8.01 nmol. This showcases how seemingly minor deviations in the standards can drastically impact the calculated values in the sample.

**(A)**

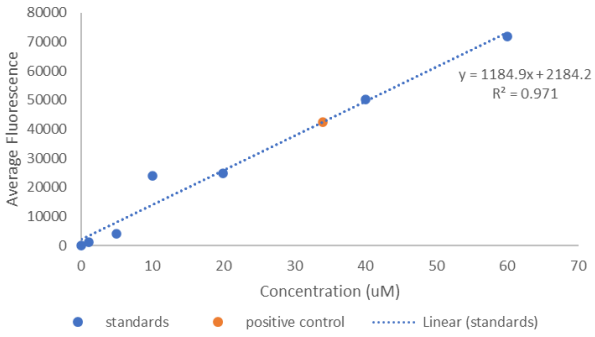


**(B)**

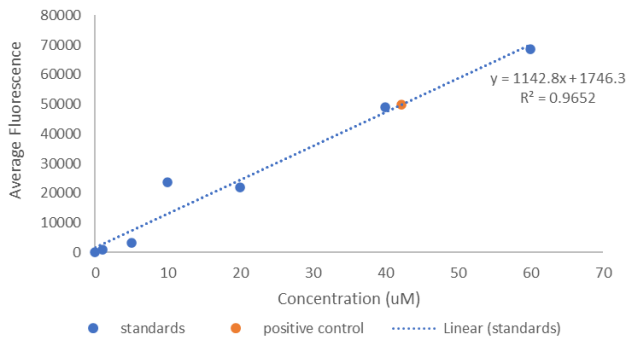


**Figure A2.2** (A) Reading one and (B) reading two of the same set of standard curves with the positive control plotted along the linear trend line of the polyP standards with concentrations ranging from 0 – 60 µM.

To address this problem, we decided to adjust the concentration of the standards (0 - 80 µM) to have a larger range of points to minimize the effect of fluctuations at the two extremes of the standards**.** The standards were made using serial dilution in hopes of getting a more consistent curves and readings. With the new set of standards ranging from concentrations of 0 - 80 µM we reduced the impact of the variability of certain points to gain accurate readings of the positive control with the first (Figure A2.3A) and second set (Figure A2.3B) of standards giving us values of 6.92 nmol and 7.14 nmol, respectively.

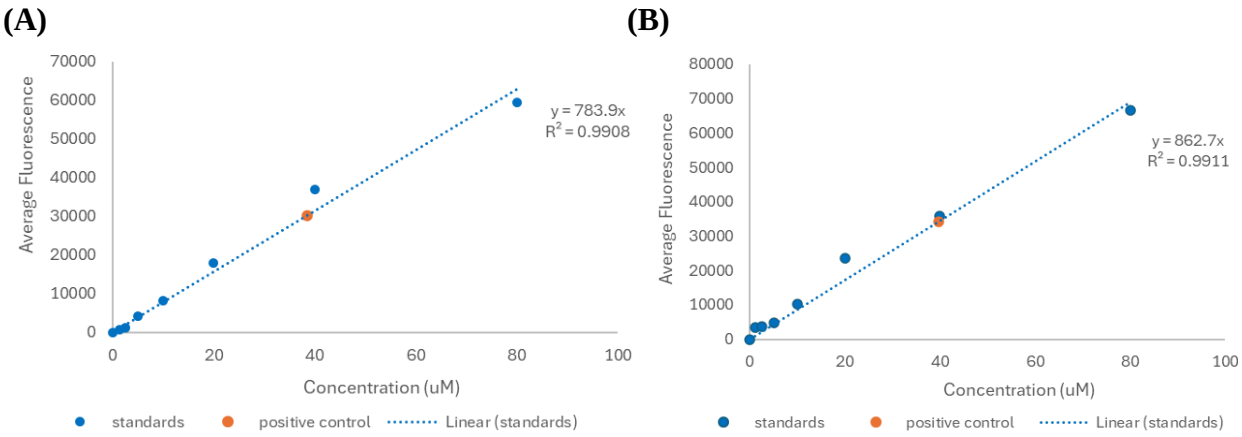


**Figure A2.3** (A) Set one and (B) set two of standard curves with the positive control plotted along the linear trend line of the polyP standards with concentrations ranging from 0 – 80 µM.

Once we were able to obtain reliable positive control readings with the 0 - 80 µM standard curve, we utilized the adjustments to begin quantifying the polyP content in the tissue constructs and spent media from our experiments. When we measured the polyP levels in both the tissue and media samples, we ran into the issue that almost all of our samples showed readings residing towards the lower concentration end of the curve with some of the samples falling below the limit of detection (Figure A2.4). The minimal level of polyP is likely attributed to the short culture period of one week, which may not be sufficient for chondrocytes to produce and accumulate substantial levels of polyP. With the samples being so close or less than the zero we decided to extend the culture period from one to two weeks to facilitate increased chondrocyte growth in hopes of elevating the production and accumulation rate of polyP.

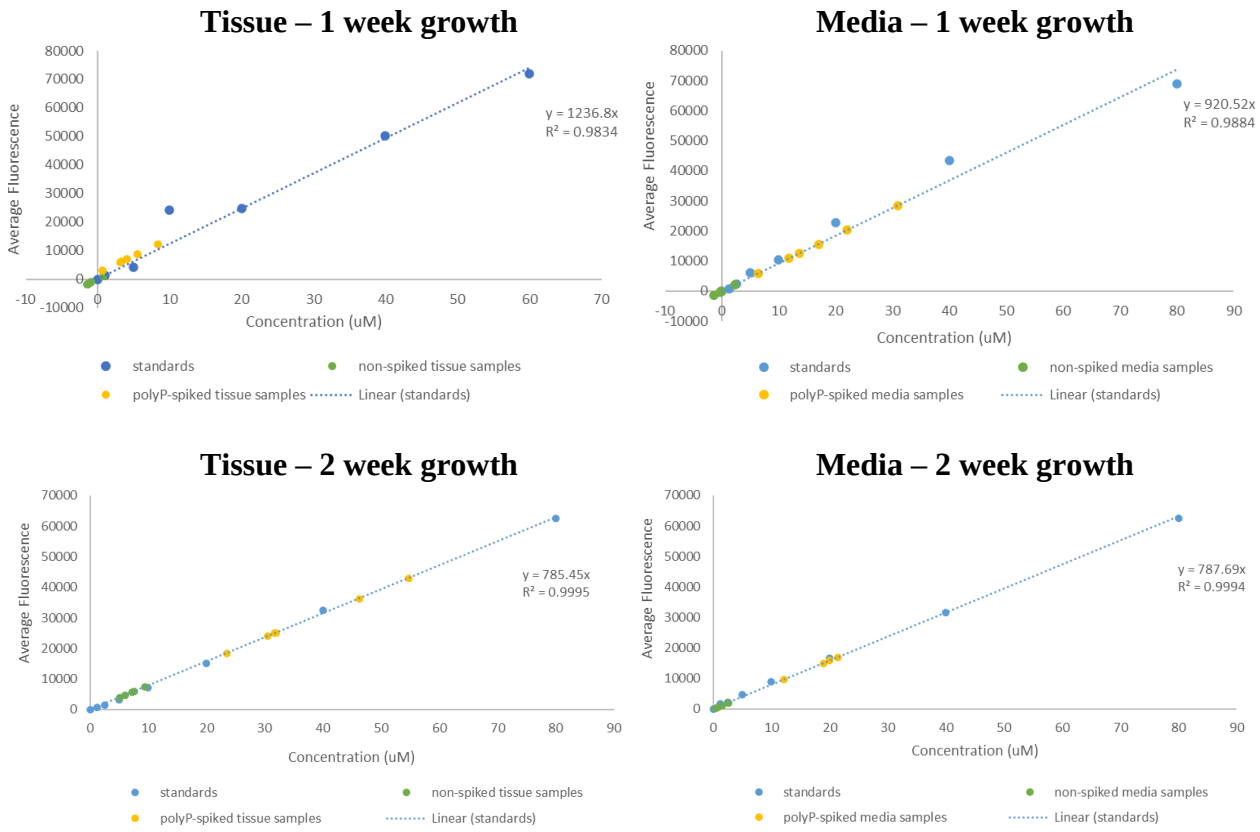


**Figure A2.4** Non-spiked and polyP-spiked tissue and media samples grown for one week versus two weeks plotted along the linear trend line of the polyP standards with concentrations ranging from 0 – 80 µM.

Despite extending the culture period, the samples still exhibited low levels of polyP. Hence, we decided to adjust our protocol in attempts to concentrate the amount of polyP measurable by the assay. Some of the adjustments we made included reducing the volume of proteinase K solution used to digest the tissue samples from 30 µL per milligram of wet weight to 10 µL per milligram of wet weight. Since the volume of proteinase K used would be reduce 3-fold the total volume of the tissue digests would be reduced to the same degree. The volume of the tissue digests was not sufficient in creating the non-spiked and spiked aliquots based on the

previous protocol, there we reduced the volume from 280 µL to 170 µL of the non-spiked and polyP-spiked samples (Figure A2.5B).

**(A)**

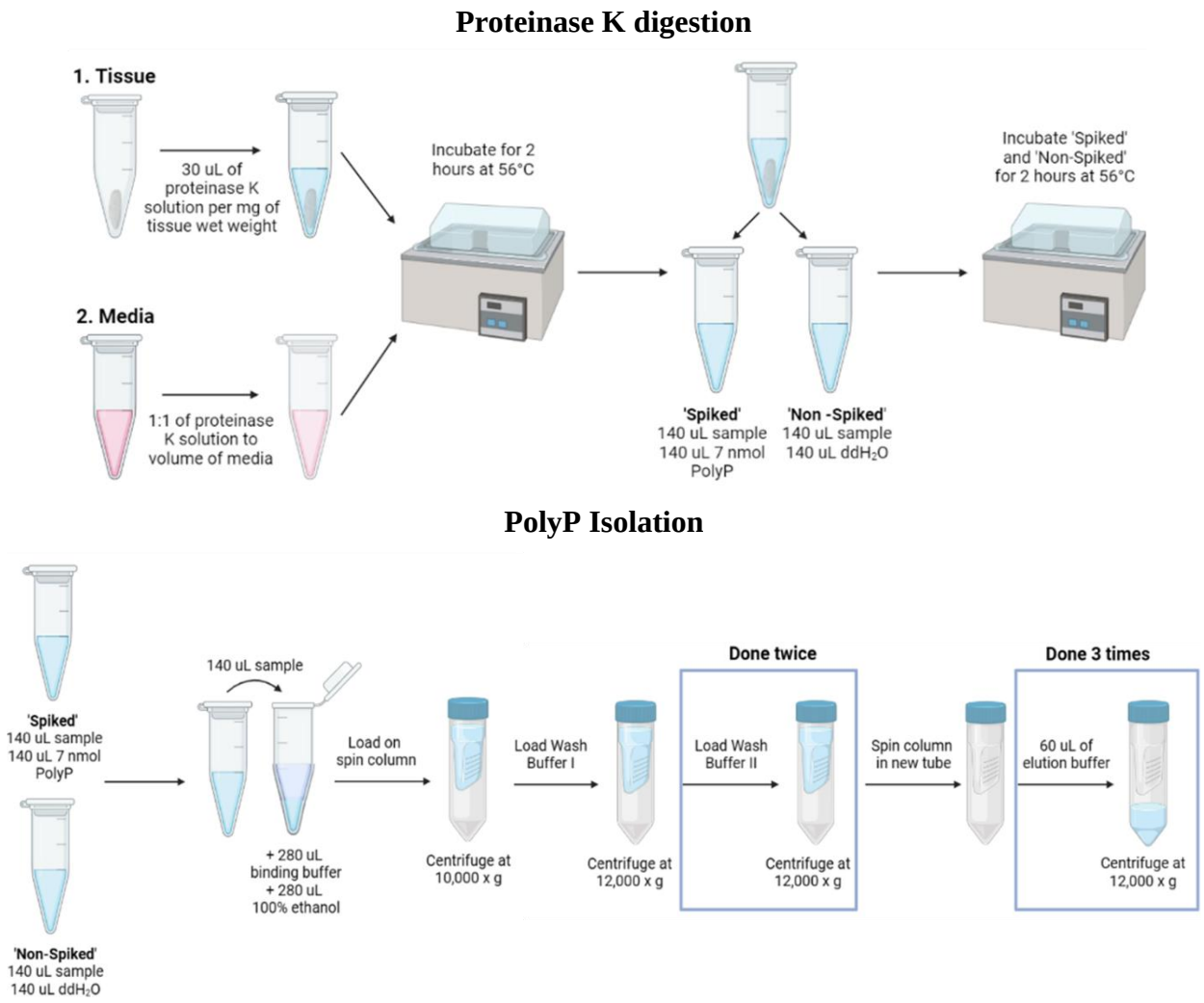

**(B)**

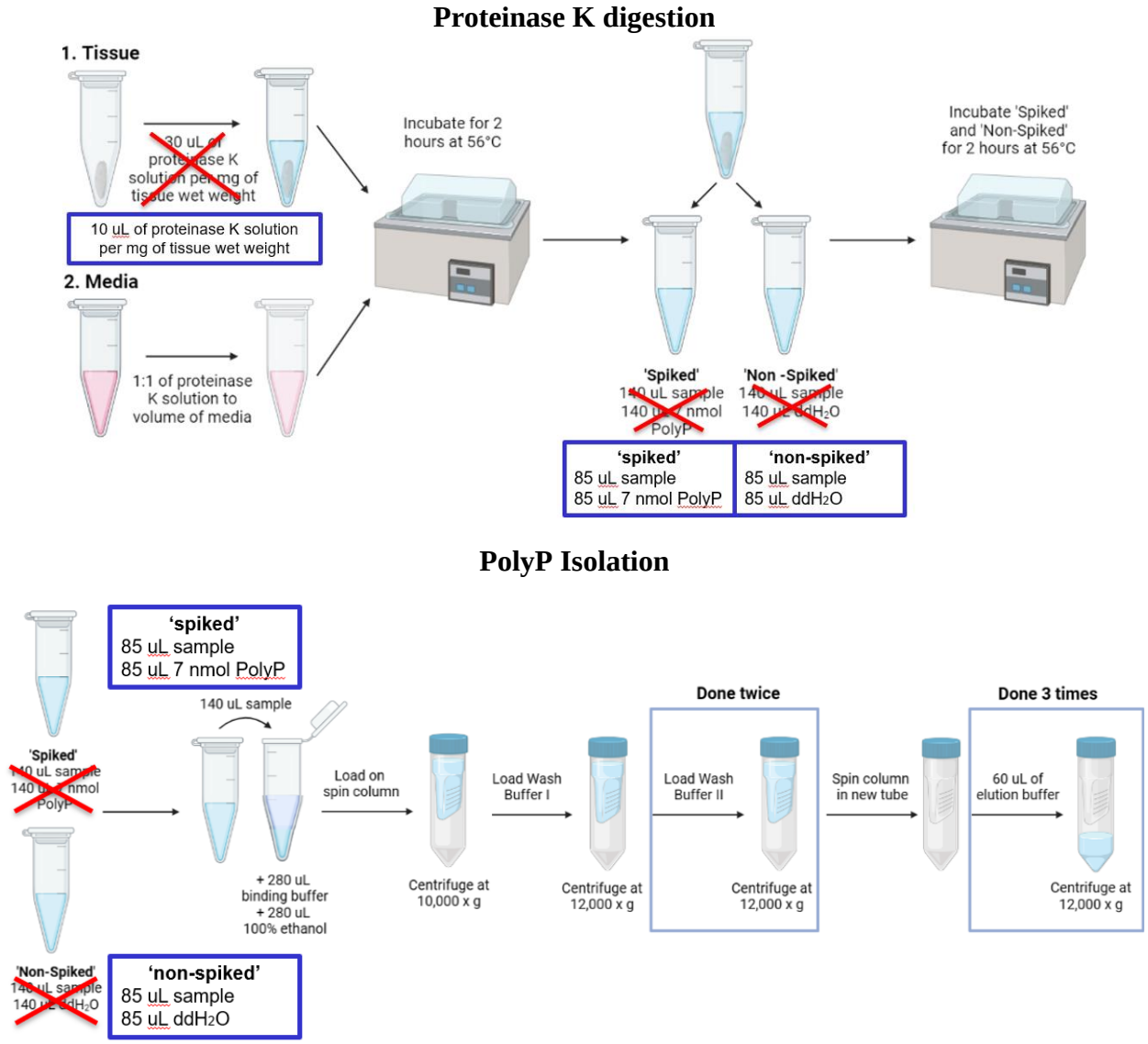


**Figure A2.5** Schematic of Proteinase K digestion protocol for tissue and media samples (A) before and (B) after the reduction of Proteinase K used for tissue digestion from 30 µL per milligram of wet weight to 10 µL per milligram of wet weight and the total volume from 280 µL to 170 µL of the non-spiked and polyP-spiked aliquots.

After concentrating the samples, we ran into the issue with our tissue samples (Figure A2.6A), especially our polyP-spiked samples, surpassing the highest concentration on our standard curve. On the other hand, our media samples all resided with the range of the standard

curve (Figure A2.6B). To correct for the readings that surpass the highest standard on the standard curve, we further diluted our tissue digests in a 1:1 ratio with distilled water during the Proteinase K digestion when creating our "spiked" and "non-spiked" samples (Figure A2.7B). This step was only done for the tissue samples in hopes of getting both the non-spiked and polyP-spiked samples within the standard curve.

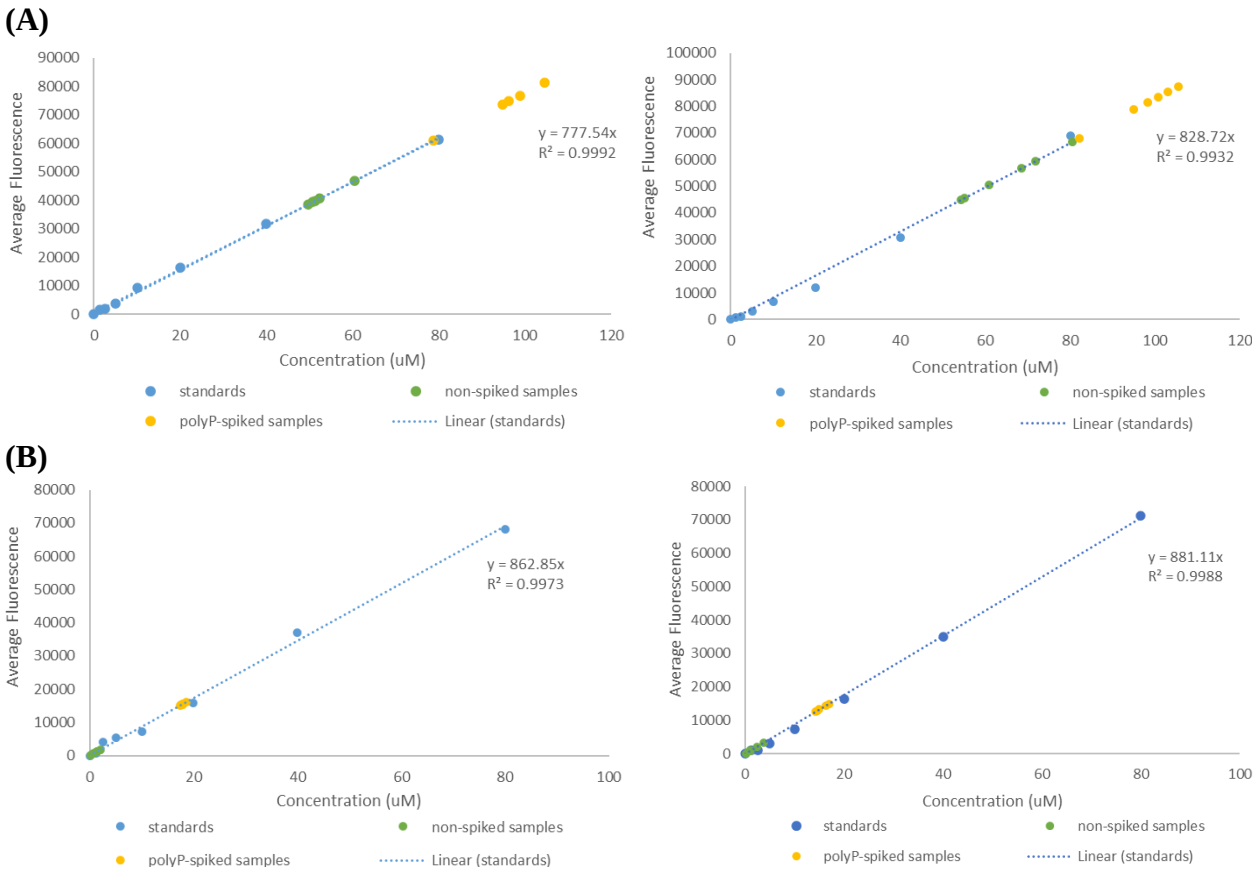


**Figure A2.6** Non-spiked and polyP-spiked (A) tissue and (B) media samples grown for two weeks and processed with the Proteinase K and polyP isolation modifications depicted in Figure A2.5B plotted along the linear trend line of the polyP standards with concentrations ranging from 0 – 80 µM.

**(A)**

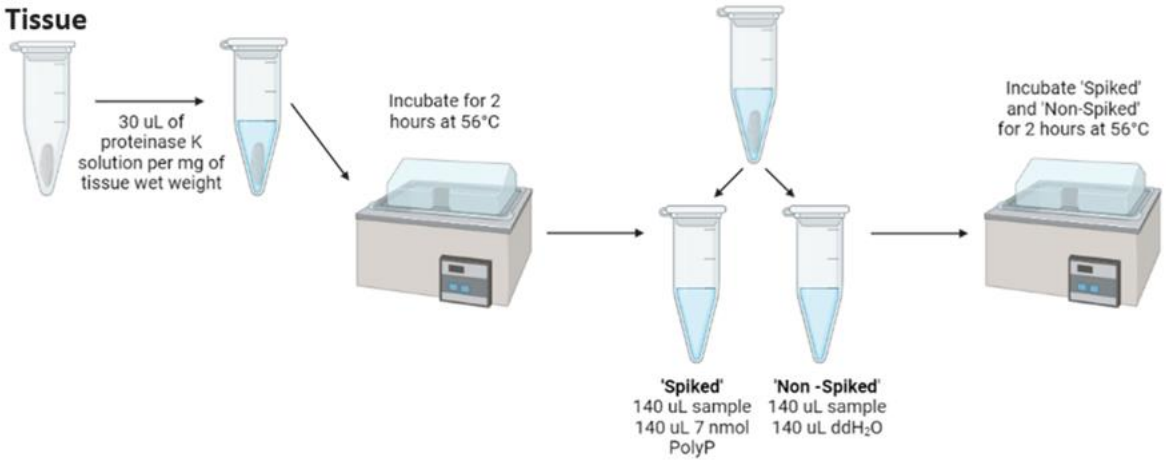


**(B)**

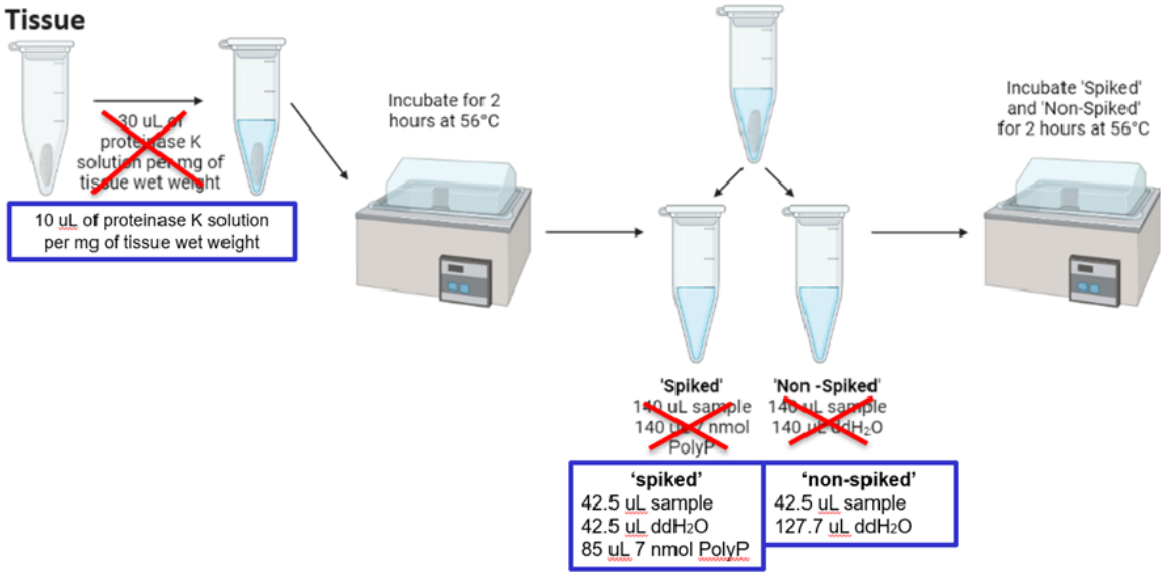


**Figure A2.7** Schematic for the creation of non-spiked and spiked aliquots (A) before and (B) after the 1:1 dilution with distilled water.

Once the 1:1 dilution with distilled water was implemented into the protocol, readings for both the non-spiked and polyp-spiked samples fell within the standard curve (Figure A2.8). The final protocol modifications to the polyP assay consisted of three main chains which include: (i) the reduction of the amount of proteinase K used to digest the tissue samples from 30 µL per milligram of wet weight to 10 µL per milligram of wet weight. (ii) the reduction of the total volume from 280 µL to 170 µL of the non-spiked and polyP-spiked samples, and (iii) the 1:1

dilution of the tissue digest with distilled water when creating the non-spiked and polyP-spiked samples.

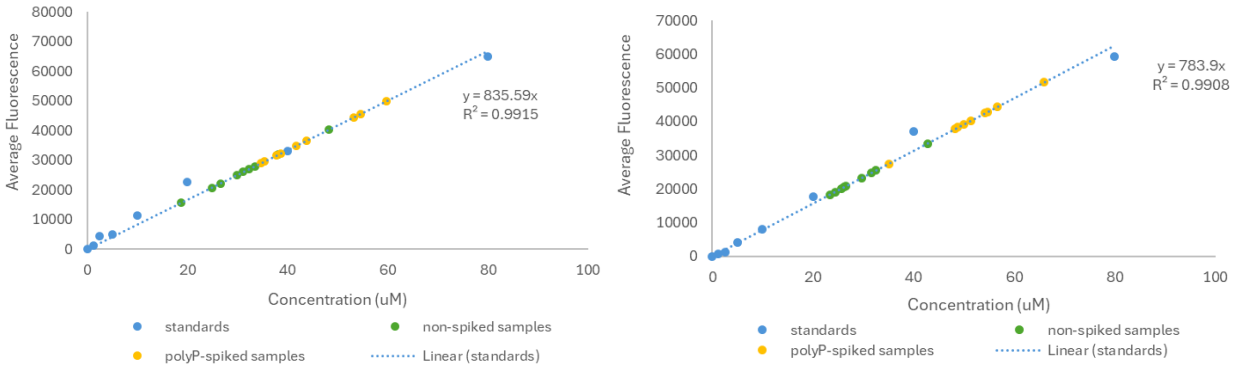


**Figure A2.8** Non-spiked and polyP-spiked tissue samples grown for two weeks and processed with the Proteinase K modification of utilizing 10 µL Proteinase K solution per milligram of wet weight, reducing the total volume from 280 µL to 170 µL and diluting the tissue digest 1:1 with distilled water for non-spiked and polyP-spiked aliquots plotted along the linear trend line of the polyP standards with concentrations ranging from 0 – 80 µM.